การสังเคราะห์คาลิกซ์[4]เอรีนควิโนนชนิดใหม่

สำหรับเป็นเซนเซอร์ของโลหะแอลคาไล

นาย ณัฐวุฒิ เกิดไพบูลย์

วิทยานิพนธ์นี้เป็นส่วนหนึ่งของการศึกษาตามหลักสูตรปริญญาวิทยาศาสตรมหาบัณฑิต

สาขาวิชา เคมี ภาควิชา เคมี

คณะวิทยาศาสตร จุฬาลงกรณ์มหาวิทยาลัย

ปีการศึกษา 2545

ISBN 974-17-2043-2

SYNTHESIS OF NEW CALIX[4]ARENEQUINONE AS ALKALI METAL SENSOR

Mr. Nuttavut Kerdpaiboon

A Thesis Submitted in Partial Fulfillment of the Requirements
for the Degree of Master of Science in Chemistry
Department of Chemistry
Faculty of Science
Chulalongkorn University
Academic Year 2002
ISBN 974-17-2043-2

Thesis Title	Synthesis of new calix[4]arenequinone as alkali metal sensor
By	Mr. Nuttavut Kerdpaiboon
Field of Study	Chemistry
Thesis Advisor	Assistant Professor Thawatchai Tuntulani, Ph.D.

Accepted by the Faculty of Science, Chulalongkorn University in Partial Fulfillment of the Requirements for the Master's Degree

…….. Deputy Dean for Administrative Affairs,
Acting Dean, Faculty of Science
(Associate Professor Pipat Karntiang, Ph.D.)

Thesis Committee

…….. Chairman
(Associate Professor Sophon Roengsumran, Ph.D.)

…….. Thesis Advisor
(Assistant Professor Thawatchai Tuntulani, Ph.D.)

…….. Member
(Associate Professor Nuanphun Chantarasiri, Ph.D.)

…….. Member
(Assistant Professor Nongnuj Muangsin, Ph.D.)

ณัฐวุฒิ เกิดไพบูลย์ : การสังเคราะห์คาลิกซ์[4]เอรีนควิโนนชนิดใหม่สำหรับเป็นเซนเซอร์ของโลหะแอลคาไล (SYNTHESIS OF NEW CALIX[4]ARENEQUINONE AS ALKALI METAL SENSOR) อาจารย์ที่ปรึกษา : ผศ.ดร. ธวัชชัย ตันฑุลานิ; 115 หน้า. ISBN 974-17-2043-2

ได้สังเคราะห์ลิแกนด์ 25,27-Di(ethyleneglycol)-bis-*p-tert*-butylcalix[4]arene **1**, 25,27-di(diethyleneglycol)-bis-*p-tert*-butylcalix[4]arene **2b** และ 25,27-di(methoxy)-26,28-di(ethyleneglycol)-bis-*p-tert*-butylcalix[4]arene **4d** อนุพันธ์ควิโนน 25,27-di(ethyleneglycol)-bis-*p-tert*-butylcalix[4]tetraquinone **5a**, 25,27-di(diethyleneglycol)-bis-*p-tert*-butylcalix[4]tetraquinone **5b** และ 25,27-di(methoxy)-26,28-di(ethyleneglycol)-bis-*p-tert*-butylcalix[4]diquinone **5c** สามารถสังเคราะห์ได้จากปฏิกิริยาระหว่าง **1**, **2b** และ **4d** ตามลำดับกับ $Tl(CF_3COO)_3$ ใน CF_3COOH การศึกษาการเกิดสารประกอบเชิงซ้อนของลิแกนด์ **5a**, **5b** และ **5c** กับแอลคาไลแคทไอออน ลิเธียม, โซเดียม, โพแทสเซียม, ซีเซียม กระทำโดยการไทเทรตด้วยเทคนิคโปรตอนนิวเคลียร์แมกเนติกเรโซแนนซ์ (เอ็นเอ็มอาร์) พบว่าลิแกนด์ **5a** และ **5c** สามารถเกิดสารประกอบเชิงซ้อนในอัตราส่วน 1:1 กับโลหะลิเธียม, โซเดียม และโพแทสเซียม โดยความสามารถในการเกิดสารประกอบเชิงซ้อนเป็นดังนี้ โซเดียม > ลิเธียม >> โพแทสเซียม และ โซเดียม >> ลิเธียม > โพแทสเซียม ตามลำดับ สำหรับลิแกนด์ **5b** สามารถเกิดสารประกอบเชิงซ้อนในอัตราส่วน 1:1 กับโลหะลิเธียม, โซเดียม, โพแทสเซียม และซีเซียม จากการที่มีโพรงขนาดใหญ่ทำให้สามารถจับกับโลหะซีเซียมได้ดี โดยความสามารถในการเกิดสารประกอบเชิงซ้อนเป็นดังนี้ ซีเซียม > โพแทสเซียม > โซเดียม >> ลิเธียม การศึกษาสมบัติทางเคมีไฟฟ้าของลิแกนด์ **5a**, **5b** และ **5c** โดยใช้เทคนิคไซคลิกโวลแทมเมทรีและ สแควร์เวฟโวลแทมเมทรี พบว่าเมื่อเติมโลหะแอลคาไลลงไปในระบบจะเห็นถึงการเปลี่ยนแปลงอย่างชัดเจนของสัญญาณโวลแทมโมแกรม และจากการเลื่อนของสัญญาณรีดักชันแสดงให้เห็นถึงผลของความเป็นฮาร์ท-ซอฟท์เอซิดของโลหะแอลคาไลที่มีผลต่อการเปลี่ยนแปลงสมบัติไฟฟ้าเคมีของลิแกนด์ทั้ง 3 ชนิด

ภาควิชา..... ลายมือชื่อนิสิต.....

สาขาวิชา..... ลายมือชื่ออาจารย์ที่ปรึกษา.....

ปีการศึกษา.....

4372258923 : MAJOR CHEMISTRY.

KEY WORDS: DOUBLECALIX[4]ARENEQUINONE, CYCLIC VOLTAMMETRY, SQUARE WAVE VOLTAMMETRY, ALKALI METAL SENSOR

NUTTAVUT KERDPAIBOON : SYNTHESIS OF NEW CALIX[4] ARENEQUINONE AS ALKALI METAL SENSOR. THESIS ADVISOR: ASSIST. PROF. THAWATCHAI TUNTULANI, Ph.D. 115 pp. ISBN 974-17-2043-2.

25,27-Di(ethyleneglycol)-bis-*p*-*tert*-butylcalix[4]arene **1**, 25,27-di (diethyleneglycol)-bis-*p*-*tert*-butylcalix[4]arene **2b** and 25,27-di(methoxy)-26,28-di (ethyleneglycol)-bis-*p*-*tert*-butylcalix[4]arene **4d** were synthesized. Quinone derivatives 25,27-di(ethyleneglycol)-bis-*p*-*tert*-butylcalix[4]tetraquinone **5a**, 25,27-di(diethylene-glycol)-bis-*p*-*tert*-butylcalix[4]tetraquinone **5b** and 25,27-di(methoxy)-26,28-di(ethylene-glycol)-bis-*p*-*tert*-butylcalix[4]diquinone **5c** were obtained from reactions of **1**, **2b** and **4d,** respectively with $Tl(CF_3COO)_3$ in CF_3COOH. Complexation studies of ligands **5a**, **5b** and **5c** with alkali metals such as Li^+, Na^+, K^+ and Cs^+ were carried out by ^{1}H-NMR titrations. Ligands **5a** and **5c** were able to form 1:1 complexes with Li^+, Na^+ and K^+ and binding abilities were as follows; $Na^+ > Li^+ >> K^+$ and $Na^+ >> Li^+ > K^+$. Ligand **5b** was able to form 1:1 complexes with Li^+, Na^+, K^+ and Cs^+. Because of its bigger cavity compared to **5a** and **5c, 5b** showed selectivity for Cs^+. The binding trend for **5b** was $Cs^+ > K^+ > Na^+ >> Li^+$. Electrochemical studies using cyclic voltammetry and square wave voltammetry showed significant changing of voltammograms of **5a**, **5b** and **5c** upon addition of alkali cations. Shifts of voltammograms signified the effect of hard-soft acid of alkali cations upon changing of electrochemical properties of the 3 ligands.

Department…….. Student's signature…….

Field of study……... Advisor's signature……

Academic year…….

Acknowledgement

I am grateful to my thesis advisor, Assist. Prof. Dr. Thawatchai Tuntulani for his suggestions, assistance, encouragement and personal friendship throughout my master degree career. I would like to thank Assoc. Prof. Dr. Sophon Roengsumran, Assist. Prof. Dr. Nuanphun Chantarasiri and Assist. Prof. Dr. Nongnuj Muangsin for their valuable suggestions and comments as committee members and thesis examiners.

This thesis cannot be completed without kindness and helps of many people. First, I am grateful to the Chulabhorn Research Institute particularly Assoc. Prof. Dr. Somsak Rujirawat for allowing me to use a 200 MHz NMR spectrometer and a FAB Mass spectrometer. I wish to thank Scientific and Technological Research Equipment Center of Chulalongkorn University, particularly Miss Amporn Aengpakornkaew for elemental analysis results. I wish to thank all former and present staffs in Supramolecular Chemistry Laboratory, especially Miss Boosayarat Tomapatanaget, Miss Gamolwan Tumcharern, Mr. Pan Tongraung and Mr. Kriengkamol Tantrakarn for idea and solving many problems arised in my experiments.

Furthermore, I would like to thank the Electroanalytical Chemistry Research Group at Chulalongkorn University headed by Assist. Prof. Dr. Orawon Chailapakul for allowing me to use a potentiostat for cyclic and square wave voltammetry experiments and for many useful comments. In addition, I would like to thank the Thailand Research Fund, the Graduate School of Chulalongkorn University and the Department of Chemistry for financial supports.

Finally, I would like to express my deepest gratitude to my family, especially my father and my mother for their kindness, encouragement, financial support and other assistance throughout my life.

CONTENTS

CONTENTS (continued)

CONTENTS (continued)

CONTENTS (continued)

LIST OF FIGURES

LIST OF FIGURES (Continued)

LIST OF FIGURES (Continued)

LIST OF TABLES

LIST OF ABBREVIATIONS AND SYMBOLS

DMAP	4-(*N*,*N*′-dimethyl amino)pyridine
δ	Chemical shift
J	Coupling constant
CV	Cyclic voltammetry
SWV	Square wave voltammetry
^{o}C	Degree Celsius
K	Kelvin
Equiv.	Equivalent
g	Gram
Hz	Hertz
mp	Melting point
Ms	Methane sulfonyl group
mmol	Millimol
mL	Mililiter
M	Molar
ppm	Part per million
psi	Pound per square inch
^{1}H-NMR	Proton nuclear magnetic resonance
^{13}C-NMR	Carbon nuclear magnetic resonance
s, d, t, m	Splitting patterns of ^{1}H-NMR (singlet, doublet, triplet and multiplet)
THF	Tetrahydrofuran

CHAPTER 1

INTRODUCTION

Electrochemical sensor is perhaps the most important application of electrochemistry in the field of supramolecular chemistry. This concept, whose use has been widespread in the past two decades, has been exploited to such an extent that a through examination of its use is well beyond the scope. The early focus of this concept in supramolecular research was primarily cation recognition. During the 1980's much interest centered on redox-switchable cation binding systems as potential mimics of biological cation transport or the emphasis has broadened to include anion and molecular recognition. Without a doubt however, the predominant interest in this field has shifted toward the development of sensored molecular devices.[1]

1.1 The Concept of Electrochemical Sensor

The IUPAC Commission on General Aspects of Analytical Chemistry has defined chemical sensors as follows.

'*A chemical sensor is a device that transforms chemical information, ranging from the concentration of a specific sample component to total composition analysis, into a useful analytical signal*'

On the basis of this definition the whole device is the sensor, for without immobilisation of the host and transduction of the interaction, it would not be possible to convert the host-guest interaction into a useful analytical signal. The physical immobilisation of the selective agent, and the transduction process have distinct effects on the performance of a sensing device, espescially in relation to selectivity, sensitivity and response time.[2] However, excellent chemical sensors that possess highly selective complexation properties and highly response time require

1. Size of the receptor should be complementary with the size of the ion to be complexed.
2. The receptor should be closed to the reporter group (signalling group) to enhance signals.[3]

Cation recognition is undoubtedly the most studied and best developed application of calixarenes in sensing devices. Molecules such as derivatives of calix[4]arene in its *cone* conformation with, for example, ester [4], ether [5], ketone [6], carboxylic acid [7], amide [8], crown ether [9], and hemispherand [10] substituents, have been extensively studied over the years.

1.2 Calix[4]arene

Condensations of *p*-substituted phenols with formaldehyde under base-catalyzed condition afford a new class of oligophenolic macrocyclic compounds called calixarenes (in Greek, calix means *chalice* or Eucharistic cup). Calixarenes are defined as [1_n] metacyclophanes comprising phenol units liked by methylene bridges.[11-13] Most common calixarenes have a number of phenol groups either 4, 6 or 8 while odd-number ring calixarenes are less studied due to the difficulty of their syntheses. Rotation of phenol units around methylene carbons causes many conformational isomers that give a great number of cavities with different size and shape.[14] Since synthetic methods were reported by Gutsche[15-16] , Calixarenes have become one of the most attractive building blocks in supramolecular chemistry. They can be modified to gain numerous types of molecular receptors by many chemical reactions. The modification can be introduced at oxygen atoms (that called 'lower rim or narrow rim'), methylene bridge carbon or *para* position of aromatic rings (which named 'upper rim or wide rim').[12,17-19] Among the calixarene family, calix[4]arene is the smallest member and served as the most popular building block in syntheses of new compound which have high selectivity towards ionic and neutral molecules. It is known that unmodified calix[4]arene exists in 'cone' conformation due to its strong intramolecular hydrogen bonding. However, chemically modified calix[4]arene can adopt other conformations as 'partial cone', '1,2-alternate' and '1,3-alternate'. All four conformation of calix[4]arene can be immobilized in only one of them by different reaction condition. Determination of conformational differences

should be deduced from ^{1}H-NMR spectra because each isomer has its unique methylene proton signals pattern.[20-21]

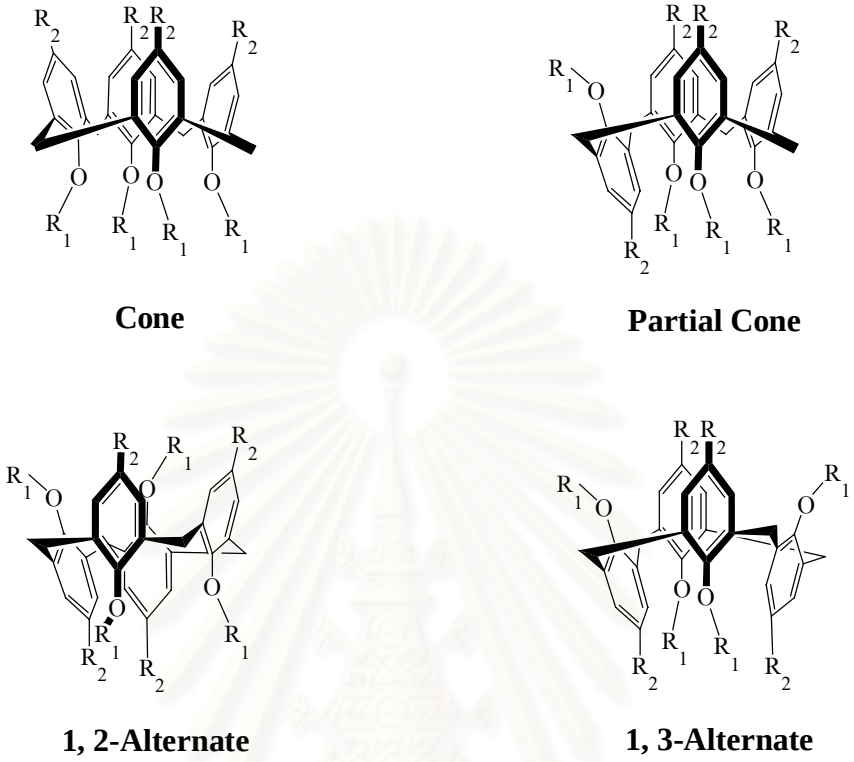

Figure 1.1: Conformational isomers of calix[4]arene

1.3 Double calix[4]arenes

Calix[4]arene are easily (and often selectively) functionalized and therefore they can be combined in various ways to larger molecules containing more than one calixarene substructure. Their connection can be separated into three types, the first type is connected via the narrow rim (also called tail-to-tail), the second type is connected via the wide rim (also called head-to-head) and the last is connected via the narrow and the wide rim (also called tail-to-head). Some examples of each type are shown in Figure 1.2. Moreover, double calix[4]arenes can be separated by the connection into three types, first is connected via single bridge, second is connected via double bridge and the last is connected via more than two bridges.

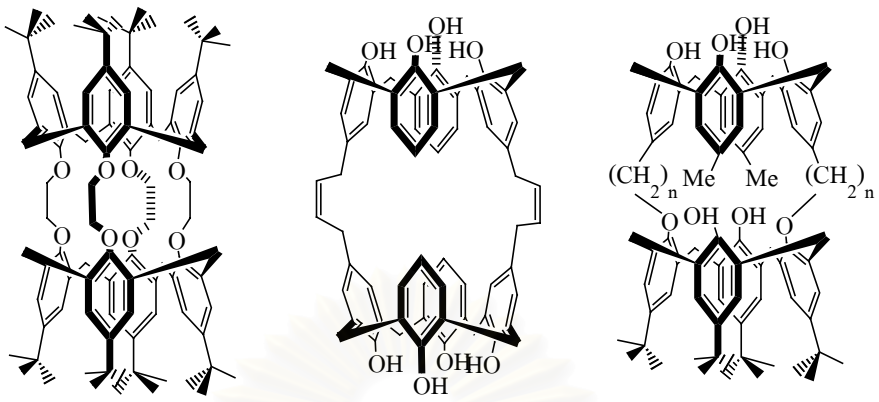

1 **2** **3**

tail-to-tail **head-to-head** **tail-to-head**

Figure 1.2: Example of double calix[4]arene, connected via double bridge

A rather rigid double calix[4]arene (calix[4]tube) **1** connecting by four ethylene bridges was obtained in 51% yield by the reaction of the tetrakis(tosyloxyethoxy)-*p-tert*-butylcalix[4]arene with *p-tert*-butylcalix[4]arene in the presence of K_2CO_3.[22] Obviously the K^+-ion acts as a template, since **1** is a selective ligand for K^+, forming kinetically and thermodynamically stable complexes, in which the K^+ is coordinated by the eight oxygens in a cubic fashion. Molecular mechanic simulations suggest that complexation occurs via a two-stage mechanism in which the intermediate involves an intracavity K^+-π complex (Figure 1.3). This is of interest as a model system for a K^+ transport by gated ion channels

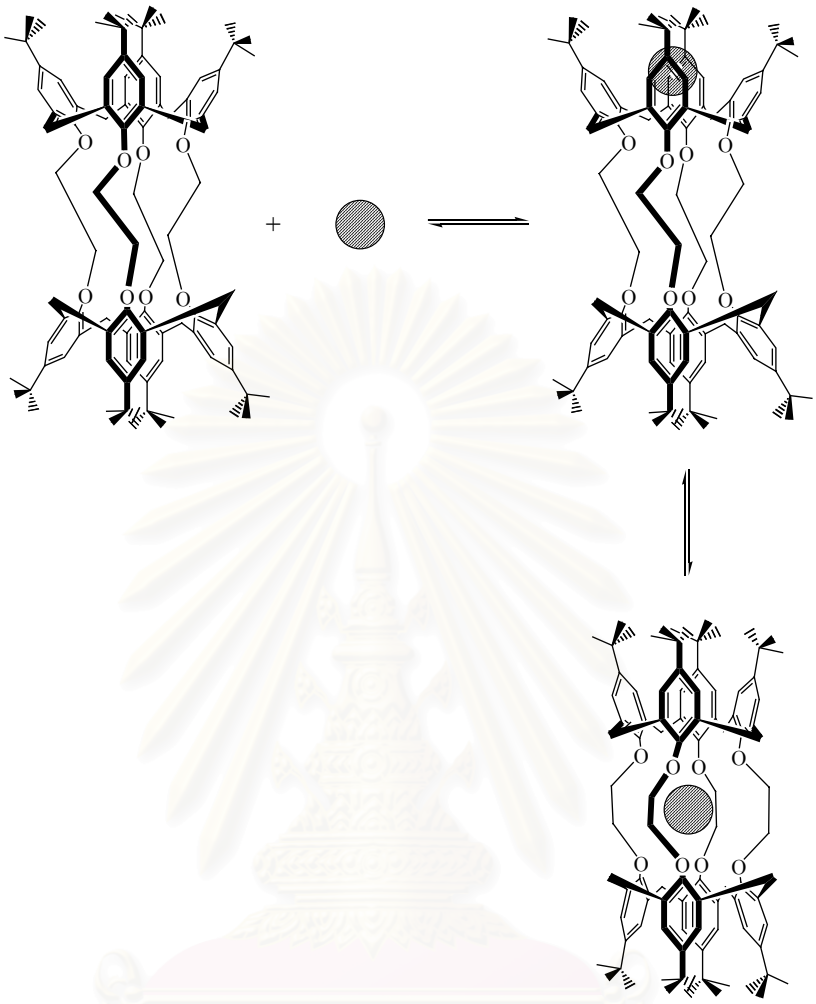

Figure 1.3: Potassium ion complexation by double calix[4]arene **1** cage host

With the larger biscalix[4]arene **4** which has two metal complexing site.[23] , two dynamic processes are observed. The intermolecular association/dissociation equilibrium in which the complex equilibrates with the uncomplexed ligand and free metal cation is slow on the NMR time scale. The complex also exhibits a faster intramolecular exchange of the metal cation such as Na^+ or K^+ from one binding site to another (Figure 1.4).

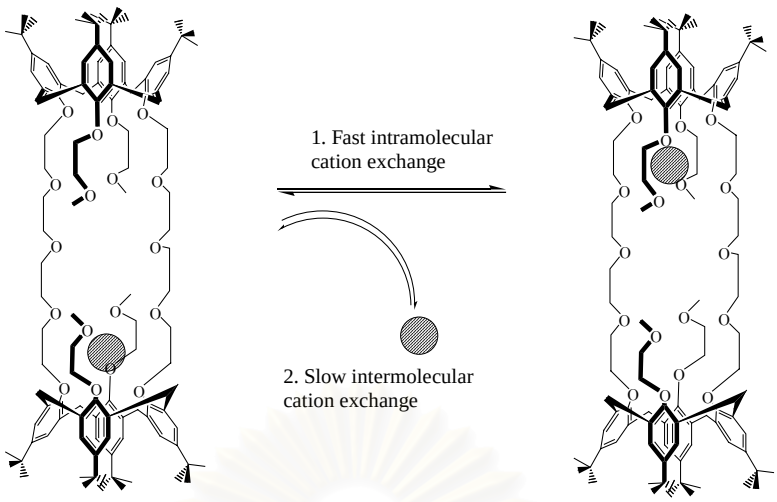

Figure 1.4: Intra- and intermolecular metal exchange processes in biscalix[4]arene **4**

1.4 Calix[4]arenequinone based Electrochemical sensor

The reaction of calix[4]arenes with strong oxidizing agents may afford derivatives in which one or several phenolic moieties have been oxidized to quinone groups ('calix-quinones').[24-25] The selective oxidation of some of the phenol rings of a calix[4]arene can be achieved by protection of one or more of the phenolic OH groups by etherification or esterification prior to the oxidation step.Using this strategy calix[4]arene with one, two or three quinone groups and four groups **5-8** have been prepared[26] (Figure 1.5) Tl-$(CF_3COO)_3$ is the reagent most commonly used for oxidation.[27]

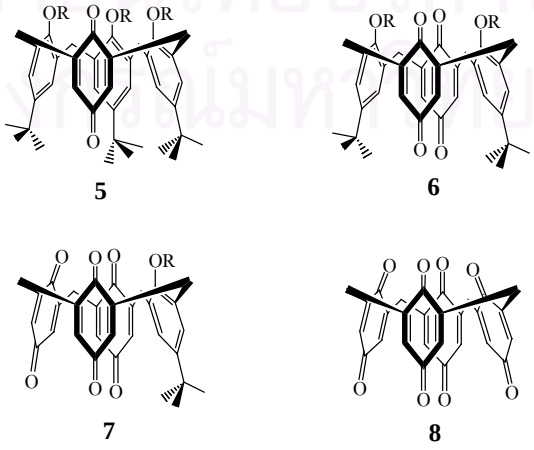

Figure 1.5: A series of calix[4]arenequinones

In recent years, the most popular signaling unit used by chemists are ferrocene and quinone.[1] An increasing interest in the synthesis of redox-active calixarenes has centered on the appropriate functionalization of phenol units since the possibility of calixarenes as enzyme mimics was suggested.[11] Calix[4]arenequinone compounds have espescially attracted chemist's attention because of their selectivity toward certain cations and electrochemical properties.[28-29] The study on the effect of electron transfer processes in spatially constrained syntems with multiple redox units of quinone made calix[4] arenequinone one of the molecular devices in redox switching studies.

Some examples of calix[4]arenequinone are shown in Figure 1.6. The tertiary amide substituents **9** have been synthesized by treatment of the respective 1,3-bis-substituted *p-tert*-butylcalix[4]arene with $Tl(OCOCF_3)_3$ in trifluoroacetic acid.[30] The electrochemical properties and its complexes have been studied using cyclic and square wave voltammetric techniques. The result showed that addition of 1 equiv. or more of sodium perchlorate or potassium hexafluorophosphate to electrochemical solutions of **5** resulted in the disappearance of waves 1 and 2 and the evolution of reversible new wave couples at more anodic potentials.(Figure 1.6)

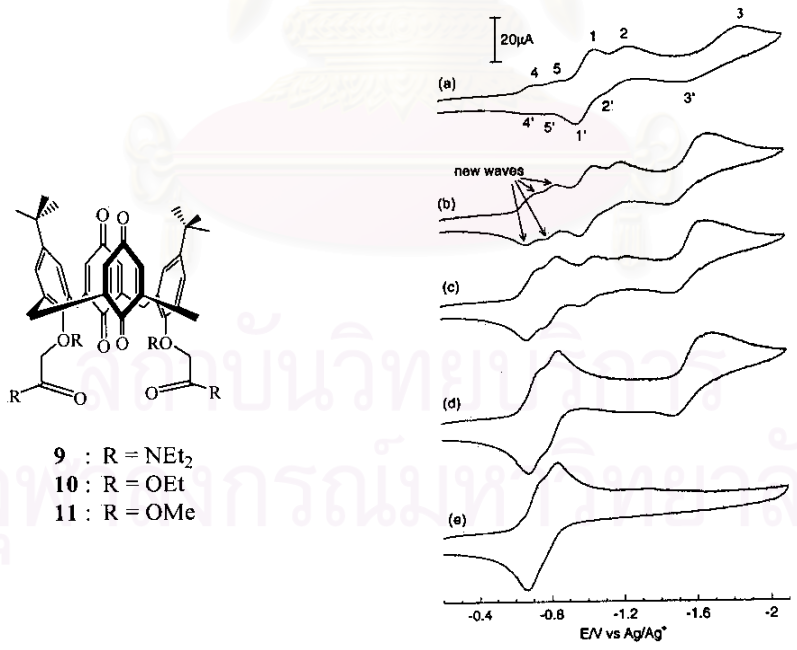

9 : R = NEt_2
10 : R = OEt
11 : R = OMe

Figure 1.6: Cyclic voltammogram of **9** ($1.17x10^{-3}$M) in a 1/1 mixture of CH_3CN and CH_2Cl_2 in the presence of different concentrations (equiv.) of sodium cations (a) 0 ; (b) 0.21 ; (c) 0.42 ; (d) 0.63 ; (e) 2.7. Scan rate : 100 mV/s

The electrochemical properties of calix[4]arenediquinone **10** and **11** have been studied.[31] Figure 1.7a and 1.7b showed voltammetric responses of variously charged metal ions. ΔE_p value of the compound **10** and **11** after complexation with a series of metal ions exhibits the trend $La^{3+} > Mg^{2+} > Ca^{2+} > Li^{+} > Na^{+} > K^{+}$.

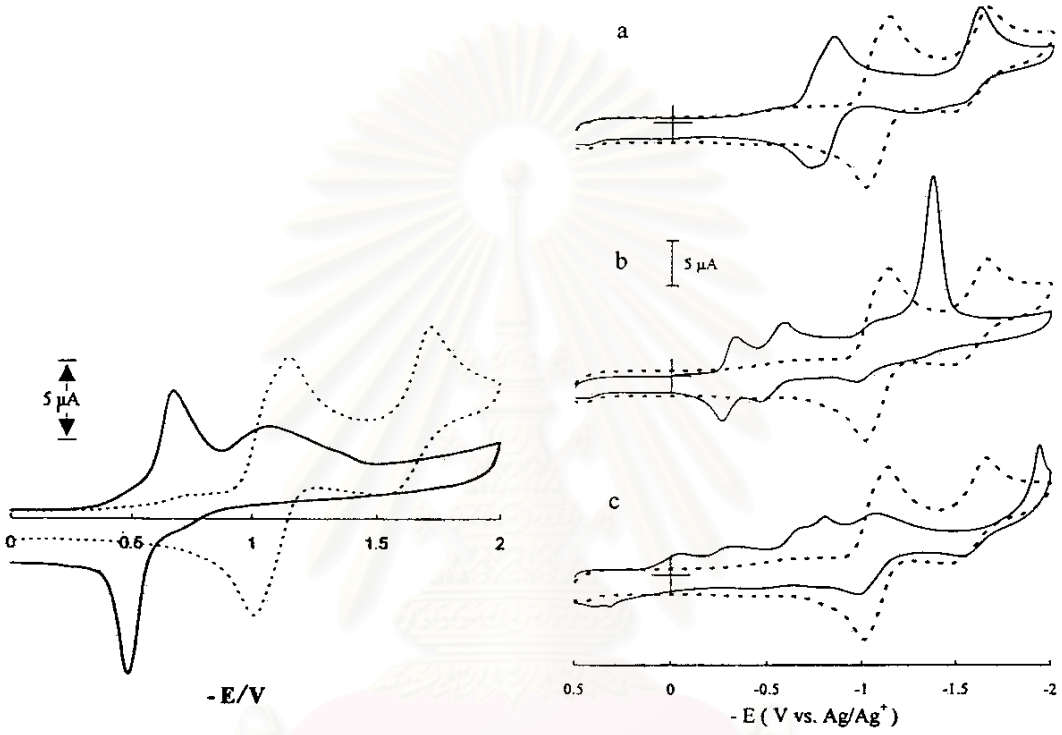

A **B**

Figure 1.7: A. Cyclic voltammogram of 0.5 mM compound **10** in the absence (-------) and presence (____) of one equiv. of Li^{+}

B. Cyclic voltammogram of 0.5 mM compound **11** in the absence (-------) and presence (____) of one equiv. of (a) Li^{+}, (b) Ca^{2+} and (c) La^{3+}

1.5 Double calix[4]arenequinone based Electrochemical sensor

A few studies of double calix[4]arenequiones has been reported. In 1996 double calix[4]arenes bridged with bpy (2,2′-bipyridine) subunits **12** (Figure 1.8) has been synthesized.[32] Spectroscopic titrations have shown that **12** form more stable complexes with K^+ with association constant of $0.8x10^5$ than with NH_4^+ $0.7x10^4$. Cyclic Voltammetry of **12** with K^+ showed the first reduction wave shifted to more positive potentials by the addition of K^+ (Figure 1.8). The addition of one equivalent of metal cation caused a potential shift to a more positive direction by 200 mV (Figure 1.8, curve (C)). Further addition of K^+ produced no change. Thus, K^+ was considered to form a 1:1 complex with **12**.

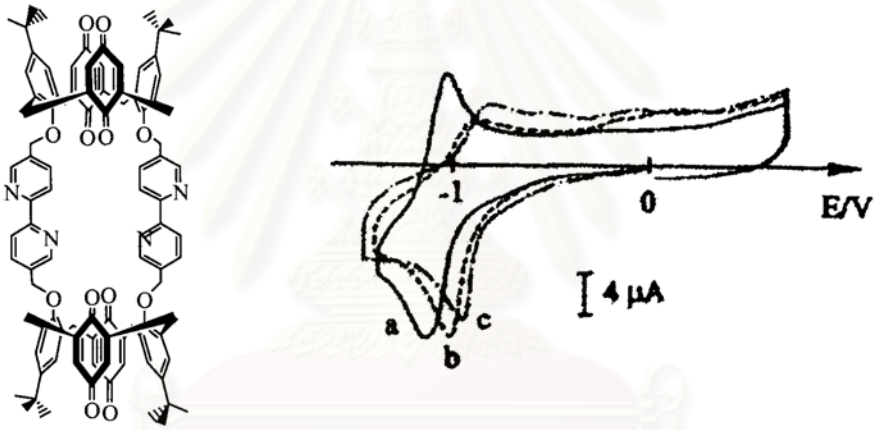

12

Figure 1.8: Cyclic voltammograms for 0.2 mM of compound **12** in CH_3CN, the absence of K^+ (curve (a), ___), and in the presence of 0.4 equiv. of K^+ (curve (b), -----) and one equiv. of K^+ (curve (c), ._._.)

In 2001 Beer synthesized novel bis(calix[4]diquinone) receptors **13**, **14** and **15** from *p-tert*-butylcalix[4]arene in acetonitrile with propane-1,3-ditosylate, 1,4-dibrobutane and 1,5-dibromopentane, respectively in the presence of potassium carbonate and then oxidized with $Tl(OCOCF_3)_3$ in trifluoroacetic acid (Figure 1.9).[33] Receptors **13** and **14** display a high selectivity for Rb^+ ($K = 6.3x10^4$) and Cs^+($K = 1.6x10^3$), respectively. The electrochemical properties of **13** and **14** with group I metal ions were studied by cyclic voltammetry (CV) and square-wave voltammetry (SWV, Figure 1.9) Both receptors exhibited essentially two broad redox waves, which implied a multielectron transfer. The two redox waves corresponded to a quasi-reversible reduction and an irreversible redox process which occurred at a more cathodic potential. The addition of Group I metal cations to electrochemical solutions of **13** and **14** led in all cases to the evolution of two new redox waves at potentials that were substantially positively shifted.

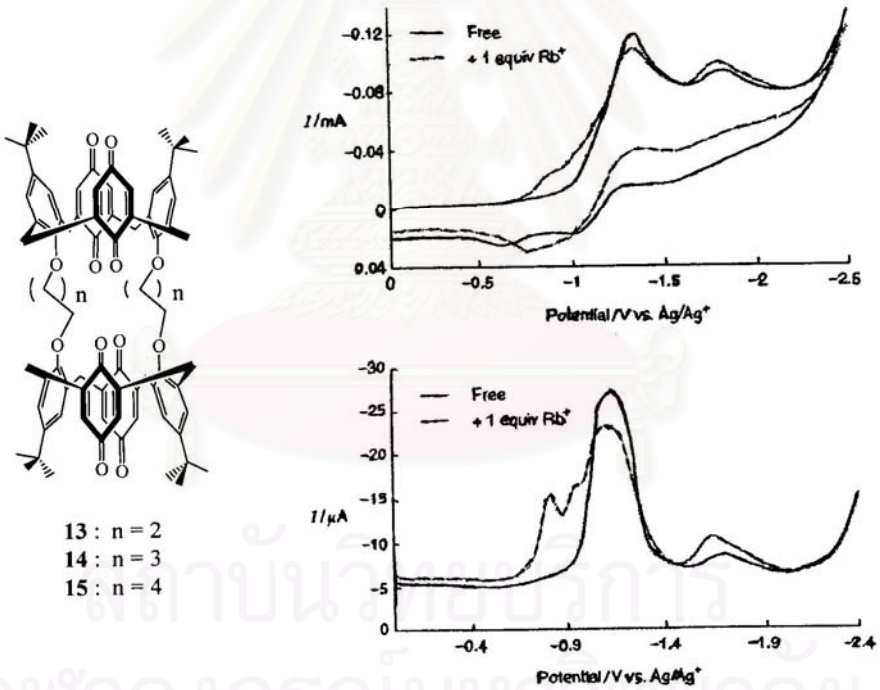

Figure 1.9: Cyclic voltammogram (top) and square wave voltammogram (bottom) of **13** + 1.0 equiv. of Rb^+ in CH_2Cl_2 : CH_3CN (4:1)

1.6 Cyclic Voltammetry

Cyclic voltammetry is the most widely use technique for acquiring qualitative information about electrochemical reactions. The power of cyclic voltammetry results from its ability to rapidly provide considerable information on the thermodynamics of redox processes and the kinetics of heterogeneous electron transfer reactions, and on coupled chemical reactions or adsorption processes. Cyclic voltammetry is often the first experiment performed in an electroanalytical study. In particular, it offers a rapid location of redox potentials of the electroactive species, and convenient evaluation of the effect of media upon the redox process.[34]

Rapid-voltage-scan technique in which the direction of voltage scan is reversed are called cyclic technique. In these technique, a ramp is applied over the full voltage-scan range and then reversed so that a descending ramp returns, almost invariably to the original potential. The scan rate in the forward and reverse directions is normally the same, so that the excitation waveform is actually an isosceles triangle. (Figure 1.10) Cyclic voltammetry can be used in single-cycle (Figure 1.11) or in multicycle modes, depending upon the electrode, the reaction in question, and the information sought. In most cases the first and later scans are not identical.[35]

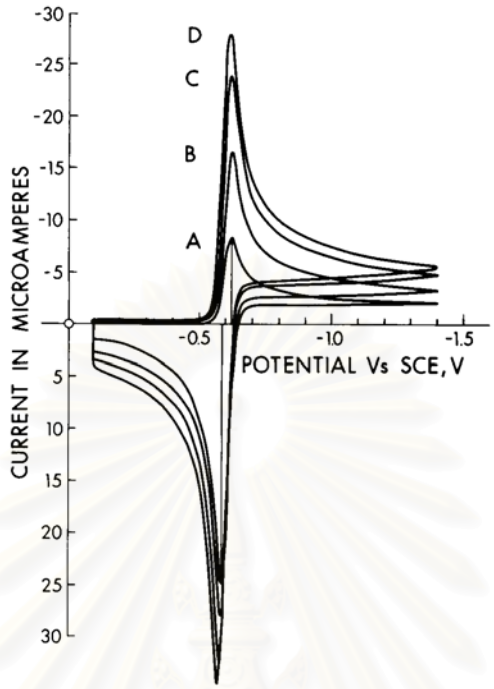

Figure 1.10: Cyclic voltammetry of a reversible process. Aqueous solution, 1.0 mol/m^3 Cd(II) in 100 mol/m^3 KCl, HMDE. Curve A, 20 mV/s; curve B, 50 mV/s; curve C, 100 mV/s; curve D, 200 mV/s. Initial scan cathodic

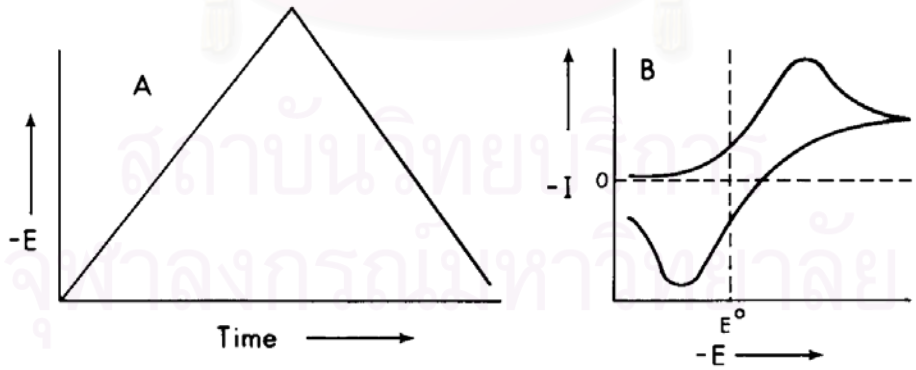

Figure 1.11: Cyclic voltammetry. (A) Excitation signal; (B) response is obtained for a single reversible reduction when the voltage-time excitation signal extends considerably on both sides of the E^o for the reversible process.

The important parameters of a cyclic voltammogram are: anodic peak current (i_{pa}) and anodic peak potential (E_{pa}) taken from the peak position of anodic current and the respective parameters i_{pc} and E_{pc} from the peak position of cathodic current. If the redox couple is reversible the half-wave potential is centered between E_{pa} and E_{pc}.

$$E_{1/2} = (E_{pa} + E_{pc}) / 2$$

Frequently $E_{1/2}$ calculated in this way is considered simply as the formal potential because the diffusion coefficients have a small effect. The difference between peak potentials is related with the number of electrons transferred in the electrode reaction.[36]

$$\Delta E_p = E_{pa} - E_{pc} = 0.059 / n$$

Electrochemical 'reversibility' means that the electrode reaction is fast enough to maintain the surface concentrations of the oxidized and reduced forms at equilibrium with each other, which is an indispensable condition for the validity of the Nernst equation.

1.7 Square Wave Voltammetry

Square wave voltammetry is a large-amplitude differential technique in which a waveform composed of a symmetrical square wave, superimposed on a base staircase potential, is applied to the working electrode (Figure 1.12). The current is sampled twice during each square-wave cycle, once at the end of the forward pulse and once at the end of the reverse pulse. Since the square wave modulation amplitude is very large, the reverse pulses cause the reverse reaction of the product (of the forward pulse). The difference between the two measurements is plotted vs. the base staircase potential. A dimensionless plot of the theoretical forward, reverse, and difference currents is given in Figure 1.13 for a rapid reversible redox system. The resulting peak-shaped voltammogram is symmetrical about the half-wave potential, and the peak current is proportional to the concentration.[34]

The major advantage of square wave voltammetry is its speed. The effective scan rate is given by $f\Delta E_s$. The term f is square wave frequency (in Hz), and ΔE_s is the step height. Frequencies of 1 to 100 cycles per second permit the use of extremely fast potential scan rates. As a result, the analysis time is drastically reduced; a complete voltammogram can be recorded within a few seconds, as compared with about 2-3 minutes in differential-pulse voltammetry.

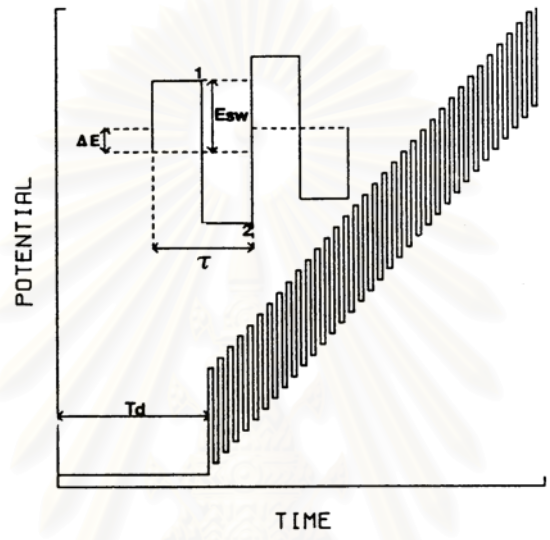

Figure 1.12: Square wave waveform showing the amplitude, E_{sw} : step height, ΔE : square wave period, τ : delay time : T_d, and current measurement times, 1 and 2.

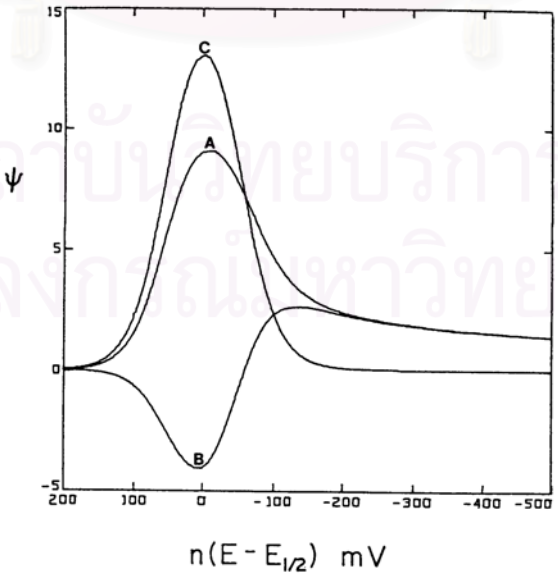

Figure 1.13: Square wave voltammogram for reversible electron transfer : (A) forward current; (B) reverse current; (C) net current. ψ is a dimensionless current function.

1.8 Objective of the Thesis

The main goals of this research are to synthesize double calix[4]arenequinone **5a**, **5b**, **5c** (Figure 1.14) by combining the lower-rim cation binding properties of calixarenes with ethylene glycol linkages similar to those found in crown ethers. Compounds **5a**, **5b** and **5c** are in cone conformation and provide oxygen donor atoms from glycol linkages that served to bind cation *via* ion-dipole interactions. The complexation studied of these compounds with alkaline cations such as Li^+, Na^+, K^+, Cs^+ are also studied by means of ^{1}H-NMR titrations. Results of this research should give information about their binding abilities toward alkaline cations. The effect of size and shape of host molecules to metal ion recognition will also be obtained.

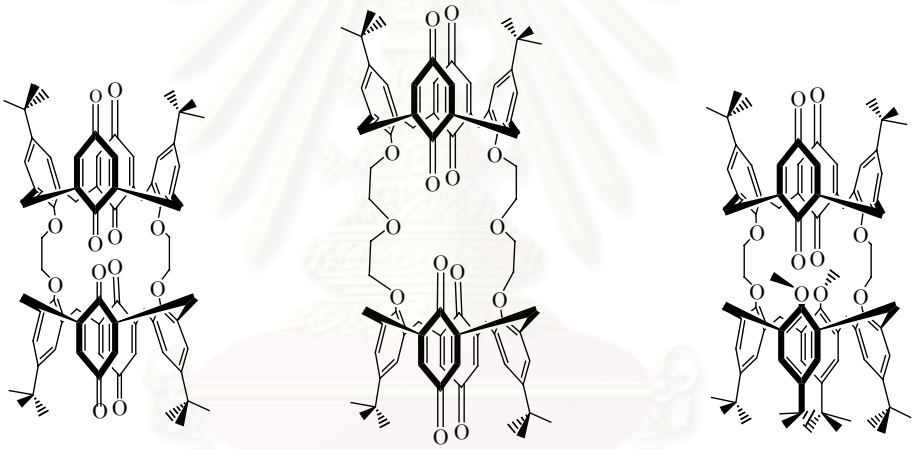

5a **5b** **5c**

Figure 1.14: Structures of double calix[4]arenequinone **5a**, **5b**, **5c**

Another aim of this work is to investigate the redox chemistry of double calix[4] arenequinones **5a**, **5b**, **5c** in non-aqueous solution in the absence and in the presence of alkaline cations by cyclic voltammetry and square wave voltammetry and at last, to explore the possibility to use them as alkali metal ion sensors.

CHAPTER 2

EXPERIMENTAL SECTION

2.1 General Procedures

2.1.1 Analytical Instruments

Nuclear Magnetic Resonance (NMR) spectra were recorded on a Varian 200, 400 and a Brucker ACF 200 MHz nuclear magnetic resonance spectrometers. In all cases, samples were dissolved in deuterated chloroform and chemical shifts were recorded in part per million (ppm) using a residual proton or carbon signals in deuterated solvents as internal reference. Elemental analysis were carried out on a CHNS/O analyzer (Perkin Elmer PE2400 series II). ESI and FAB Mass spectra were recorded on a Bruker Mass spectrometer and a GCQ Finigan Mass spectrometer. Infrared spectra were obtained on a Nicolet Impact 410 using KBr pellet. All melting points were obtained on an Electrothermal 9100 apparatus and uncorrected.

2.1.2 Materials

All materials were standard analytical grade, purchased from Fluka, Aldrich, BHD, Carlo Erba, Merck or J.T. Baker and used without further purification. Commercial grade solvents such as acetone, hexane, dichloromethane, methanol and ethyl acetate were distilled before used. Acetonitrile was dried over CaH_2 and freshly distilled under nitrogen prior to use. THF was dried with Na in benzophenone under nitrogen atmosphere and distrilled before used.

Column chromatography was carried out using silica gel (Kieselgel 60, 0.063-0.200 mm, Merck). Thin layer chromatography (TLC) was performed on silica gel plates (Kieselgel 60 F_{254}, 1 mm, Merck).

Starting materials such as *p-tert*-butylcalix[4]arene were prepared according to the literature procedure.[37] . Synthesis of compound **1**, **3a**, **3b**, **3c** and **3d** was adapted from the literature procedure.[38-39] All compounds were characterized by ^{1}H-NMR spectroscopy, ^{13}C-NMR spectroscopy, mass spectrometry and elemental analysis.

2.2 Synthesis

2.2.1 Preparation of 25,27-di(ethyleneglycol)-bis-*p-tert*-butylcalix[4]arene (1)

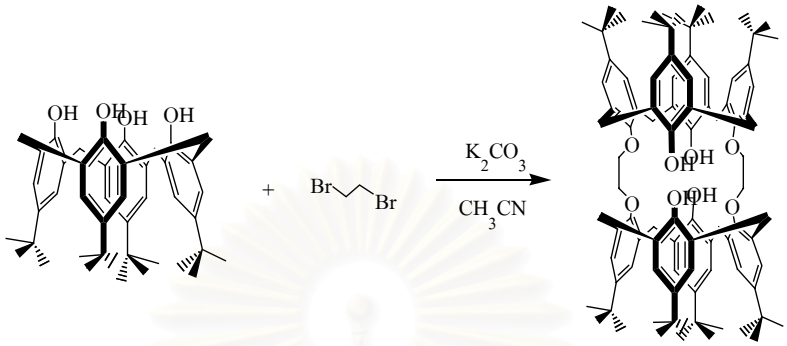

1

In a 100 mL two-necked round bottom flask, *p-tert*-butylcalix[4]arene (3.24 g, 5 mmol) and potassium carbonate (0.69 g, 5 mmol) were suspended in dried acetonitrile (50 mL). After the mixture was stirred for 30 minutes, 1,2-dibromoethane (5 mL, 58 mmol) was then added. The mixture was stirred overnight and heated at 70 ^{o}C under nitrogen atmosphere. The solution was allowed to cool to room temperature and evaporated to dryness under reduced pressure. The residue was dissolved in dichloromethane (50 mL) and stirred with an aqueous solution of 3 M hydrochloric acid (50 mL) for 30 minutes and then extracted with dichloromethane (2x50 mL). The organic layer was dried over anhydrous sodium sulfate, filtered and evaporated to dryness. The residue was dissolved in a minimum amount of dichloromethane and methanol was added to precipitate a white crystalline solid (0.42 g, 12% yield). The product was dried in *vacuo* and kept in a desiccator.

Characterization data for Preparation of 25,27-di(ethyleneglycol)-bis-*p-tert*-butylcalix[4]arene (1)

mp. > 300 ^{o}C (decompose)

^{1}H-NMR spectrum ($CDCl_3$, 200 MHz) : δ (in ppm) 7.65 (s, 4H, O<u>H</u>), 7.00 (s, 8H, *m*-<u>H</u>ArOH), 6.82 (s, 8H, *m*-<u>H</u>ArOCH$_2$CH$_2$OAr<u>H</u>), 4.55 (s, 8H, ArOC<u>H$_2$</u>C<u>H$_2$</u>OAr), 3.35,

4.50 (dd, *J* = 14.0 Hz, 16H, ArC<u>H</u>$_2$Ar), 1.25 (s, 36H, HOAr-*t*-C$_4$<u>H</u>$_9$), 0.99 (s, 36H, *t*-C$_4$<u>H</u>$_9$-ArOH)

^{13}C-NMR spectrum ($CDCl_3$, 50 MHz) : δ (in ppm) 151.16, 150.42, 147.08, 141.27, 132.34, 127.78, 127.70, 125.54, 124.62, 75.88, 33.74, 33.48, 32.13, 31.26, 30.73

FAB mass (m/z) : 1367.8 [$M^+ + NH_4^+$]

Elemental analysis : Calculate ($C_{92}H_{116}O_8$) C, 81.86 ; H, 8.66
Found C, 81.86 ; H, 8.86

2.2.2 Preparation of diethyleneglycol ditosylate (2a)

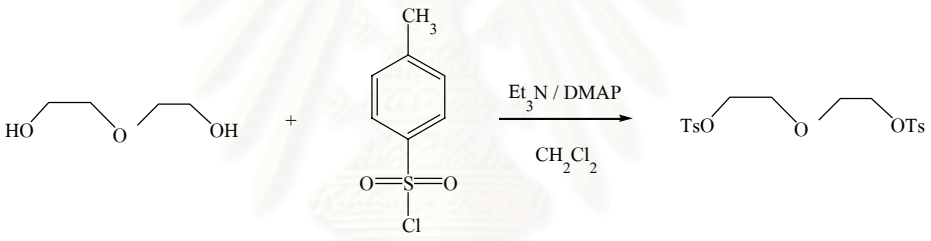

2a

In a 250 mL two-necked round bottom flask, a dichloromethane solution (50 mL) of diethyleneglycol (3 g, 28.28 mmol), triethylamine (11.76 mL, 84.84 mmol) and a catalytic amount of DMAP was chilled to 10 ^{o}C with an ice bath and stirred under nitrogen for 30 minutes. The solution of tosylchloride (11.86 g, 62.22 mmol) in dichloromethane (100 mL) was then added dropwise. The reaction mixture was allowed to stir overnight at room temperature under nitrogen. After the reaction was completed, the mixture was then poured into an aqueous solution of 3 M hydrochloric acid (100 mL) and stirred for 30 minutes and then extracted with dichloromethane (2x50 mL). The organic layer was dried over anhydrous sodium sulfate, filtered and evaporated to dryness. The residue was dissolved in a minimum amount of dichloromethane and methanol was added to precipitate a white crystalline solid (7.66 g, 65% yield). The product was dried in *vacuo* and kept in a desiccator.

Characterization data for Preparation of diethyleneglycol ditosylate (2a)

^{1}H-NMR spectrum ($CDCl_3$, 200 MHz) : δ (in ppm) 7.76 (d, *J* = 8.3 Hz, 4H, Ar<u>H</u>), 7.33 (d, *J* = 8.3 Hz, 4H, Ar<u>H</u>), 4.07 (t, J = 4.6 Hz, 4H, TsOC<u>H</u>$_2$CH$_2$), 3.59 (t, *J* = 4.8 Hz, 4H, CH$_2$C<u>H</u>$_2$OH), 2.43 (s, 6H, ArC<u>H</u>$_3$)

2.2.3 Preparation of 25,27-di(diethyleneglycol)-bis-*p-tert*-butylcalix[4]arene (2b)

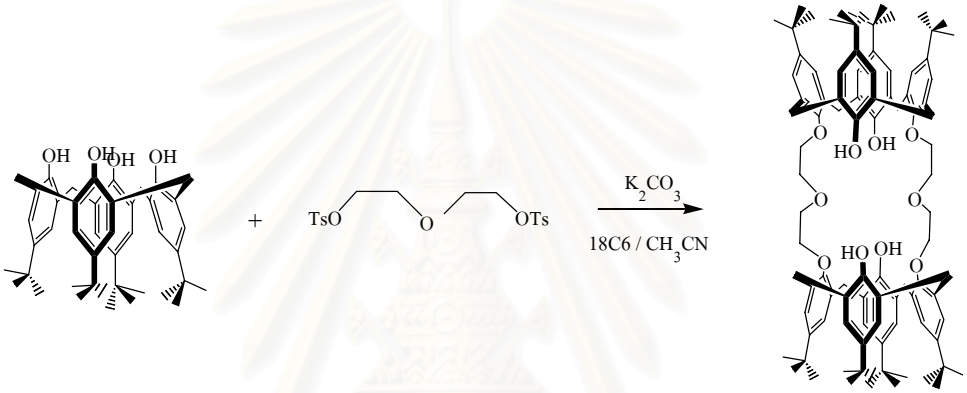

2a **2b**

In a high pressure tube equipped with valves and a pressure gauge, *p-tert*-butylcalix [4]arene (3 g, 4.62 mmol), diethyleneglycol ditosylate, **2a** (1.91 g, 4.62 mmol), catalytic amount of 18-crown-6 and potassium carbonate (1.28 g, 9.24 mmol) were suspened in dried acetonitrile (10 mL). The tube was then pressurized with N_2 at 50 psi. The mixture was stirred and heated at 70 ^oC for 2 days. The solution was allowed to cool to room temperature and evaporated to dryness under reduced pressure to yield a crude product. The residue was dissolved in dichloromethane (50 mL) and stirred with an aqueous solution of 3 M hydrochloric acid (2x50 mL) for 30 minutes, and then extracted with dichloromethane (2x50 mL). The organic layer was dried over anhydrous sodium sulfate, filtered and evaporated to dryness. The residue was dissolved in a minimum amount of dichloromethane and methanol was added to precipitate a white crystalline solid (0.44 g, 14% yield). The product was dried in *vacuo* and kept in a desiccator.

Characterization data for Preparation of 25,27-di(diethyleneglycol)-bis-*p-tert*-butylcalix[4]arene (2b)

mp. > 300 ^{o}C (decompose)

^{1}H-NMR spectrum ($CDCl_3$, 200 MHz) : δ (in ppm) 8.09 (s, 4H, O<u>H</u>), 7.00 (s, 8H, *m*-<u>H</u>ArOH), 6.85 (s, 8H, *m*-<u>H</u>ArOCH$_2$CH$_2$OAr<u>H</u>), 4.50-4.10 (m, 24H, ArOC<u>H$_2$</u>C<u>H$_2$</u>OAr, ArC<u>H$_2$</u>Ar), 3.18, (dd, *J* = 14.0 Hz, 8H, ArC<u>H$_2$</u>Ar), 1.25 (s, 36H, HOAr-*t*-C$_4$<u>H$_9$</u>), 1.05 (s, 36H, *t*-C$_4$<u>H$_9$</u>-ArOH)

^{13}C-NMR spectrum ($CDCl_3$, 50 MHz) : δ (in ppm) 150.49, 149.51, 147.20, 141.43, 133.45, 127.76, 125.62, 125.10 , 74.82, 70.44, 34.04, 33.78, 31.64, 31.11

FAB mass (m/z) : 1437 [$M^+ + H^+$]

Elemental analysis : Calculate ($C_{96}H_{124}O_{10}$) C, 80.18 ; H, 8.69
Found C, 80.21 ; H, 8.43

2.2.4 Preparation of 25,27-di(methoxy)-*p-tert*-butylcalix[4]arene (3a)

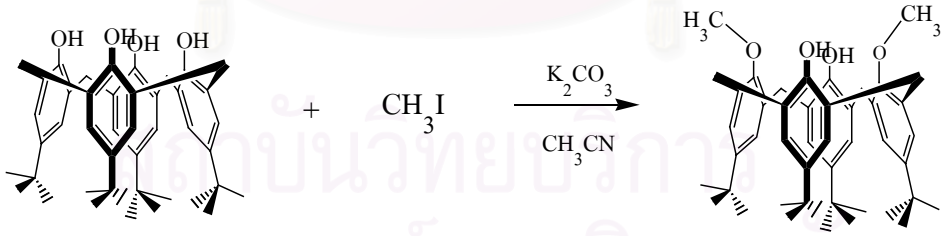

3a

In a 100 mL two-necked round bottom flask, *p-tert*-butylcalix[4]arene (5 g, 7.70 mmol) and potassium carbonate (1.60 g, 11.55 mmol) were suspended in dried acetonitrile (50 mL). The mixture was stirred at room temperature for 30 minutes. Methyl iodide (1.20 mL, 19.25 mmol) was then added by syringe. The mixture was stirred overnight and heated at 70 ^{o}C under nitrogen. The solution was allowed to cool to room temperature and evaporated to dryness under reduced pressure. The residue was dissolved

in dichloromethane (50 mL) and stirred with aqueous solution of 3 M hydrochloric acid (50 mL) for 30 minutes and then extracted with dichloromethane (2x50 mL). The organic layer was dried over anhydrous sodium sulfate, filtered and evaporated to dryness. The residue was dissolved in a minimum amount of dichloromethane and methanol was added to precipitate a white powder (4.75 g, 91% yield). The product was dried in *vacuo* and kept in a desiccator.

Characterization data for Preparation of 25,27-di(methoxy)-*p*-*tert*-butylcalix[4]arene (3a)

^{1}H-NMR spectrum ($CDCl_3$, 200 MHz) : δ (in ppm) 7.25 (s, 2H, ArO<u>H</u>), 7.08 (s, 4H, *m*-ROAr<u>H</u>), 6.77 (s, 4H, *m*-HOAr<u>H</u>), 3.94 (s, 6H, ArOC<u>H</u>$_3$), 4.25 and 3.29 (dd, *J* = 13 Hz, 8H, ArC<u>H</u>$_2$Ar), 1.30 (s, 18H, ROAr-*t*-C$_4$<u>H</u>$_9$), 0.94 (s, 18H, HOAr-*t*-C$_4$<u>H</u>$_9$)

2.2.5 Preparation of 25,27-di(carboethoxymethoxy)-*p*-*tert*-butylcalix[4]arene (3b)

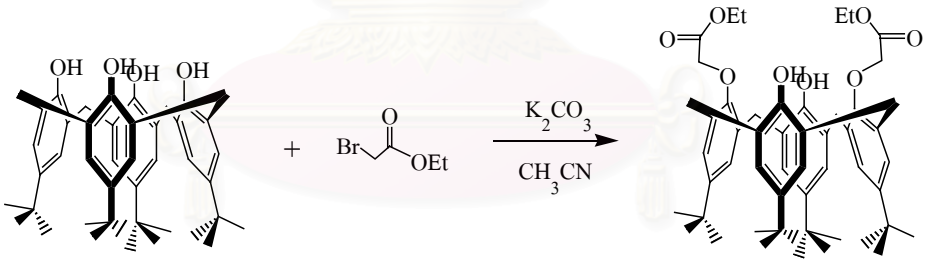

3b

In a 250 mL two-necked round bottom flask, *p*-*tert*-butylcalix[4]arene (3 g, 4.62 mmol) and potassium carbonate (1.6 g, 11.35 mmol) were suspended in dried acetonitrile (100 mL). The mixture was stirred for 30 minutes. Ethyl bromoacetate (1.03 mL, 9.24 mmol) was then added by syringe. The mixture was stirred and heated at 70 ^{o}C under nitrogen atmosphere for 4 hours. The solution was allowed to cool to room temperature and evaporated to dryness under reduced pressure. The residue was dissolved in dichloromethane (50 mL) and the saturated solution of ammonium chloride (50 mL) was subsequently added to destroy excess ethyl bromoacetate, followed by washing with

saturated sodium chloride solution (50 mL). Water (50 mL) was added and the mixture was stirred for 30 minutes and extracted with dichloromethane (2x50 mL). The organic layer was dried over anhydrous sodium sulfate, filtered and evaporated to dryness. The residue was dissolved in a minimum amount of dichloromethane and methanol was added to precipitate a white powder (2.55 g, 67% yield). The product was dried in *vacuo* and kept in a desiccator.

Characterization data for 25,27-di(carboethoxymethoxy)-*p*-*tert*-butylcalix[4]arene (3b)

^{1}H-NMR spectrum ($CDCl_3$, 200 MHz) : δ (in ppm) 7.09 (s, 2H, ArO<u>H</u>), 7.01 (s, 4H, *m*-HOAr<u>H</u>), 6.81 (s, 4H, *m*-ROAr<u>H</u>), 4.70 (s, 4H, OC<u>H</u>$_2$CO), 4.30 (q, *J* = 7.8 Hz, 4H, OC<u>H</u>$_2$CH$_3$), 3.34 and 4.40 (dd, *J* = 14.0 Hz, 8H, ArC<u>H</u>$_2$Ar), 1.30 (t, 6H, OCH$_2$C<u>H</u>$_3$), 1.24 (s, 18H, HOAr-*t*-C$_4$<u>H</u>$_9$), 0.97 (s, 18H, ROAr-*t*-C$_4$<u>H</u>$_9$)

2.2.6 Preparation of 25,27-di(2-hydroxyethoxy)-*p*-*tert*-butylcalix[4]arene (3c)

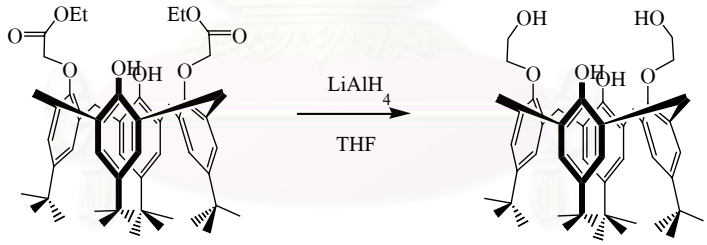

3b **3c**

In a 100 mL two-necked round bottom flask, a solution of 25,27-di (carboethoxymethoxy)-*p*-*tert*-butylcalix[4]arene (**3b**) (2 g, 2.44 mmol) in dried tetrahydrofuran (50 mL) was stirred for 10 minutes at 10 ^{o}C under nitrogen atmosphere. $LiAlH_4$ (0.4 g, 10.54 mmol) was then added gradually. The mixture was allowed to stir overnight at room temperature under nitrogen atmosphere. An aqueous solution of 3 M hydrochloric acid was subsequently added until a precipitate of lithium had formed which was then filtered. Water (30 mL) was added and stirred for 30 minutes and extracted with dichloromethane (2x30 mL). The organic layer was dried over anhydrous sodium sulfate, filtered and evaporated to dryness under reduced pressure. The residue was dissolved in a

minimum amount of dichloromethane and methanol was added to precipitate a white powder (1.58 g, 88% yield). The product was dried in *vacuo* and kept in a desiccator.

Characterization data for 25,27-di(2-hydroxyethoxy)-*p*-*tert*-butylcalix[4]arene (3c)

^{1}H-NMR spectrum ($CDCl_3$, 200 MHz) : δ (in ppm) 9.23 (s, 2H, ArO<u>H</u>), 7.07 (s, 4H, *m*-<u>H</u>OArH), 7.01 (s, 4H, *m*-ROAr<u>H</u>), 5.25 (s, 2H, CH_2O<u>H</u>), 4.25 (t, 8H, ArOC<u>H</u>$_2$C<u>H</u>$_2$OH), 4.30 and 3.43 (dd, *J* = 14.0 Hz, 8H, ArC<u>H</u>$_2$Ar), 1.20 (s, 18H, ROAr-*t*-C_4<u>H</u>$_9$), 1.19 (s, 18H, HOAr-*t*-C_4<u>H</u>$_9$)

2.2.7 Preparation of 25,27-di(methanesulfonyloxyethoxy)-*p*-*tert*-butylcalix[4] arene (3d)

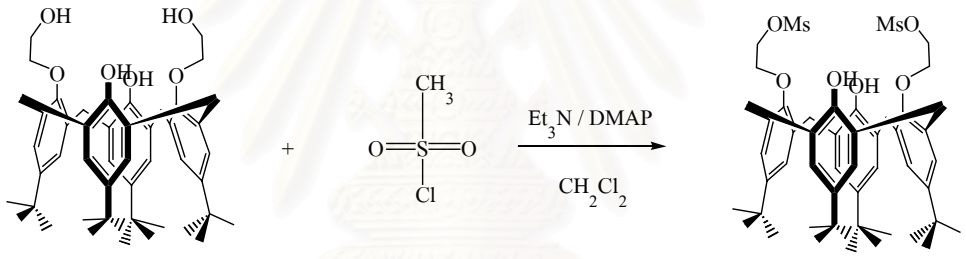

3c **3d**

In a 50 mL two-necked round bottom flask, a dichloromethane solution (30 mL) of 25,27-di(2-hydroxyethoxy)-*p*-*tert*-butylcalix[4]arene (**3c**) (0.5 g, 0.68 mmol), triethylamine (0.37 mL, 2.71 mmol) and a catalytic amount of DMAP was chilled to 10 ^{o}C with an ice bath and stirred under nitrogen for 30 minutes. MsCl (0.21 mL, 2.71 mmol) was then added by syringe. The reaction mixture was stirred at room temperature under nitrogen for 4 hours. After the reaction was completed, an aqueous solution of 3 M hydrochloric acid (30 mL) was added and stirred for 30 minutes and extracted with dichloromethane (2x30 mL). The organic layer was dried over anhydrous sodium sulfate, filtered and evaporated to dryness. The residue was dissolved in a minimum amount of dichloromethane and methanol was added to precipitate a white powder (0.54 g, 87% yield). The product was dried in *vacuo* and kept in a desiccator.

Characterization data for 25,27-di(methanesulfonyloxyethoxy)-*p-tert*-butylcalix[4] arene (3d)

^{1}H-NMR spectrum ($CDCl_3$, 200 MHz) : δ (in ppm) 7.06 (s, 4H, RAr<u>H</u>), 6.75 (s, 4H, HOAr<u>H</u>), 6.67 (s, 2H, ArO<u>H</u>), 4.64 (m, 4H, MsC<u>H</u>$_2$C<u>H</u>$_2$O), 3.36 (m, 8H, ArC<u>H</u>$_2$Ar and MsC<u>H</u>$_2$C<u>H</u>$_2$O), 4.24 (d, *J* = 13 Hz, 4H, ArC<u>H</u>$_2$Ar), 3.23 (s, 6H, $SO_2C\underline{H}_3$), 1.28 (s, 18H, HOAr-*t*-$C_4\underline{H}_9$), 0.90 (s, 18H, ROAr-*t*-$C_4\underline{H}_9$).

2.2.8 Attempt to synthesize 25,27-di(methoxy)-26,28-di(ethyleneglycol)-bis-*p-tert*-butylcalix[4]arene (3e)

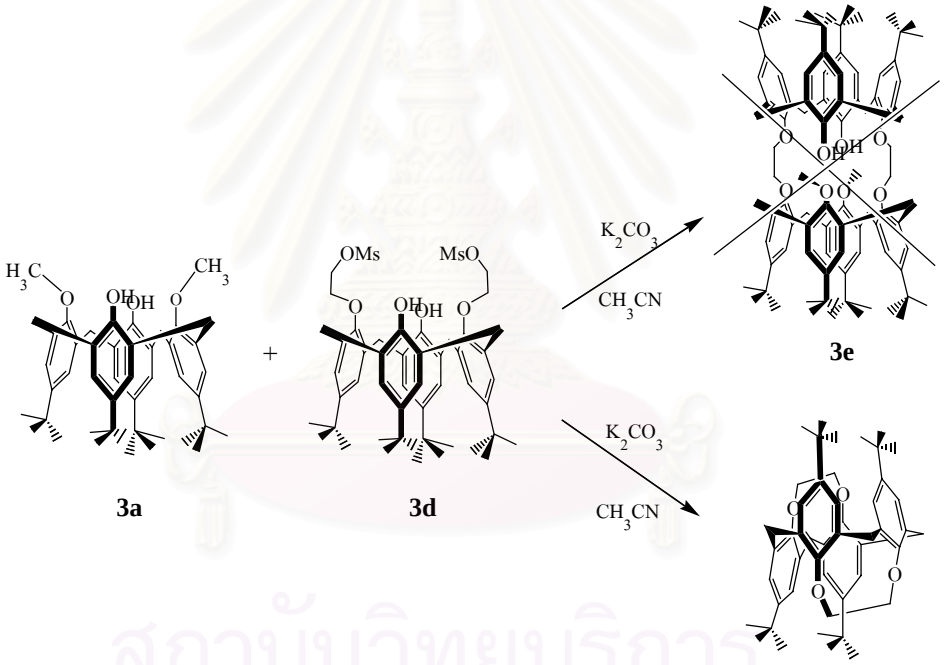

In a 100 mL two-necked round bottom flask, 25,27-di(methoxy)-*p-tert*-butylcalix [4]arene **(3a)** (0.4 g, 0.6 mmol) and potassium carbonate (0.34 g, 2.4 mmol) were suspended in dried acetonitrile (50 mL). The mixture was stirred at room temperature for 1 hour. A solution of 25,27-di(methanesulfonyloxyethoxy)-*p-tert*-butylcalix[4]arene **(3d)** (0.54 g, 0.6 mmol) in dried acetonitrile (10 mL) was then added. The mixture was stirred and heat at 70 ^{o}C under nitrogen atmosphere for 3 days. After the reaction was completed, the solution was allowed to cool to room temperature and evaporated to dryness under

reduced pressure. The residue was dissolved in dichloromethane (50 mL) and stirred with an aqueous solution of 3 M hydrochloric acid (50 mL) for 30 minutes and then extracted with dichloromethane (2x30 mL). The organic layer was dried over anhydrous sodium sulfate, filtered and evaporated to dryness. The residue was dissolved in a minimum amount of dichloromethane and methanol was added to precipitate a white crystalline solid (0.33 g, 78% yield). The product was characterized by ^{1}H-NMR and the result indicated that the desired product (**3e**) was not obtained. However, the intramolecular alkylated product (**3f**) was obtained instead.

Characterization data for (3f)

mp. > 300 ^{o}C (decompose)

^{1}H-NMR spectrum ($CDCl_3$, 400 MHz) : δ (in ppm) 7.06, 6.96 (m, 8H, RAr<u>H</u>), 4.57 (d, 2H, ArC<u>H</u>$_2$Ar axial), 4.05 (s, 4H, ArC<u>H</u>$_2$Ar), 3.58 (m, 4H, ArOC<u>H</u>$_2$-C<u>H</u>$_2$O), 3.32 (d, 2H, ArC<u>H</u>$_2$Ar equatorial), 3.14 (m, 4H, ArOC<u>H</u>$_2$-C<u>H</u>$_2$O), 1.25 (s, 36H, HOAr-*t*-C_4<u>H</u>$_9$).

^{13}C-NMR spectrum ($CDCl_3$, 50 MHz) : δ (in ppm) 153.10, 144.88, 134.73, 132.80, 125.21, 70.64, 34.19, 34.08, 31.46

FAB mass (m/z) : 701 [$M^+ + H^+$]

2.2.9 Preparation of 25,27-di(methoxy)-26,28-di(carbomethoxymethoxy)-*p-tert*-butylcalix[4]arene (4a)

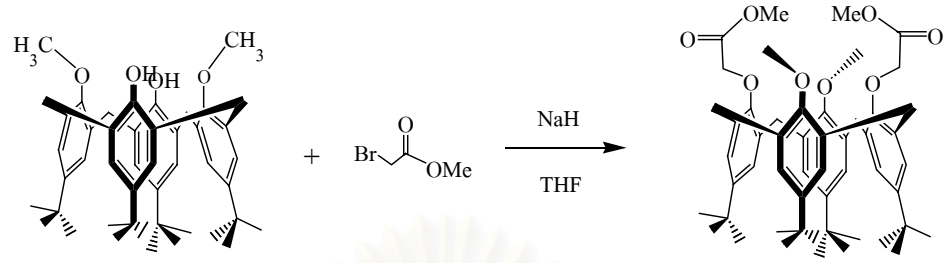

3a **4a**

In a 100 mL two-necked round bottom flask, 25,27-di(methoxy)-*p-tert*-butylcalix [4]arene **(3a)** (3 g, 4.32 mmol) and sodium hydride (0.31 g, 12.96 mmol) were suspended in dried tetrahydrofuran (60 mL). The mixture was stirred for 30 minutes. Methyl bromoacetate (1.23 mL, 12.96 mmol) was then added by syringe. The mixture was stirred overnight and heated at 70 ^{o}C under nitrogen. After the reaction was completed, the solution was allowed to cool to room temperature and evaporated to dryness under reduced pressure. The residue was dissolved in dichloromethane (50 mL) and the saturated solution of ammonium chloride (50 mL) was subsequently added to destroy excess methyl bromoacetate and followed by washing with saturated sodium chloride solution (50 mL). Water (50 mL) was added and the mixture was stirred for 30 minutes and extracted with dichloromethane (2x50 mL). The organic layer was dried over anhydrous sodium sulfate, filtered and evaporated to dryness. The residue was dissolved in a minimum amount of dichloromethane and methanol was added to precipitate a white powder (2.82 g, 80% yield). The product was dried in *vacuo* and kept in a desiccator.

Characterization data for 25,27-di(methoxy)-26,28-di(carbomethoxymethoxy)-*p-tert*-butylcalix[4]arene (4a)

mp. 170-172 ^{o}C

^{1}H-NMR spectrum ($CDCl_3$, 400 MHz) : δ (in ppm) 7.13 (br, 4H, *m*-ROAr<u>H</u>), 6.95-6.42 (br, 4H, *m*-ROAr<u>H</u>), 4.03 (s, 4H, OC<u>H</u>$_2$CO), 3.82 (br, 6H, ArOC<u>H</u>$_3$), 3.40-3.10 and

4.70-4.10 (br, 8H, ArC$\underline{H}_2$Ar), 1.37 (s, 18H, ROAr-*t*-$C_4\underline{H}_9$), 1.03 (2s, 18H, ROAr-*t*-$C_4\underline{H}_9$), 0.8 (s, 6H, OC$\underline{H}_3$)

^{13}C-NMR spectrum ($CDCl_3$, 50 MHz) : δ (in ppm) 169.87, 155.74, 153.74, 145.15, 144.73, 135.70, 131.87, 127.66, 125.38, 124.57, 72.04, 70.84, 60.43, 58.11, 51.61, 37.62, 34.05, 33.60, 31.63, 31.17

FAB mass (m/z) : 821 [$M^+ + H^+$]

Elemental analysis : Calculate ($C_{52}H_{68}O_8$) C, 76.06 ; H, 8.35
Found C, 76.14 ; H, 8.18

2.2.10 Preparation of 25,27-di(methoxy)-26,28-di(2-hydroxyethoxy)-*p-tert*-butylcalix[4]arene (4b)

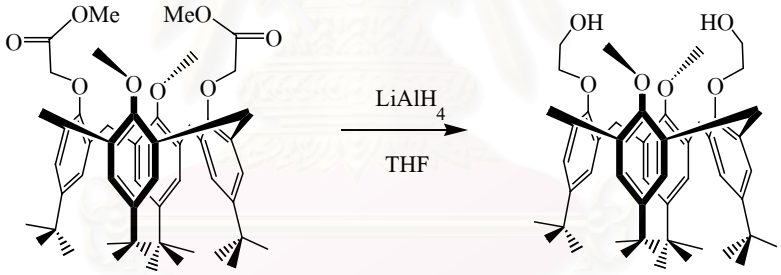

4a **4b**

In a 100 mL two-necked round bottom flask, a solution of 25,27-di(methoxy)-26, 28-di(carbomethoxymethoxy)-*p-tert*-butylcalix[4]arene **(4a)** (1.6 g, 1.95 mmol) in dried tetrahydrofuran (40 mL) was stirred for 10 minutes at 10 ^oC under nitrogen atmosphere. $LiAlH_4$ (0.37 g, 9.75 mmol) was then added gradually. The mixture was allowed to stir overnight at room temperature under nitrogen atmosphere. After the reaction was completed, an aqueous solution of 3 M hydrochloric acid was subsequently added until a precipitate had formed which was then filtered. Water (30 mL) was added and stirred for 30 minutes and extracted with dichloromethane (2x30 mL). The organic layer was dried over anhydrous sodium sulfate, filtered and evaporated to dryness under reduced pressure. The residue was dissolved in a minimum amount of dichloromethane and

methanol was added to precipitate a white powder (1.23 g, 82% yield). The product was dried in *vacuo* and kept in a desiccator.

Characterization data for 25,27-di(methoxy)-26,28-di(ethoxyl)-*p*-*tert*-butylcalix[4] arene (4b)

mp. 135 ^{o}C

^{1}H-NMR spectrum ($CDCl_3$, 400 MHz) : δ (in ppm) 7.20-6.50 (m, 8H, *m*-ROAr<u>H</u>), 5.30-4.90 (m, 2H, CH_2O<u>H</u>), 4.07 (m, 8H, $ArOC$<u>H_2</u>C<u>H_2</u>OH), 3.72 (s, 6H, $ArOC$<u>H_3</u>), 4.30 and 3.20 (dd, *J* = 12.0 Hz, 8H, ArC<u>H_2</u>Ar), 1.25 (s, 18H, ROAr-*t*-C_4<u>H_9</u>), 0.82 (s, 18H, HOAr-*t*-C_4<u>H_9</u>)

^{13}C-NMR spectrum ($CDCl_3$, 50 MHz) : δ (in ppm) 153.74, 153.39, 151.90, 146.23, 145.67, 145.04, 135.29, 133.65, 133.32, 132.15, 131.72, 126.35, 125.64, 124.94, 75.74, 62.86, 61.72, 61.46, 58.76, 38.36, 33.94, 33.87, 33.57, 31.58, 31.49, 30.97, 30.43

FAB mass (m/z) : 765 [$M^+ + H^+$]

Elemental analysis :	Calculate ($C_{50}H_{68}O_6$)	C, 78.49 ; H, 8.96
	Found	C, 78.41 ; H, 8.88

2.2.11 Preparation of 25,27-di(methoxy)-26,28-di(methanesulfonyloxyethoxy)-*p-tert*-butylcalix[4]arene (4c)

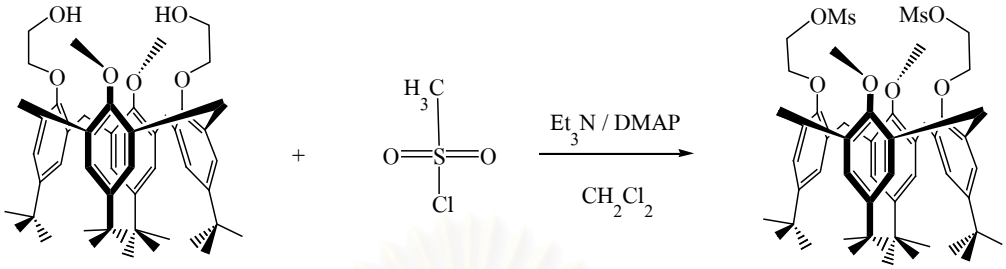

4b **4c**

In a 50 mL two-necked round bottom flask, dichloromethane solution (30 mL) of 25,27-di(methoxy)-26,28-di(2-hydroxyethoxy)-*p-tert*-butylcalix[4]arene (**4b**) (0.5 g, 0.65 mmol), triethylamine (1.02 mL, 6.5 mmol) and a catalytic amount of DMAP was chilled to 10^{o}C with an ice bath and stirred under nitrogen for 30 minutes. MsCl (0.45 mL, 6.5 mmol) was then added by syringe. The reaction mixture was stirred at room temperature under nitrogen for 3 hours. After the reaction was complete, an aqueous solution of 3 M hydrochloric acid (30 mL) was added and stirred for 30 minutes and extracted with dichloromethane (2x30 mL). The organic layer was dried over anhydrous sodium sulfate, filtered and evaporated to dryness. The residue was dissolved in a minimum amount of dichloromethane and methanol was added to precipitate a white powder (0.52 g, 88% yield). The product was dried in *vacuo* and kept in a desiccator.

Characterization data for 25,27-di(methoxy)-26,28-di(methanesulfonyloxyethoxy)-*p-tert*-butylcalix[4]arene (4c)

mp. 234-236 ^{o}C

^{1}H-NMR spectrum ($CDCl_3$, 400 MHz) : δ (in ppm) 7.05 (br, 4H, RAr<u>H</u>), 6.54 (br, 4H, HOAr<u>H</u>), 4.61 (br, 2H, MsC<u>H</u>$_2$C<u>H</u>$_2$O), 4.30 (br, 2H, MsC<u>H</u>$_2$C<u>H</u>$_2$O), 3.95 (br, 6H, ArOC<u>H</u>$_3$), 3.18 (br, 6H, $SO_2C\underline{H}_3$), 4.10 and 3.03 (br, 8H, ArC<u>H</u>$_2$Ar), 1.32 (br, 18H, ROAr-*t*-$C_4\underline{H}_9$), 1.10-0.90 (br, 18H, ROAr-*t*-$C_4\underline{H}_9$).

^{13}C-NMR spectrum ($CDCl_3$, 75 MHz) : δ (in ppm) 155.21, 152.63, 145.02, 134.74, 132.33, 125.39, 71.46, 68.15, 60.23, 33.99, 33.63, 37.58, 31.55, 31.14

FAB mass (m/z) : 921 [$M^+ + H^+$]

Elemental analysis : Calculate ($C_{52}H_{72}O_{10}S_2$) C, 67.79 ; H, 7.88
Found C, 67.83 ; H, 7.84

2.2.12 Preparation of 25,27-di(methoxy)-26,28-di(ethyleneglycol)-bis-*p-tert*-butylcalix[4]arene (4d)

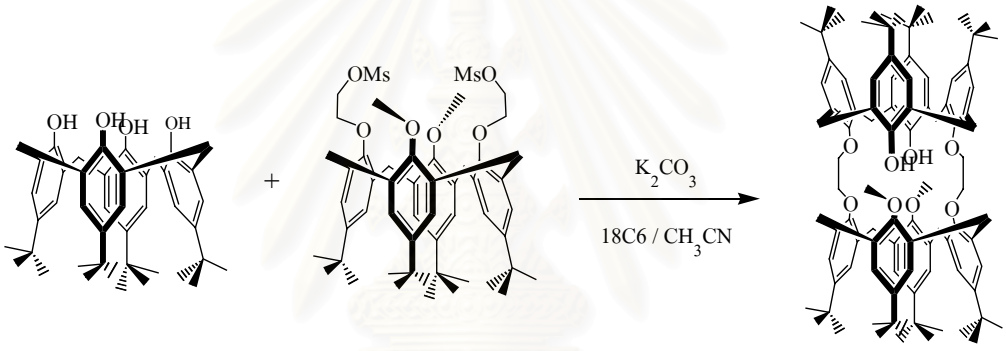

4c **4d**

In a high pressure tube equipped with valves and a pressure gauge, *p-tert*-butylcalix [4]arene (0.21 g, 0.33 mmol), 25,27-di(methoxy)-26,28-di(methanesulfonyloxyethoxy)-*p-tert*-butylcalix[4]arene **(4c)** (0.3 g, 0.33 mmol), catalytic amount of 18-crown-6 and potassium carbonate (0.11 g, 0.82 mmol) were suspended in dried acetonitrile (5 mL). The tube was then pressurized with N_2 at 50 psi. The mixture was stirred and heated at 80 ^{o}C for 4 days. The solution was allowed to cool to room temperature and evaporated to dryness under reduce pressure. The residue was dissolved in dichloromethane (50 mL) and an aqueous solution of 3 M hydrochloric acid (50 mL) was subsequently added and stirred for 30 minutes and then extracted with dichloromethane (2x50 mL). The organic layer was dried over anhydrous sodium sulfate, filtered and evaporated to dryness. The residue was dissolved in a minimum amount of dichloromethane and methanol was added to precipitate a white crystalline solid (0.23 g, 52% yield). The product was dried in *vacuo* and kept in a desiccator.

Characterization data for 25,27-di(methoxy)-26,28-di(ethyleneglycol)-bis-*p-tert*-butylcalix[4]arene (4d)

mp. > 300 ^{o}C (decompose)

^{1}H-NMR spectrum ($CDCl_3$, 200 MHz) : δ (in ppm) 10.37 (s, 2H, ArO<u>H</u>), 7.09-6.70 (m, 16H, <u>H</u>Ar), 4.78-4.12 (m, 22H, OC<u>H</u>$_2$C<u>H</u>$_2$O, ArC<u>H</u>$_2$Ar and –OC<u>H</u>$_3$), 3.40-3.15 (m, 8H, ArC<u>H</u>$_2$Ar), 1.30 (s, 18H, Ar-*t*-C$_4$<u>H</u>$_9$), 1.25 (s, 18H, Ar-*t*-C$_4$<u>H</u>$_9$), 0.95 (s, 36H, Ar-*t*-C$_4$<u>H</u>$_9$)

^{13}C-NMR spectrum ($CDCl_3$, 50 MHz) : δ (in ppm) 154.56, 144.45, 144.26, 141.33, 134.47, 132.98, 132.56, 127.91, 127.67, 125.82, 125.17, 124.89, 75.42, 72.81, 62.52, 33.92, 33.80, 33.61, 32.67, 32.45, 31.58, 31.48, 31.38, 31.29, 31.13, 30.96

ESI mass (m/z) : 1395.2 ($M^+ + NH_4^+$)

Elemental analysis : Calculate ($C_{94}H_{120}O_8$) C, 80.01 ; H, 8.43
Found C, 80.40 ; H, 8.43

2.2.13 Preparation of 25,27-di(ethyleneglycol)-bis-*p-tert*-butylcalix[4] tetraquinone (5a)

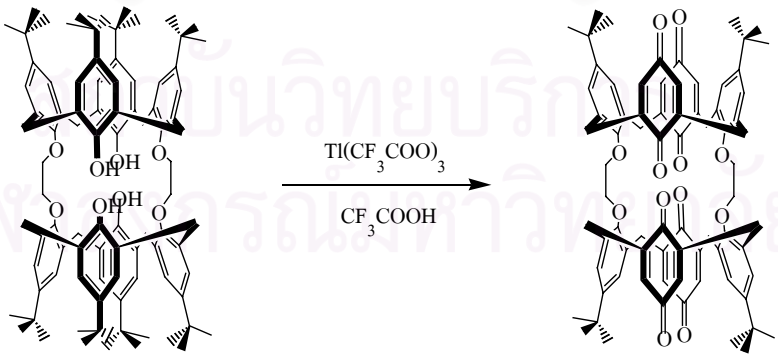

1 **5a**

In a 50 mL two-necked round bottom flask, a suspension of thallium trifluoroacetate (0.8 g, 1.48 mmol) in trifluoroacetic acid (5 mL) was stirred in the dark under nitrogen for 1 hour. 25,27-Di(ethyleneglycol)-bis-*p-tert*-butylcalix[4]arene **(1)** (0.2

g, 0.15 mmol) was then added. The mixture was stirred in the dark for another 2 hours. The solution was then poured into ice. Chloroform (50 mL) was added and stirred with water until the organic phase having pH 7 and then extracted with chloroform (2x30 mL). The organic layer was dried over anhydrous magnesium sulfate, filtered and evaporated to dryness. The residue was dissolved in a minimum amount of chloroform and methanol was added to precipitate a yellow crystalline solid (0.091 g, 52% yield). The product was dried in *vacuo* and kept in a desiccator.

Characterization data for 25,27-di(ethyleneglycol)-bis-*p*-*tert*-butylcalix[4] tetraquinone (5a)

mp. > 260 ^{o}C (decompose)

^{1}H-NMR spectrum ($CDCl_3$, 200 MHz) : δ (in ppm) 7.10 (s, 8H, ROAr<u>H</u>), 5.86 (s, 8H, Hquinone), 4.39 (s, 8H, OC<u>H</u>$_2$C<u>H</u>$_2$O), 4.52, 3.00 (dd, *J* = 13.9 Hz, 16H, ArC<u>H</u>$_2$Ar), 1.33 (s, 36H, Ar-*t*-C$_4$<u>H</u>$_9$)

^{13}C-NMR spectrum ($CDCl_3$, 50 MHz) : δ (in ppm) 187.02, 184.97, 154.20, 149.66, 147.58, 133.97, 133.22, 126.67, 72.57, 33.61, 31.63, 30.84

ESI mass (m/z) : 1203.4 ($M^+ + 4H + NH_4^+$)

IR spectrum (KBr (cm^{-1})) : 1658 (C=O)

Elemental analysis : Calculate ($C_{76}H_{76}O_{12}.2H_2O$) C, 74.98 ; H, 6.62
Found C, 74.99 ; H, 6.20

2.2.14 Preparation of 25,27-di(diethyleneglycol)-bis-*p-tert*-butylcalix[4] tetraquinone (5b)

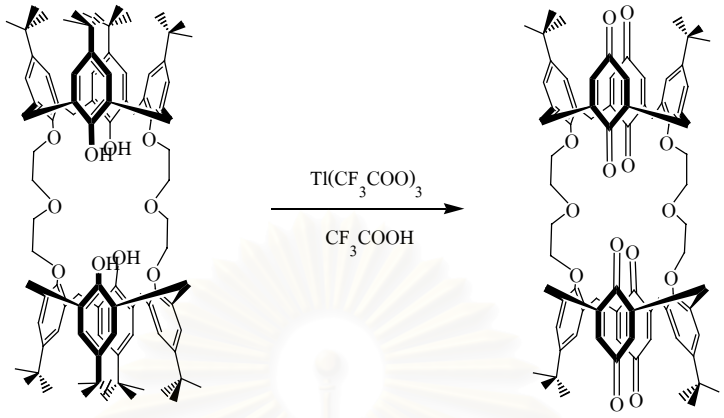

2b **5b**

In a 50 mL two-necked round bottom flask, a suspension of thallium trifluoroacetate (0.76 g, 1.39 mmol) in trifluoroacetic acid (5 mL) was stirred in the dark under nitrogen for 1 hour. 25,27-Di(diethyleneglycol)-bis-*p-tert*-butylcalix[4]arene **(2b)** (0.2 g, 0.14 mmol) was then added. The mixture was stirred in the dark for another 2 hours. The solution was then poured into ice. Chloroform (50 mL) was added and stirred with water until the organic phase having pH 7 and then extracted with chloroform (2x30 mL). The organic layer was dried over anhydrous magnesium sulfate, filtered and evaporated to dryness. The residue was dissolved in a minimum amount of chloroform and methanol was added to precipitate a yellow brown crystalline solid (0.12 g, 68% yield). The product was dried in *vacuo* and kept in a desiccator.

Characterization data for 25,27-di(diethyleneglycol)-bis-*p-tert*-butylcalix[4] tetraquinone (5b)

mp. > 260 ^{o}C (decompose)

^{1}H-NMR spectrum ($CDCl_3$, 200 MHz) : δ (in ppm) 6.95 (s, 8H, ROAr<u>H</u>), 6.39 (s, 8H, Hquinone), 4.35-3.90 (m, 24H, ArOC<u>H</u>$_2$C<u>H</u>$_2$OAr, ArC<u>H</u>$_2$Ar), 3.12 (dd, *J* = 13.9 Hz, 8H, ArC<u>H</u>$_2$Ar), 1.20 (s, 36H, Ar-*t*-C$_4$<u>H</u>$_9$)

^{13}C-NMR spectrum ($CDCl_3$, 50 MHz) : δ (in ppm) 187.98, 185.27, 153.95, 148.79, 146.46, 132.77, 131.10, 126.58, 74.30, 71.29, 34.07, 31.37

IR spectrum (KBr (cm^{-1})) : 1661 (C=O)

Elemental analysis :	Calculate ($C_{80}H_{84}O_{14}.2H_2O$)	C, 72.60 ; H, 6.85
	Found	C, 72.86 ; H, 6.12

2.2.15 Preparation of 25,27-di(methoxy)-26,28-di(ethyleneglycol)-bis-*p-tert*-butylcalix[4]diquinone (5c)

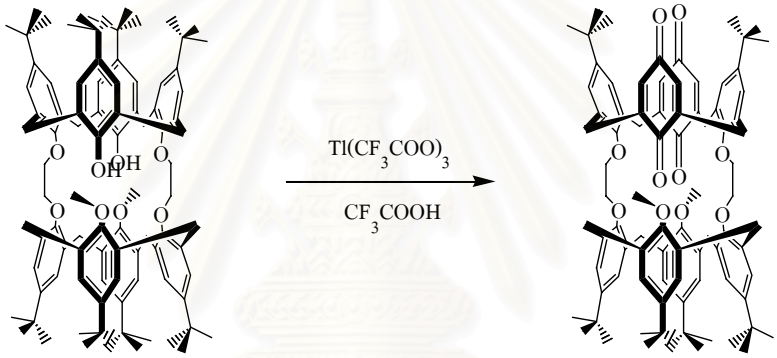

4d **5c**

In a 50 mL two-necked round bottom flask, a suspension of thallium trifluoroacetate (0.76 g, 1.39 mmol) in trifluoroacetic acid (5 mL) was stirred in the dark under nitrogen for 1 hour. 25,27-Di(methoxy)-26,28-di(ethyleneglycol)-bis-*p-tert*-butylcalix[4]arene **(4d)** (0.2 g, 0.14 mmol) was then added. The mixture was stirred in the dark for another 2 hours. The solution was then poured into ice. Chloroform (50 mL) was added and stirred with water until the organic phase having pH 7 and then extracted with chloroform (2x30 mL). The organic layer was dried over anhydrous magnesium sulfate, filtered and evaporated to dryness. The residue was dissolved in a minimum amount of chloroform and methanol was added to precipitate a yellow crystalline solid (0.036 g, 38% yield). The product was dried in *vacuo* and kept in a desiccator.

Characterization data for 25,27-di(methoxy)-26,28-di(ethyleneglycol)-bis-*p-tert*-butylcalix[4]diquinone (5c)

mp. > 260 ^{o}C (decompose)

^{1}H-NMR spectrum ($CDCl_3$, 200 MHz) : δ (in ppm) 7.15 (s, 8H, HArOR), 6.36 (s, 4H, HArOR), 5.68 (s, 4H, Hquinone), 4.60-4.40 (m, 16H, OCH_2CH_2O, $ArCH_2Ar$), 4.17 (s, 6H, $-OCH_3$), 3.30-2.90 (m, 8H, $ArCH_2Ar$), 1.33 (s, 36H, Ar-*t*-C_4H_9), 0.83 (s, 18H, Ar-*t*-C_4H_9)

^{13}C-NMR spectrum ($CDCl_3$, 50 MHz) : δ (in ppm) 187.00, 185.50, 155.73, 154.65, 154.23, 150.89, 146.84, 144.99, 144.15, 135.23, 134.50, 132.62, 130.93, 126.55, 125.73, 124.20, 73.65, 71.42, 63.02, 34.28, 33.99, 33.55, 31.63, 31.52, 31.22, 30.88, 29.65

ESI mass (m/z) : 1315.8 ($M^+ + 4H + NH_4^+$)

IR spectrum (KBr (cm^{-1})) : 1660 (C=O)

Elemental analysis :	Calculate ($C_{86}H_{100}O_{10}.3H_2O$)	C, 76.64 ; H, 7.93
	Found	C, 77.20 ; H, 8.52

2.3 Complexation studies

2.3.1 Complexation studies of ligands 5a, 5b and 5c with Li^+ ion

A solution of 0.005 M of ligands **5a**, **5b** and **5c** ($2.5x10^{-6}$ mol) in $CDCl_3$ (0.5 mL) was prepared in NMR tubes. A solution of 0.05 M of $LiClO_4$ ($5.32x10^{-3}$ g, $5x10^{-5}$ mol) in CD_3CN (1 mL) was prepared in a vial. The solution of $LiClO_4$ was added directly to the NMR tube by microsyringe to have cation : ligand ratios shown in Table 2.1. ^{1}H-NMR spectra were recorded after each addition.

2.3.2 Complexation studies of ligands 5a, 5b and 5c with Na^+ ion

A solution of 0.005 M of ligands **5a**, **5b** and **5c** ($2.5x10^{-6}$ mol) in $CDCl_3$ (0.5 mL) was prepared in NMR tubes. A solution of 0.05 M of $NaClO_4$ ($6.12x10^{-3}$ g, $5x10^{-5}$ mol) in CD_3CN (1 mL) was prepared in a vial. The solution of $NaClO_4$ was added directly to the NMR tube by microsyringe to have cation : ligand ratios shown in Table 2.1. ^{1}H-NMR spectra were recorded after each addition.

2.3.3 Complexation studies of ligands 5a, 5b and 5c with K^+ ion

A solution of 0.005 M of ligands **5a**, **5b** and **5c** ($2.5x10^{-6}$ mol) in $CDCl_3$ (0.5 mL) was prepared in NMR tubes. A solution of 0.05 M of KPF_6 ($9.2x10^{-3}$ g, $5x10^{-5}$ mol) in CD_3CN (1 mL) was prepared in a vial. The solution of KPF_6 was added directly to the NMR tube by microsyringe to have cation : ligand ratios shown in Table 2.1. ^{1}H-NMR spectra were recorded after each addition.

2.3.4 Complexation studies of ligands 5a, 5b and 5c with Cs^+ ion

A solution of 0.005 M of ligands **5a**, **5b** and **5c** ($2.5x10^{-6}$ mol) in $CDCl_3$ (0.5 mL) was prepared in NMR tubes. A solution of 0.05 M of $CsPF_6$ ($1.39x10^{-2}$ g, $5x10^{-5}$ mol) in CD_3CN (1 mL) was prepared in a vial. The solution of $CsPF_6$ was added directly to the NMR tube by microsyringe to have cation : ligand ratios shown in Table 2.1. ^{1}H-NMR spectra were recorded after each addition.

Table 2.1: Ratios of cation : ligand in $CDCl_3$: CD_3CN

Ratios of cation : ligand	Volumn cation added (mL)	Mole cation added (mol)	Total volumn in NMR tube(mL)
0.0 : 1.0	0	0	0.500
0.1 : 1.0	0.005	$2.5x10^{-7}$	0.505
0.2 : 1.0	0.005	$5.0x10^{-7}$	0.510
0.3 : 1.0	0.005	$7.5x10^{-7}$	0.515
0.4 : 1.0	0.005	$1.0x10^{-6}$	0.520
0.5 : 1.0	0.005	$1.25x10^{-6}$	0.525
0.6 : 1.0	0.005	$1.5x10^{-6}$	0.530
0.7 : 1.0	0.005	$1.75x10^{-6}$	0.535
0.8 : 1.0	0.005	$2.0x10^{-6}$	0.540
0.9 : 1.0	0.005	$2.25x10^{-6}$	0.545
1.0 : 1.0	0.005	$2.5x10^{-6}$	0.550
1.2 : 1.0	0.01	$3.0x10^{-6}$	0.560
1.4 : 1.0	0.01	$3.5x10^{-6}$	0.570
1.6 : 1.0	0.01	$4.0x10^{-6}$	0.580
1.8 : 1.0	0.01	$4.5x10^{-6}$	0.590
2.0 : 1.0	0.01	$5.0x10^{-6}$	0.600
3.0 : 1.0	0.05	$7.5x10^{-6}$	0.650
4.0 : 1.0	0.05	$1.0x10^{-5}$	0.700

2.4 Electrochemical studies

2.4.1 Apparatus

Cyclic voltammetry and square wave voltammetry was perfomed using an AUTOLAB PGSTAT 100 (Ecochemie, Netherlands) with a three electrode consisting of a glassy carbon electrode with a conducting area of 3mm diameter, a platinum wire counter electrode and a $Ag/AgNO_3$ reference electrode. All CV measurements were digitized using the GPES software (Version 4.7). All scans were carried out at room temperature and scan rates were varied.

2.4.2 Cleaning procedure for electrode

Cleaning of the glassy carbon electrode was done using a BAS polishing kit with stepwise finer abrasives down to 0.05 and 0.1 μm alumina powder slurry. The electrode was then sonicated in 0.005 M H_2SO_4 for 5 minutes and then soaked with dichloromethane. This cleaning procedure was repeated after each measurement. The platinum wire counter electrode was cleaned by immerged in 3 M HNO_3 for 30 minutes, rinsed with distilled water and wiped to dryness before use. The reference electrode was cleaned by immerging in 3 M HNO_3 for 30 minutes and by rinsing with distilled water.

2.4.3 Preparation of the main solution

Unless otherwise indicated, all experiments were carried out in an electrolyte solution of 0.1 M tetrabutyl ammonium hexafluorophosphate ($TBAPF_6$) in 20% acetonitrile in dichloromethane. The reference electrode contained 0.01 M $AgNO_3$ + 0.1 M $TBAPF_6$ in 20% acetonitrile in dichloromethane. The background solution contained only 0.1 M $TBAPF_6$ (0.19372 g, $5x10^{-4}$ mmol) in 5 mL of 20% acetonitrile in dichloromethane.

2.4.4 CV and SWV measurement

All CV and SWV measurements were carried out in a cell compartment enclosed with a build-in Teflon cap. To avoid the interference from O_2, All solution was bubbled with nitrogen at least 5 minutes before each measurement.

Cyclic voltammograms were recorded over a range of scan rate from 0.05 to 1.0 V/s. The values of E_p and i_p were determined graphically from the CV by plotting a tangent to the leading baseline of the peak to correct for the background current. At a scan rate of 0.050 V/s the half-wave potential $E_{1/2}$ was determined as $(E_{pa} + E_{pc})/2$

Square wave voltammograms were recorded in Frequency 60 Hz at amplitude 0.050 V.

2.4.5 CV and SWV measurements of ligands 5a, 5b and 5c with Li^+ ion

A solution of 0.001 M of ligands **5a**, **5b** and **5c** ($5x10^{-6}$ mol) + $TBAPF_6$ (0.19372 g, $5x10^{-4}$ mmol) in 5 mL of 20% acetonitrile in dichloromethane was prepared in a volumetric flask. $NaClO_4$ 0.1 M (0.05317 g, $5x10^{-4}$ mol) and $TBAPF_6$ (0.19372 g, $5x10^{-4}$ mmol) in 5 mL of acetonitrile was prepared in a volumetric flask. All solutions were sonicated for 30 minutes before used. The solution of $LiClO_4$ was added directly to the Cell by microsyringe to have cation : ligand ratios shown in Table 2.2. Redox currents were determined from CV scans of the complex solutions at a scan rate of 0.050 V/s using the method as described above.

2.4.6 CV and SWV measurements of ligands 5a, 5b and 5c with Na^+ ion

A solution of 0.001 M of ligands **5a**, **5b** and **5c** ($5x10^{-6}$ mol) + $TBAPF_6$ (0.19372 g, $5x10^{-4}$ mmol) in 5 mL of 20% acetonitrile in dichloromethane was prepared in a volumetric flask. $NaClO_4$ 0.1 M (0.06122 g, $5x10^{-4}$ mol) and $TBAPF_6$ (0.19372 g, $5x10^{-4}$ mmol) in 5 mL of acetonitrile was prepared in a volumetric flask. All solutions were sonicated for 30 minutes before used. The solution of $NaClO_4$ was added directly to the Cell by microsyringe to have cation : ligand ratios shown in Table 2.2. Redox currents were determined from CV scans of the complex solutions at a scan rate of 0.050 V/s using the method as described above.

2.4.7 CV and SWV measurements of ligands 5a, 5b and 5c with K^+ ion

A solution of 0.001 M of ligands **5a**, **5b** and **5c** ($5x10^{-6}$ mol) and $TBAPF_6$ (0.19372 g, $5x10^{-4}$ mmol) in 5 mL of 20% acetonitrile in dichloromethane was prepared in a volumetric flask. KPF_6 0.1 M (0.09203 g, $5x10^{-4}$ mol) and $TBAPF_6$ (0.19372 g, $5x10^{-4}$ mmol) in 5 mL of acetonitrile was prepared in a volumetric flask. All solutions were sonicated for 30 minutes before used. The solution of KPF_6 was added directly to the Cell by microsyringe to have cation : ligand ratios shown in Table 2.2. Redox currents were determined from CV scans of the complex solutions at a scan rate of 0.050 V/s using the method as described above.

2.4.8 CV and SWV measurements of ligand 5b with Cs^+ ion

A solution of 0.001 M of ligand **5b** ($5x10^{-6}$ mol) and $TBAPF_6$ (0.19372 g, $5x10^{-4}$ mmol) in 5 mL of 20% acetonitrile in dichloromethane was prepared in a volumetric flask. $CsPF_6$ 0.1 M (0.13894 g, $5x10^{-4}$ mol) and $TBAPF_6$ (0.19372 g, $5x10^{-4}$ mmol) in 5 mL of acetonitrile was prepared in a volumetric flask. All solutions were sonicated for 30 minutes before used. The solution of $CsPF_6$ was added directly to the Cell by microsyringe to have cation : ligand ratios shown in Table 2.2. Redox currents were determined from CV scans of the complex solutions at a scan rate of 0.050 V/s using the method as described above.

Table 2.2: Ratios of cation : ligand in CH_2Cl_2 : CH_3CN

Ratios of cation : ligand	Volumn cation added (mL)
0.0 : 1.0	0
0.2 : 1.0	0.010
0.4 : 1.0	0.010
0.6 : 1.0	0.010
0.8 : 1.0	0.010
1.0 : 1.0	0.010
1.5 : 1.0	0.025
2.0 : 1.0	0.025

CHAPTER 3

RESULTS AND DISCUSSION

3.1 Synthesis and characterization of double calix[4]arene derivatives

3.1.1 Synthesis and characterization of 25,27-di(ethyleneglycol)-bis-*p-tert*-butylcalix[4]arene (1)

The method to synthesized double calix[4]arene **1** was first reported by Tomapatanaget et. al. in 1998 by nucleophilic substitution reactions of *p-tert*-butylcalix [4]arene with bromoethyl tosylate using anhydrous potassium carbonate as base and yielded **1** in 41%.[40] In the year 2001, Tantrakarn applied high pressure in the same reaction and improved the yield of **1** to 69%.[41] However, the easier way to synthesize compound **1** was adapted from the report by Chen and coworkers as shown in Figure 3.1.[38] *p-tert*-Butylcalix[4]arene was prepared by the condensation of *p-tert*-butylphenol with formaldehyde in a minimum amount of sodium hydroxide as previously reported by Gutsche.[37] Treating *p-tert*-butylcalix[4]arene with 12 equiv. of 1,2-dibromoethane in acetonitrile in the presence of anhydrous potassium carbonate (1 equiv.) for one night. The white crystalline solid double calix[4]arene **1** was obtained in 12% yield. From ^{1}H-NMR spectrum, this compound is in cone conformation due to the presence of Ar$C\underline{H}_2$Ar protons as two doublets at 4.50 and 3.35 ppm with coupling constant (J) = 13 Hz. The bridging glycolic protons ($OC\underline{H}_2C\underline{H}_2O$) appeared at 4.55 ppm. FAB mass spectra also supported the structure of this ligand showing an intense line at m/z 1367.8 due to the [$M^+ + NH_4^+$] and elemental analysis was in good agreement with the structure.

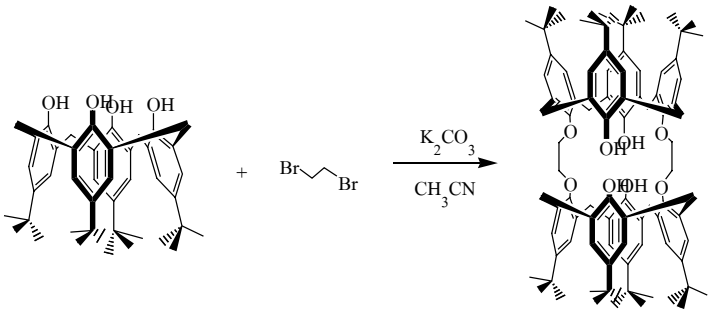

1 (12%)

Figure 3.1: Synthesis of double calix[4]arene (**1**)

3.1.2 Synthesis and characterization of 25,27-di(diethylene glycol)-bis-*p*-*tert*-butylcalix[4]arene (2b)

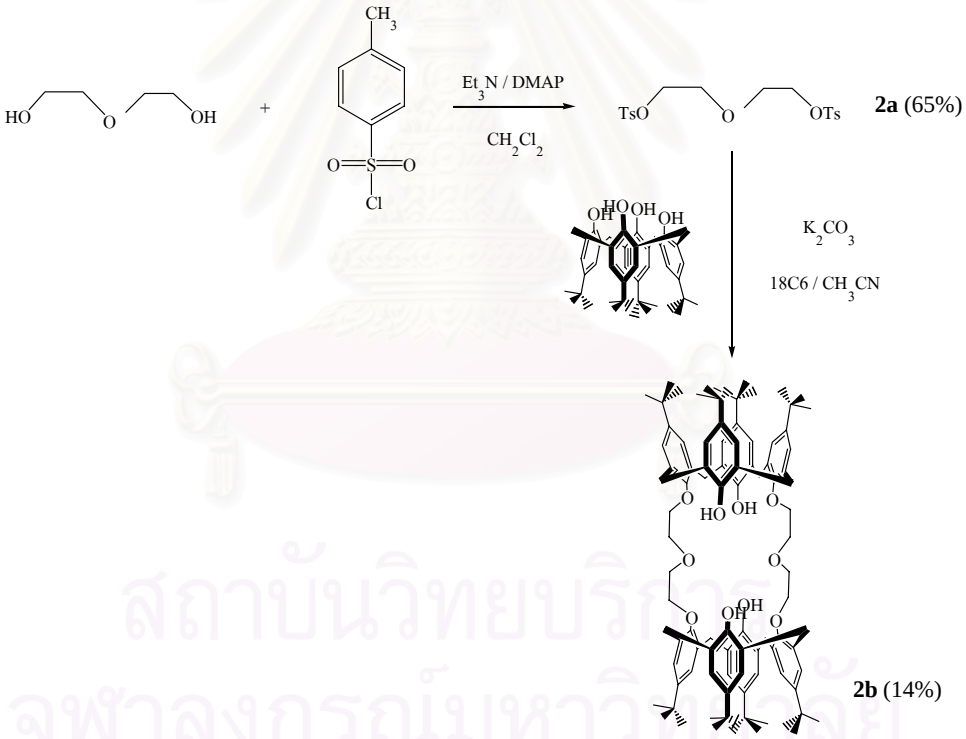

Figure 3.2: Synthetic pathway of double calix[4]arene **2b**

The synthetic pathway shown in Figure 3.2, adapted from Asfari's report, [42] started with a preparation of diethylene glycol ditosylate (**2a**) by tosylation of diethylene glycol in the presence of 3 equiv. of triethylamine and a catalytic amount of DMAP in dichloromethane at room temperature overnight. A white crystalline solid of compound

2a was obtained in 65% yield. ^{1}H-NMR spectrum of compound **2a** showed the characteristic peaks of tosyl groups: singlet of C<u>H</u>$_3$ at 2.43 ppm and two doublets of Ar<u>H</u> at 7.76 and 7.33 ppm with coupling constant (*J*) of 8 Hz. They are accordance with the structure of diethyleneglycol ditosylate (**2a**).

The coupling reaction of **2a** with *p-tert*-butylcalix[4]arene in acetonitrile (10 mL) using anhydrous potassium carbonate as base with a catalytic amount of 18-crown-6 as phase transfer was done by using high pressure technique which was reported by Tantrakarn K.[41] The tube was compressed with N_2 at 50 psi and heated at 70 ^{o}C for 2 days. After recrystallization with methanol, compound **2b** was obtained in 14% yield as a white crystalline solid. ^{1}H-NMR spectrum of compound **2b** indicated that it is in cone conformation due to the presence of ArC<u>H</u>$_2$Ar protons as two doublets at 4.30 and 3.18 ppm with coupling constant (*J*) = 14.0 Hz. The bridging glycolic protons (OC<u>H</u>$_2$C<u>H</u>$_2$O) appeared at 4.50-4.10 ppm. FAB mass spectra also supported the structure of this ligand showing an intense line at m/z 1437 and elemental analysis was in good agreement with the structure.

3.1.3 Synthesis and characterization of 25,27-di(methoxy)-26,28-di(ethylene glycol)-bis-*p-tert*-butylcalix[4]arene (4d)

The synthesis of double calix[4]arene **4d** is more complicate than double calix[4] arene **1** and **2b** because the structure of compound **4d** was asymmetric. The only way to synthesize this compound was to coupling two units of calix[4]arene derivatives together. One unit must have a good leaving group that makes the coupling procudure more easily. By using this strategy, the synthesis of double calix[4]arene **4d** was carried out in two pathways as shown in Figure 3.3 and Figure 3.4.

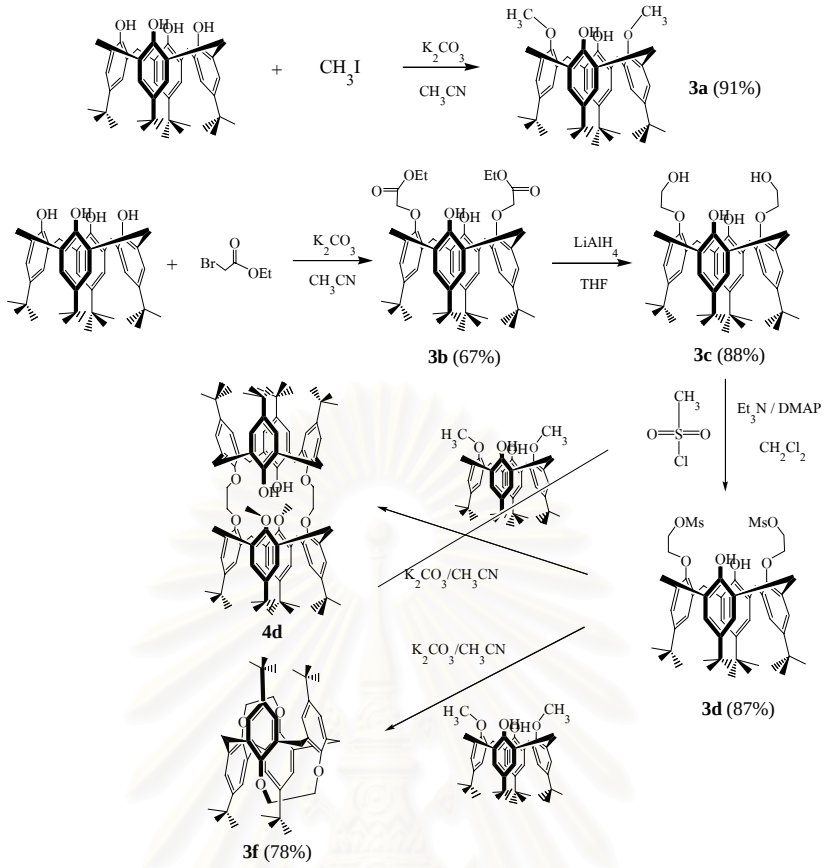

Figure 3.3: Synthetic pathway I of double calix[4]arene **4b**

In early attempt, we tried to synthesize compound **4d** by the synthetic pathway I shown in Figure 3.3. In the first step, compound **3a** was synthesized by a nucleophilic substitution reaction of *p-tert*-butylcalix[4]arene with methyliodide (2.5 equiv.) using anhydrous potassium carbonate as base in dried acetonitrile yielding dimethoxy derivative **3a** as white powder in 91% yield. The ^{1}H-NMR spectrum of **3a** showed singlet peak of the methyl proton at 3.94 ppm. In the second step, compound **3b** was synthesized by nucleophilic substitution reaction of *p-tert*-butylcalix[4]arene with ethylbromoacetate (2 equiv.) using anhydrous potassium carbonate as base in dried acetonitrile yielding diester product **3b** as white powder in 67% yield. The ^{1}H-NMR spectrum of **3b** showed quartet and triplet peaks of the ethylester proton at 4.30 and 1.30 ppm, respectively. After that diester product **3b** was then reduced by adding 4.3 equiv. of $LiAlH_4$ into the solution of **3b** in dried THF to afford an alcohol derivative **3c** as a white powder in 88% yield. The ^{1}H-NMR spectrum of **3c** exhibited two broader peaks due to phenolic hydroxy and alkyl hydroxy protons at 9.23 and 5.25 ppm, respectively with the integral ratio of 1:1. The hydroxy protons of alcohol derivative **3c** was then underwent nucleophilic substitution with methanesulfonyl groups (mesyl) by treating with 4.0 equiv. of triethylamine and a

catalytic amount of DMAP in dichloromethane. A white powder product, **3d** was obtained in 87% yield. The ^{1}H-NMR spectrum of **3d** indicated methyl proton signals of methane sulfonyl groups at 3.23 ppm.

Finally, The coupling reaction between the methane sulfonyl derivative **3d** and dimethoxy derivative **3a** was done in the presence of 4.0 equiv. of anhydrous potassium carbonate as base in dried acetonitrile and heated at 70 ^{o}C for 3 days. The product was then characterized by ^{1}H-NMR, Mass spectrometry and the result indicated that the desired product **4d** was not obtained, but the product **3f** which its conformation was in 1,2-alternate was obtained instead. The compound **3f** resulted from an intramolecular alkylated reaction. ^{1}H-NMR spectrum of **3f** showed characteristic peaks due to 1,2 alternate conformation by the presence of a singlet at 4.05 ppm and two doublets at 4.57 and 3.32 ppm for the methylene bridge protons of the calixarene. In the mean time the four protons of the diethylene glycol units face the two opposite aromatic walls appear as a multiplet at 3.58 and 3.14 ppm.[43] In addition, there are 2 ^{13}C-NMR signals appear in the ^{13}C-NMR spectrum of **3f** at 34.2 and 34.1 ppm due to the anti orientation of the adjacent phenol rings.[44]

From the failure of coupling reaction of the pathway I, a new pathway was used. A new unit for the coupling reaction was employed. Figure 3.4 showed the pathway II for synthesize double calix[4]arene **4d**.

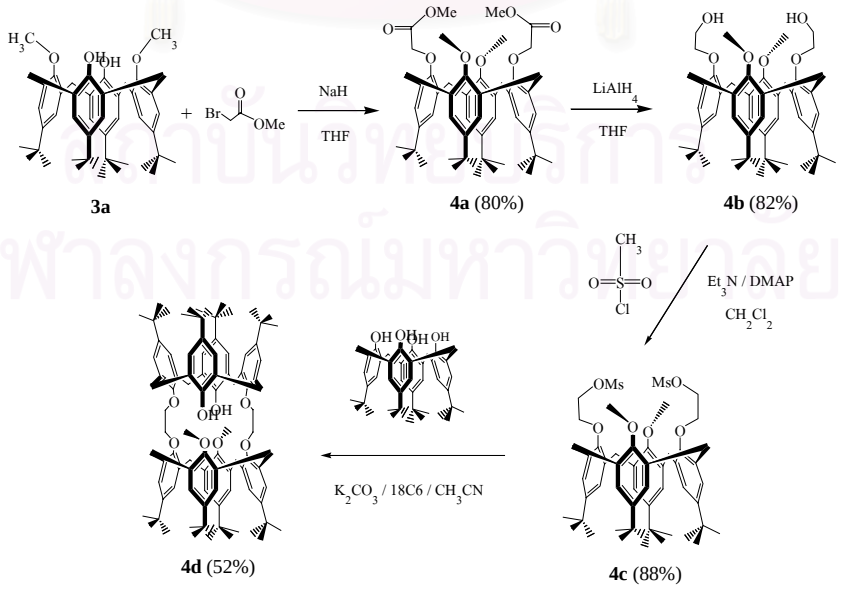

Figure 3.4: Synthetic pathway II of double calix[4]arene **4b**

The synthetic pathway II started with nucleophilic substition of dimethoxy *p-tert*-butylcalix[4]arene **3a** with 3.0 equiv. of methyl bromoacetate in the presence of 3.0 equiv. of sodium hydride as base in dried tetrahydrofuran. The tetra-substituted product **4a** was obtained as white powder in 80% yield. The ^{1}H-NMR spectrum of **4a** showed broad signals due to the phenyl ring inversion from the lack of intramolecular hydrogen bonding. FAB mass spectra supported the structure of this compound showing an intense line at m/z 821 and elemental analysis was in good agreement with the structure. Diester product **4a** was then reduced by adding 5 equiv. of $LiAlH_4$ into the solution of **4a** in dried THF to afford an alcohol derivative **4b** as white powder in 82% yield. As the same as **4a**, the ^{1}H-NMR spectrum of **4b** showed broad signals due to the phenyl ring inversion from the lack of intramolecular hydrogen bonding. FAB mass spectra also supported the structure of this compound showing an intense line at m/z 765 and elemental analysis was in good agreement with the structure. The hydroxy protons of alcohol derivative **4b** was then underwent nucleophilic substitution with methanesulfonyl groups (mesyl) by treating with 10 equiv. of triethylamine and a catalytic amount of DMAP in dichloromethane. A white powder product, **4c** was obtained in 88% yield. The ^{1}H-NMR spectrum of **4c** was not resolved due to the ring inversion from lacking of intramolecular hydrogen bonding. However, FAB mass spectra supported the structure of this compound showing an intense line at m/z 921 and elemental analysis was in good agreement with the structure.

Finally, The coupling reaction between the tetra-substituted methane sulfonyl derivative **4c** and *p-tert*-butylcalix[4]arene in the presence of 2.5 equiv. of anhydrous potassium carbonate as base in dried acetonitrile (5 mL) with a catalytic amount of 18-crown-6 as phase transfer was done by using a high pressure technique. The reaction tube was compressed with nitrogen at 50 psi and heated at 80^{o}C for 4 days. After recrystallization with methanol, compound **4d** was obtained in 52% yield as a white crystalline solid. ^{1}H-NMR spectrum of compound **4d** at 4.78-4.12 and 3.40-3.15 ppm indicated that it existed in cone conformation with methyl group due to the presence of Ar$C\underline{H}_2$Ar and –O$C\underline{H}_3$, respectively. The bridging glycolic protons (O$C\underline{H}_2C\underline{H}_2$O) appeared at 4.78-4.12 ppm. ESI mass spectra also supported the structure of this ligand showing an intense line at m/z 1395.2 due to the $[M^+ + NH_4^+]$ and elemental analysis was in good agreement with the structure.

3.1.4 Synthesis and characterization of double calix[4]arenequinone 5a, 5b and 5c

Double calix[4]arenes **1**, **2b** and **4d** were then transformed to their quinone derivatives. From Figure 3.5, compounds **5a**, **5b** and **5c** were synthesized by using Tl $(OCOCF_3)_3$ in CF_3COOH as oxidizing reagent in darkness under nitrogen. The final products, **5a**, **5b** and **5c** were obtained as yellow crystalline solid in 52%, 68% and 38% yield, respectively. ^{1}H-NMR spectrum of ligand **5a** showed the absence of the hydroxy proton signal at 7.65 ppm of compound **1** and a signal of quinone protons was found at 5.86 ppm instead. ESI mass spectra also supported the structure of this ligand showing an intense line at m/z 1203.4 due to the $[M^+ + 4H + NH_4^+]$ and elemental analysis was in good agreement with the structure. ^{1}H-NMR spectrum of ligand **5b** showed the same pattern as that of ligand **5a,** which a signal of quinone protons was found at 6.39 ppm. For ligand **5c**, ^{1}H-NMR spectrum showed absence of two hydroxy proton signals at 10.37 ppm of compound **4d** and a signal of quinone protons was found at 6.50 ppm instead. The methyl protons in structure appeared at 4.15 ppm. ESI mass spectra also supported the structure of this ligand showing an intense line at m/z 1315.8 due to the $[M^+ + 4H + NH_4^+]$ and elemental analysis was in good agreement with the structure. All three final products **5a**, **5b** and **5c** showed the CO stretching in their IR spectra at 1660 cm^{-1}.

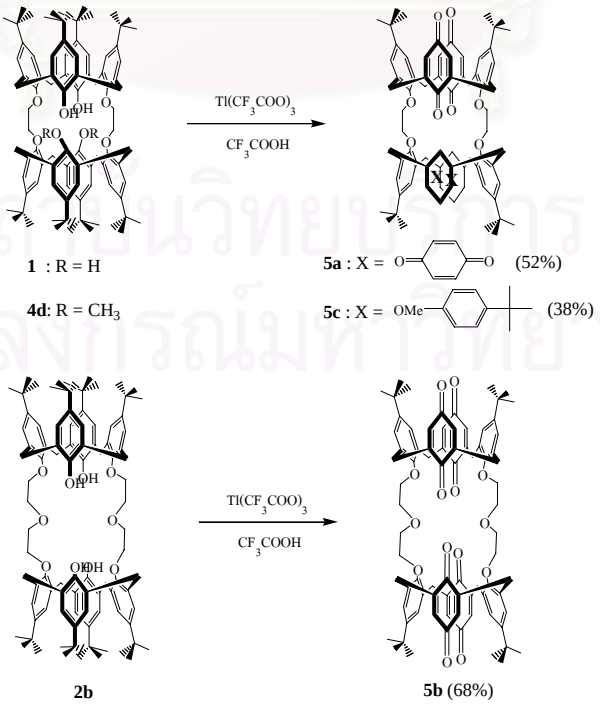

Figure 3.5: Synthetic pathway of double calix[4]arenequinones **5a**, **5b** and **5c**

3.2 Cation complexation studies

Ligands **5a**, **5b** and **5c** contain glycol linkages which have oxygen donor atoms for binding alkaline cations. Like the crown ether derivative calixarenes, they have different cavity size suitable for recognition studies with cations having various sizes. Thus, complexation studies of ligands **5a**, **5b** and **5c** with alkaline cations such as Li^+, Na^+, K^+ and Cs^+ were carried out.

3.2.1 Complexation studies of ligand 5a with Li^+, Na^+, K^+ and Cs^+ ions

Upon addition of $LiClO_4$ to the solutions, The signal of aromatic and quinone protons at 7.11 and 5.88 ppm in ^{1}H-NMR spectra (Figure 3.6) decreased rapidly and a new aromatic signal at 6.80 ppm increased significantly. The new doublet signal of methylene bridge protons of calixarene at 4.03 and 3.35 ppm was also found while doublet signals of the methylene bridge protons of the free ligand at 4.52 and 3.00 (dd, J = 13.9 Hz) decreased gradually. After adding 1.0 equiv. of $LiClO_4$, the signal of aromatic protons and quinone protons at 7.11 and 5.88 ppm of the free ligand totally disappeared and only a new signal of aromatic protons at 6.80 ppm of the complex was found instead. The signal of glycol linkage at 4.42 ppm shifted upfield to 4.31 ppm and the signal of methylene bridge protons of calixarenes at 4.52 and 3.00 (dd, J = 13.9 Hz) moved to 4.03 and 3.35 ppm for the complex. These results indicated that lithium cation bind oxygen atom of the glycol linkages and quinone moieties. The conformation of calixarene was changed, so that the lower rim of calixarene units were closely orientated to each other and suggested that the cavity of double calixarene **5a** was changed after complexation with lithium ion. Addition of more than 1.0 equiv. showed no change of the spectra, indicated that **5a** formed complex with lithium cation in a 1:1 stoichiometry.

When 1.0 equiv. of $NaClO_4$ was added to the $CDCl_3$ solution of **5a**, the signals of aromatic protons and quinone protons at 7.11 and 5.88 ppm disappeared and a new signal of aromatic protons at 6.76 ppm was found in the ^{1}H-NMR spectra (Figure 3.7). The signal of the glycolic chain at 4.42 ppm was shifted upfield to 4.31 ppm. The doublet signals of the methylene bridge protons of the free ligand at 4.52 and 3.00 (dd, J = 13.9 Hz) became a doublet signal at 4.42 and 3.20 ppm. From these results, suggested that the sodium cation bind oxygen atom of the glycol linkages and the cavity of double

calixarene **5a** changed after complexation with sodium but compare with the case of lithium, the cavity after complexation was bigger due to a little shift of methylene bridge protons. Addition more than 1.0 equiv. showed no change of the spectra, indicated that **5a** formed complex with sodium cation in a 1:1 stoichiometry.

In the case of KPF_6, at 1.0 equiv of KPF_6, the signal of aromatic protons and quinone protons at 7.11 and 5.88 ppm disappeared from the ^{1}H-NMR spectra (Figure 3.7) and a new signal of aromatic protons at 6.66 ppm was found. The signal of the glycol chain at 4.42 ppm shifted upfield to 4.26 ppm. The doublet signal of methylene bridge protons of calixarenes at 4.52 and 3.00 (dd, J = 13.9 Hz) became a doublet signal at 4.35 and 3.10 ppm. From these results, suggested that the potassium cation bind oxygen atom of the glycol linkage and the cavity of double calixarene **5a** changed after complexation with potassium. Addition more than 1.0 equiv. showed no change of the spectra, indicated that **5a** formed complex with potassium ion in a 1:1 stoichiometry.

Upon addition of $CsPF_6$ to the solution, no new signal was observed in the ^{1}H-NMR spectra (Figure 3.8). The result shows that **5a** cannot form complexes with cesium ion.

In conclusion, double calix[4]arene quinone **5a** can act as an alkali ion receptor. This ligand can bind Li^+, Na^+ and K^+ with oxygen donor atom in the ethylene glycol linkage and after binding cations, the cavity of double calix[4]arenequinone **5a** changed upon complexation. The quinone units can flip up and down to accommodate a particular cation (Li^+, Na^+ or K^+). In the case of Cs^+, no complexation between ligand **5a** and Cs^+ occurred due to the radius of Cs^+ is bigger than the cavity size. These results lead us to propose the structure of complexation between ligand **5a** with various cations as shown in Figure 3.10.

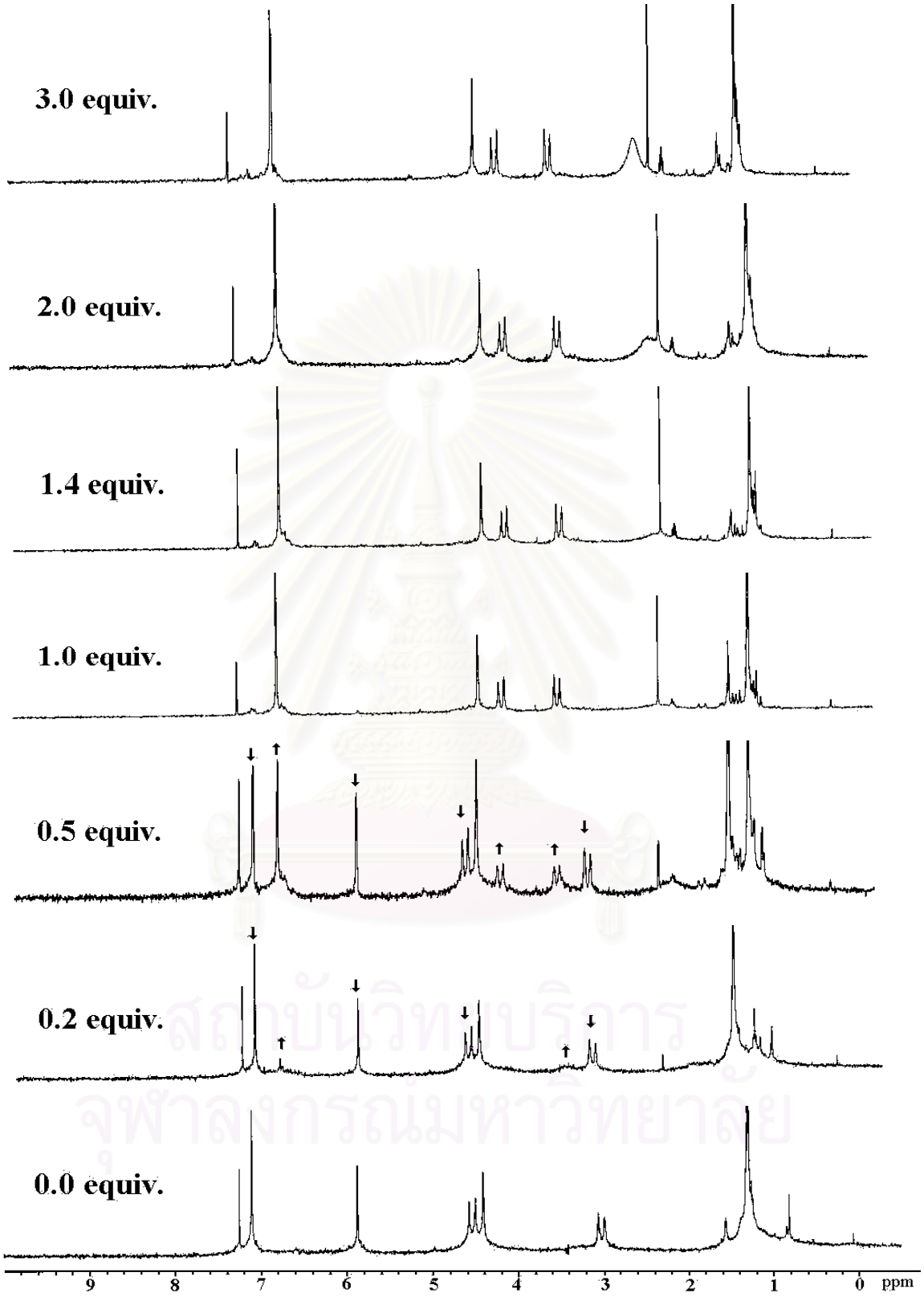

Figure 3.6 : ^{1}H-NMR ($CDCl_3$, 200 MHz) spectra of ligand **5a** with $LiClO_4$

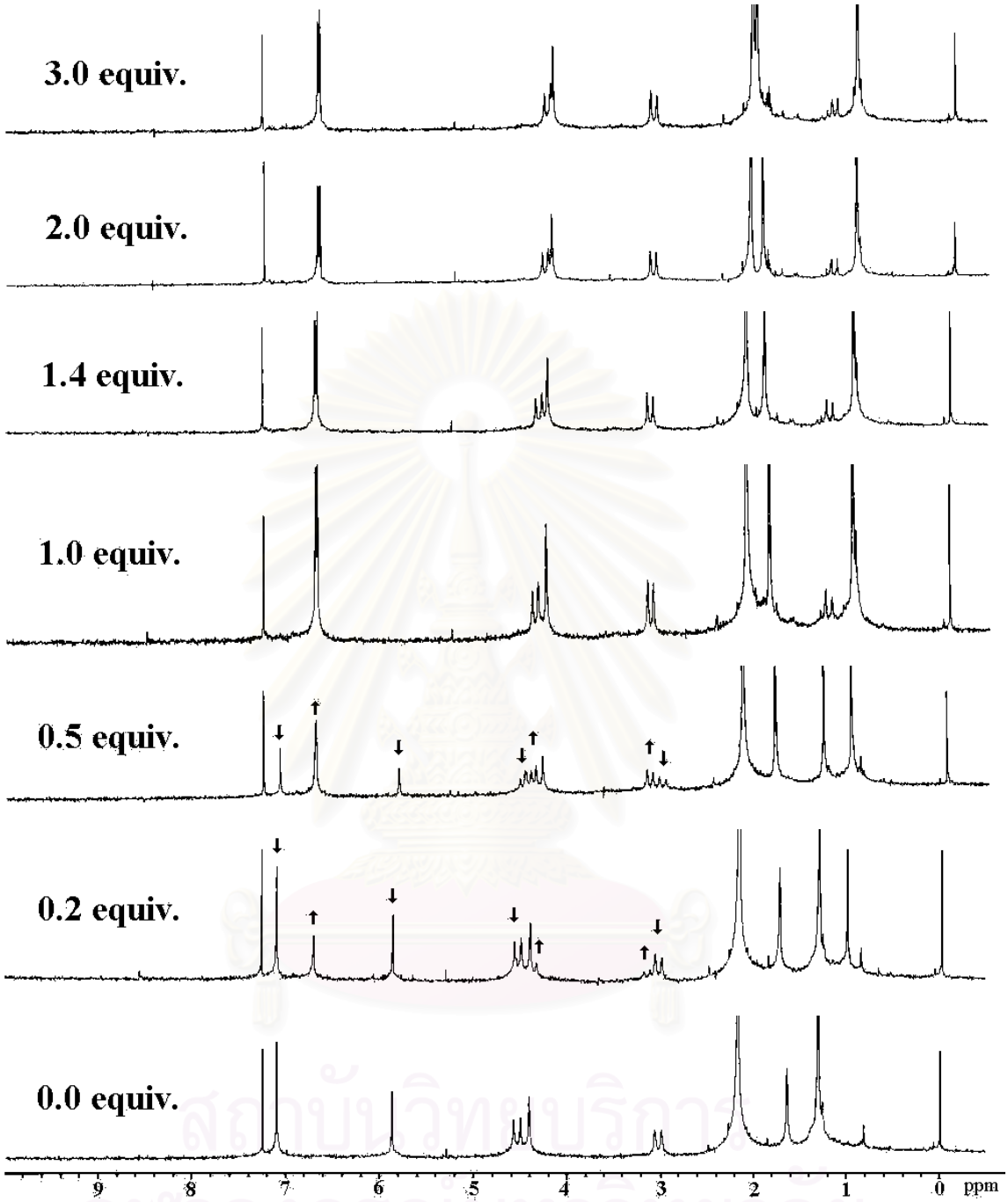

Figure 3.7 : ^{1}H-NMR ($CDCl_3$, 200 MHz) spectra of ligand **5a** with $NaClO_4$

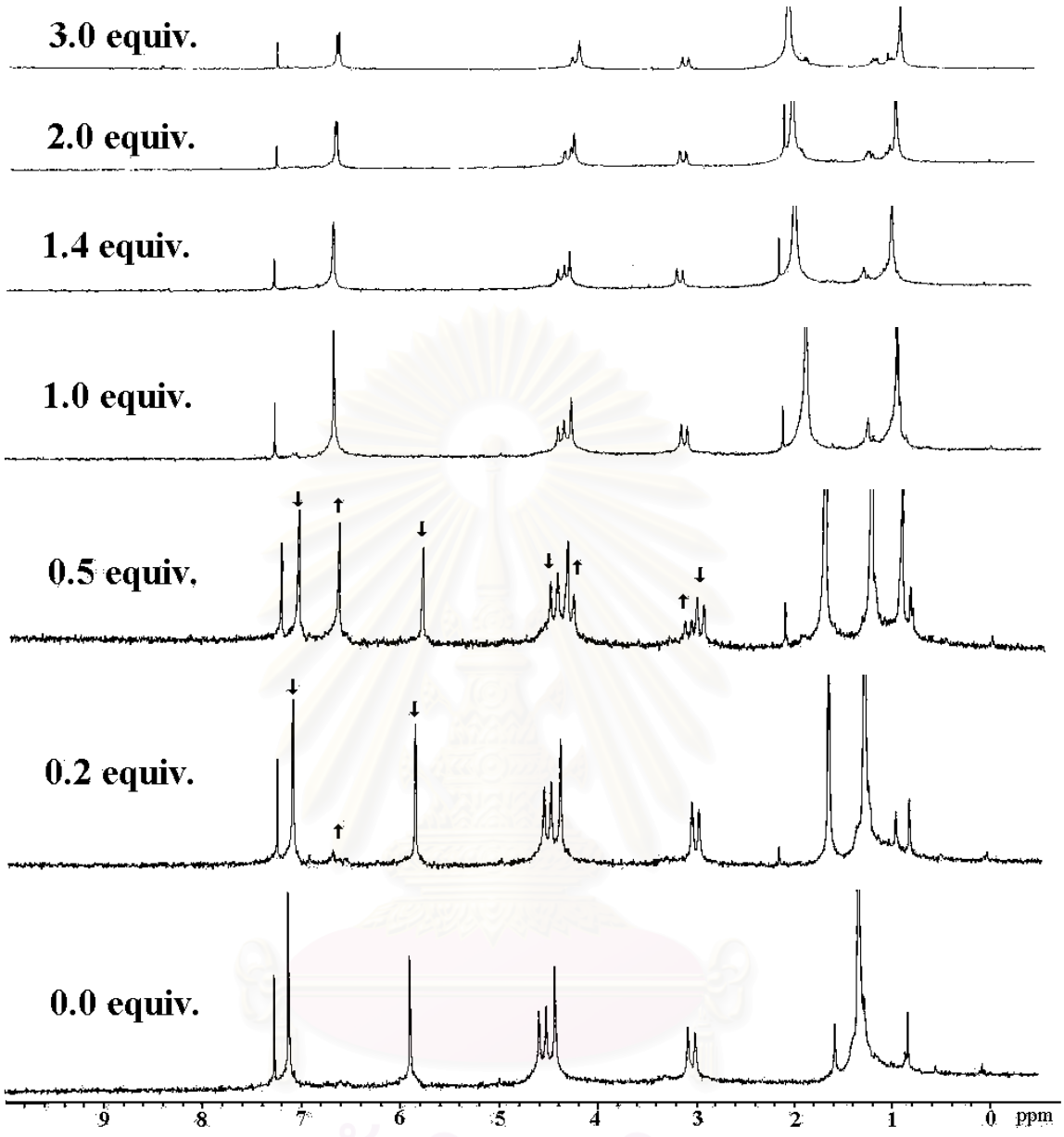

Figure 3.8 : ^{1}H-NMR ($CDCl_3$, 200 MHz) spectra of ligand **5a** with KPF_6

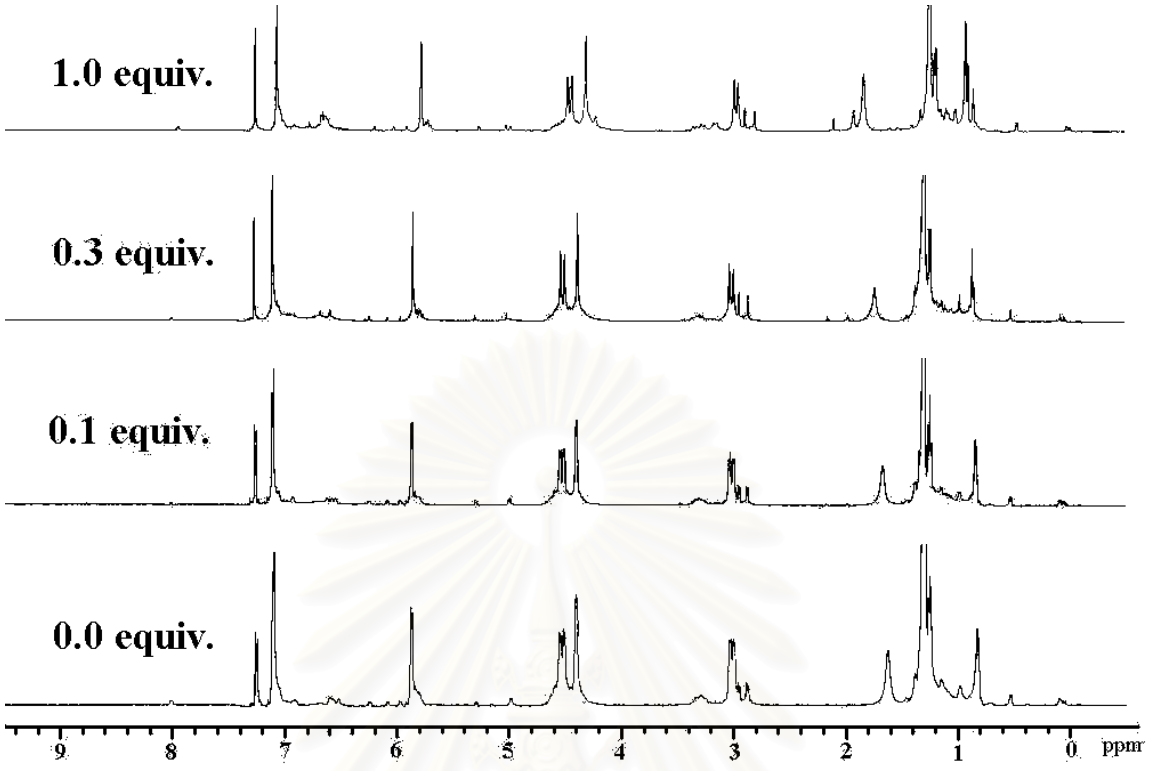

Figure 3.9 : ^{1}H-NMR ($CDCl_3$, 400 MHz) spectra of ligand **5a** with $CsPF_6$

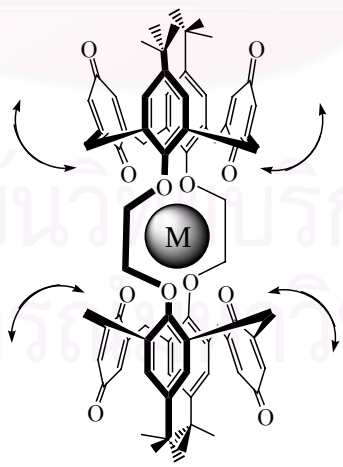

M = Li^+, Na^+ and K^+

Figure 3.10 : A proposed structure of complexation between ligand **5a** with various cations

3.2.2 Complexation studies of ligand 5b with Li^+ , Na^+, K^+ and Cs^+ ions

Upon addition of $LiClO_4$ to the solutions, signals of aromatic and quinone protons at 6.95 and 6.37 ppm in ^{1}H-NMR spectra (Figure 3.11) decreased rapidly and a new aromatic signal at 6.66 ppm increased significantly. The signal of the diethylene glycol linkage at 4.01 ppm became a broad signal. Signals of methylene bridge protons of calixarene at 4.20 and 3.10 ppm were unchanged. After adding $LiClO_4$ to 1.0 equiv., signals of aromatic protons and quinone protons at 6.95 and 6.37 ppm of the free ligand totally disappeared and only a new signal of aromatic protons at 6.66 ppm of the complex was found instead. The signal of glycol linkage at 4.01 ppm shifted upfield to 3.90 ppm and signals of methylene bridge protons of calixarene were unchanged. These results indicated that lithium cation bind oxygen atom of the diethylene glycol linkages and the cavity of calixarene was unchanged. Addition more than 1.0 equiv. showed no change of the spectra, indicated that **5b** formed complex with lithium ion a in 1:1 stoichiometry.

When 1.0 equiv. of $NaClO_4$ was added to the $CDCl_3$ solution of **5b**. The signal of aromatic protons and quinone protons at 6.95 and 6.38 ppm disappeared and a new signal of aromatic protons at 6.65 ppm was found in the ^{1}H-NMR spectra (Figure 3.12). The signal of the glycolic chain at 4.01 ppm shifted upfield to 3.94 ppm and became a broad signal. Unlike with the case of lithium, new doublet signals of methylene bridge protons of calixarene at 4.14 and 3.06 ppm were found. From these results, suggested that the sodium cation bind oxygen atom of the diethylene glycol linkages and the cavity of the ligand changes a little due to a little shift of methylene bridge proton signals. Addition of more than 1.0 equiv. showed only changes at the diethylene glycol signal, indicated that **5b** formed complex with sodium ion in a 1:1 stoichiometry.

In the case of KPF_6 at 1.0 equiv. of KPF_6, signals of aromatic protons and quinone protons at 6.95 and 6.38 ppm disappeared and a new signal of aromatic protons at 6.65 ppm was found in the ^{1}H-NMR spectra (Figure 3.13). The signal of the glycolic chain at 4.01 ppm shifted upfield to 3.90 ppm. New doublet signals of methylene bridge protons of calixarenes at 4.14 and 3.04 ppm were found. From these results, suggested that the potassium cation bind oxygen atom of the diethylene glycol linkages and the cavity of double calixarene **5a** changes due to a little shift of methylene bridge proton signals.

Addition of more than 1.0 equiv. showed no change of the spectra, indicated that **5b** formed complex with potassium cation in a 1:1 stoichiometry.

Upon addition of $CsPF_6$ to the solution at 1.0 equiv. of $CsPF_6$, signals of aromatic protons and quinone protons at 6.95 and 6.38 ppm disappeared and a new signal of aromatic protons at 6.65 ppm was found in the ^{1}H-NMR spectra (Figure 3.14). The signal of the glycol chain at 4.01 ppm shifted upfield to 3.90 ppm. New doublet signals of methylene bridge protons of calixarenes at 4.20 and 3.01 ppm were found. These results suggested that cesium ion binds oxygen atom of the diethylene glycol linkage and the cavity of double calixarene **5a** changes due to a little shift of methylene bridge protons to accommodate Cs^+. Addition of more than 1.0 equiv. showed no change of the spectra and indicated that **5b** formed complex with cesium ion in a 1:1 stoichiometry.

In conclusion, double calix[4]arene quinone **5b** can act as an alkali cation receptor. This ligand can bind Li^+, Na^+, K^+ and Cs^+ with oxygen donor atoms in diethylene glycol linkages and quinone units. Due to its large cavity size, ligand **5b** can bind Cs^+ and show a little change in calixarene conformation when bind with large alkali cations such as Na^+, K^+ and Cs^+. These results lead us to propose the structure of complexation between ligand **5b** with various cations as shown in Figure 3.15.

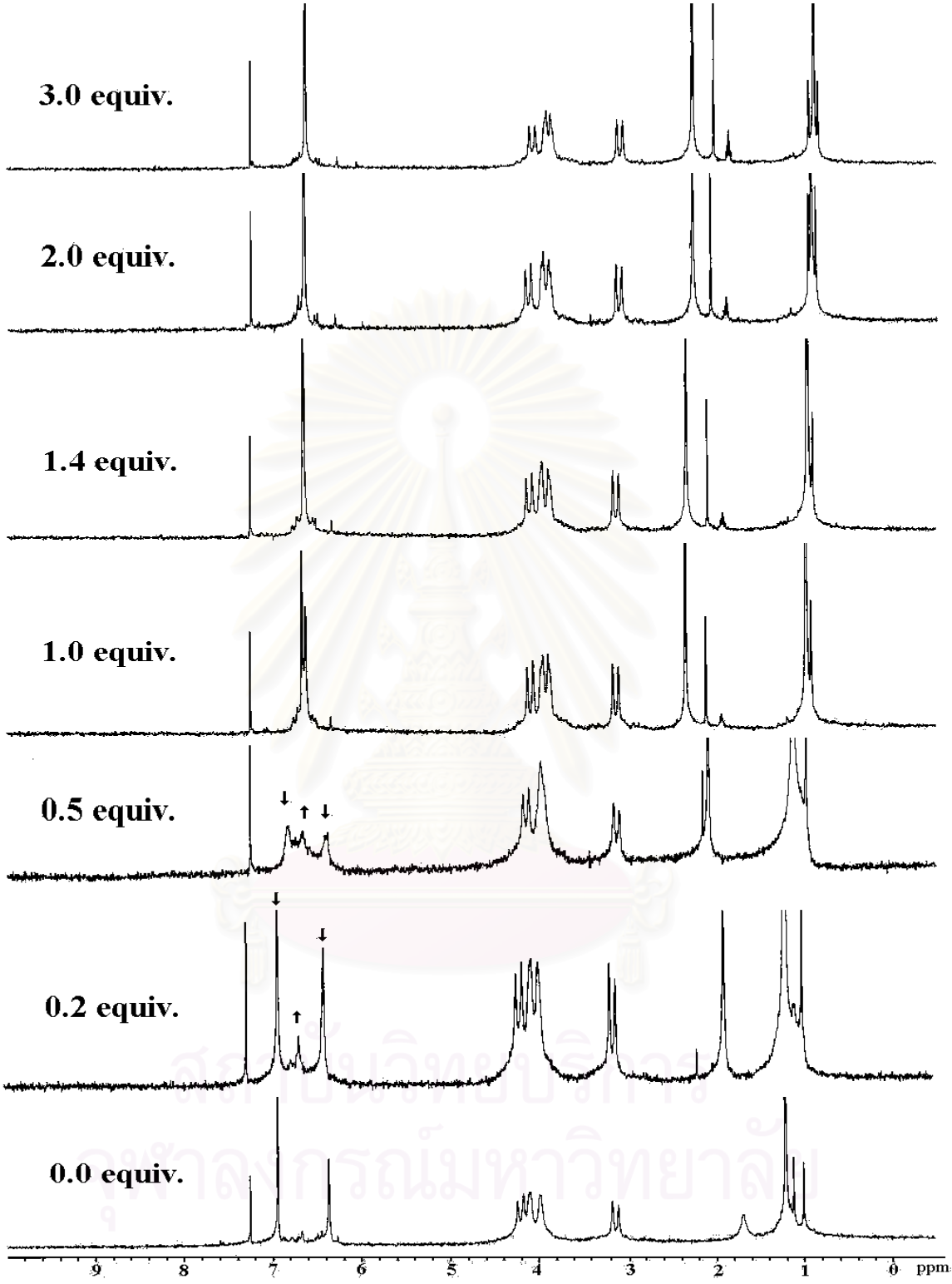

Figure 3.11 : ^{1}H-NMR ($CDCl_3$, 200 MHz) spectra of ligand **5b** with $LiClO_4$

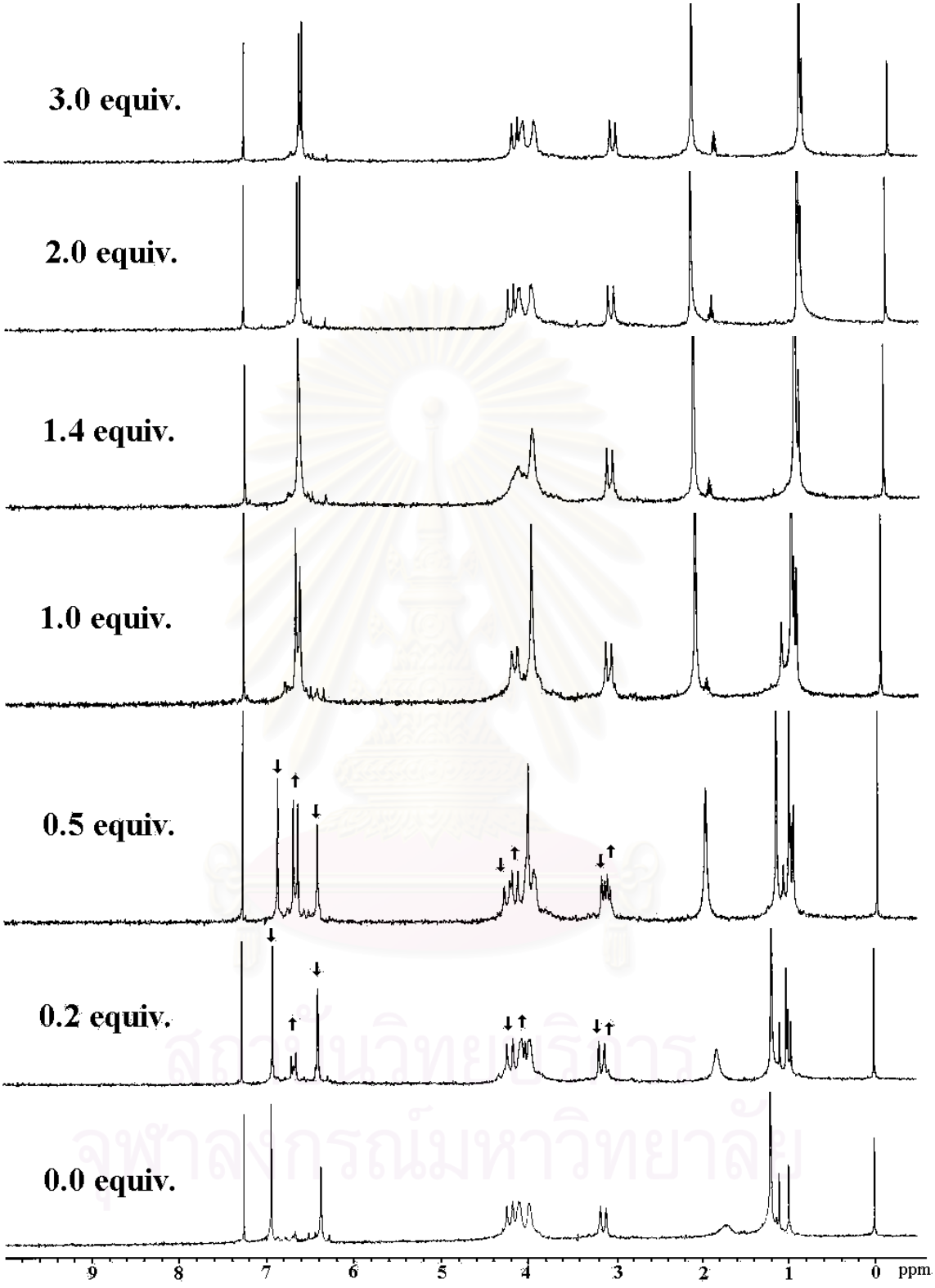

Figure 3.12 : ^{1}H-NMR ($CDCl_3$, 200 MHz) spectra of ligand **5b** with $NaClO_4$

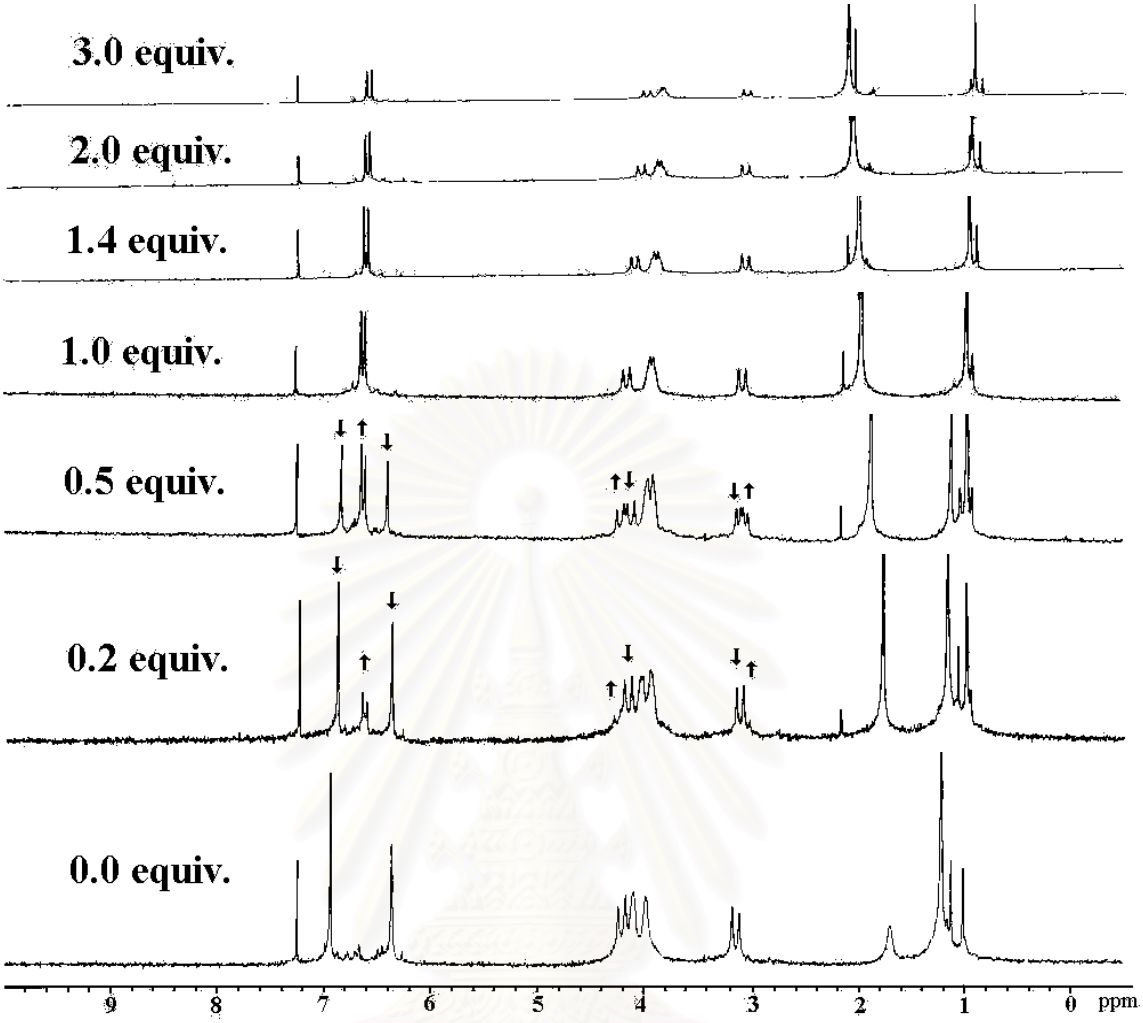

Figure 3.13 : ^{1}H-NMR ($CDCl_3$, 200 MHz) spectra of ligand **5b** with KPF_6

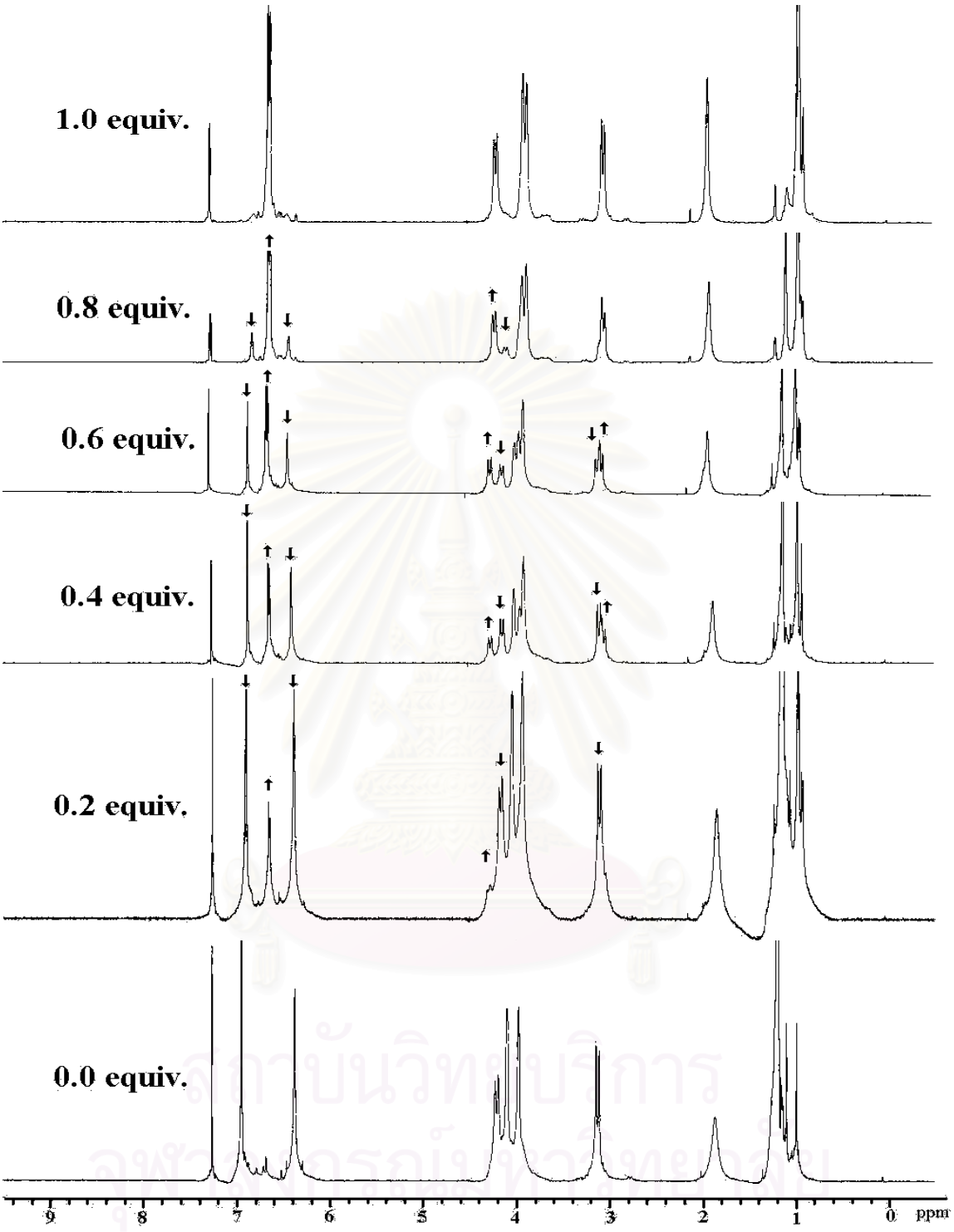

Figure 3.14 : ^{1}H-NMR ($CDCl_3$, 400 MHz) spectra of ligand **5b** with $CsPF_6$

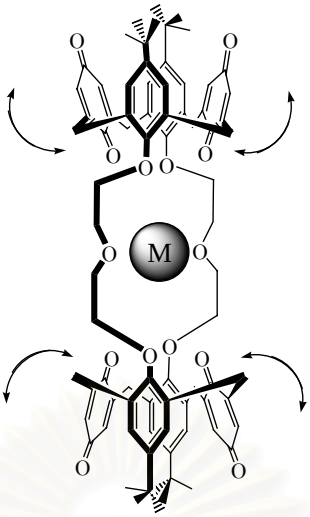

M = Li^+, Na^+, K^+ and Cs^+

Figure 3.15 : A proposed structure of complexation between ligand **5b** with various cations

3.2.3 Complexation studies of ligand 5c with Li^+, Na^+, K^+ and Cs^+ ions

Upon addition of $LiClO_4$ to the solutions, signals of aromatic and quinone protons at 7.15, 6.36 and 5.68 ppm in ^{1}H-NMR spectra (Figure 3.16) decreased rapidly and a new set of aromatic proton signals at 7.40-5.80 ppm increased significantly. These signals imply that upon complexing a cation the conformation of the methoxy phenyl units were frozen or their movement was prohibited and caused the phenyl ring moving slower than the NMR time scale. This results in various conformations appeared in the NMR spectrum of the complex. New doublet signals of methylene bridge protons of calixarene at 5.00-2.80 ppm was also found and increasing. After adding 1.4 equiv. of $LiClO_4$, the signal of aromatic protons and quinone protons at 6.36 and 5.68 ppm of the free ligand totally disappeared and a new set of aromatic proton signals at 7.40-6.50 ppm of the complex was found instead. New signals of glycolic linkages and methylene bridge protons were found at 5.00-2.80 ppm. The signal of methyl protons in the structure shifted downfield from 4.17 to 4.29 ppm. These results indicated that the cavity size of double calix[4]arene **5c** was small due to the steric from two methyl groups in the structure and when lithium cation bind oxygen atom of the ethylene glycol linkage, the conformation of calixarene changed (Figure 3.20) upon complexation. Addition of more

than 1.4 equiv. showed no change of the spectra, suggested that **5c** formed complex with lithium cation in a 1:1 stoichiometry.

When 1 equiv. of $NaClO_4$ was added to the $CDCl_3$ solution of **5c**, signals of aromatic protons and quinone protons at 7.15, 6.36 and 5.68 ppm disappeared from the ^{1}H-NMR spectra (Figure 3.17) and new signals of aromatic protons at 7.40-6.50 ppm were found. Signals of methyl protons at 4.17 ppm shifted downfield to 4.24 ppm. New methylene bridge protons and ethylene glycol linkages signal were found at 5.00-3.40 ppm. From these results, as the same as lithium case, suggested that the sodium cation bind oxygen atom of the glycol linkages and the conformation of double calixarene **5a** changed for accommodating sodium ion. Addition of more than 1.0 equiv. showed no change of the spectra, indicated that **5c** formed complex with sodium ion in a 1:1 stoichiometry.

In the case of KPF_6, adding of more than 0.6 equiv of KPF_6 changed the spectra. From ^{1}H-NMR spectra (Figure 3.18) at 1.8 equiv., signals of aromatic protons and quinone protons at 6.36 and 5.68 ppm disappeared and a new signal of aromatic protons at 6.76 ppm was found. The signal of methyl protons at 4.17 ppm disappeared and became a signal at 3.52 ppm. New methylene bridge protons and ethylene glycolic linkages signal were found at 4.50-3.20 ppm. These results suggested that the potassium ion bind with oxygen atom of the glycol linkages moderately due to its large radius. Addition of more than 1.8 equiv. showed no change of the spectra, suggested that **5c** formed complex with potassium cation in a 1:1 stoichiometry.

Upon addition of $CsPF_6$ to the solution, no new signal was observed in the ^{1}H-NMR spectra (Figure 3.19). The result shows that **5c** cannot form a complex with cesium.

In conclusion, double calix[4]arene quinone **5c** can act as an alkali ion receptor. From the results, this ligand can bind Na^+, Li^+ and K^+ with oxygen donor atom in the ethylene glycol linkage and after binding cations, the conformation of double calix[4] arenequinone **5c** changed upon complexation. In the case of Cs^+, no complexation between ligand **5c** and Cs^+ occurred because the radius of Cs^+ is bigger than the cavity size. These results lead us to propose the structure of complexation between ligand **5c** with various cations as shown in Figure 3.20.

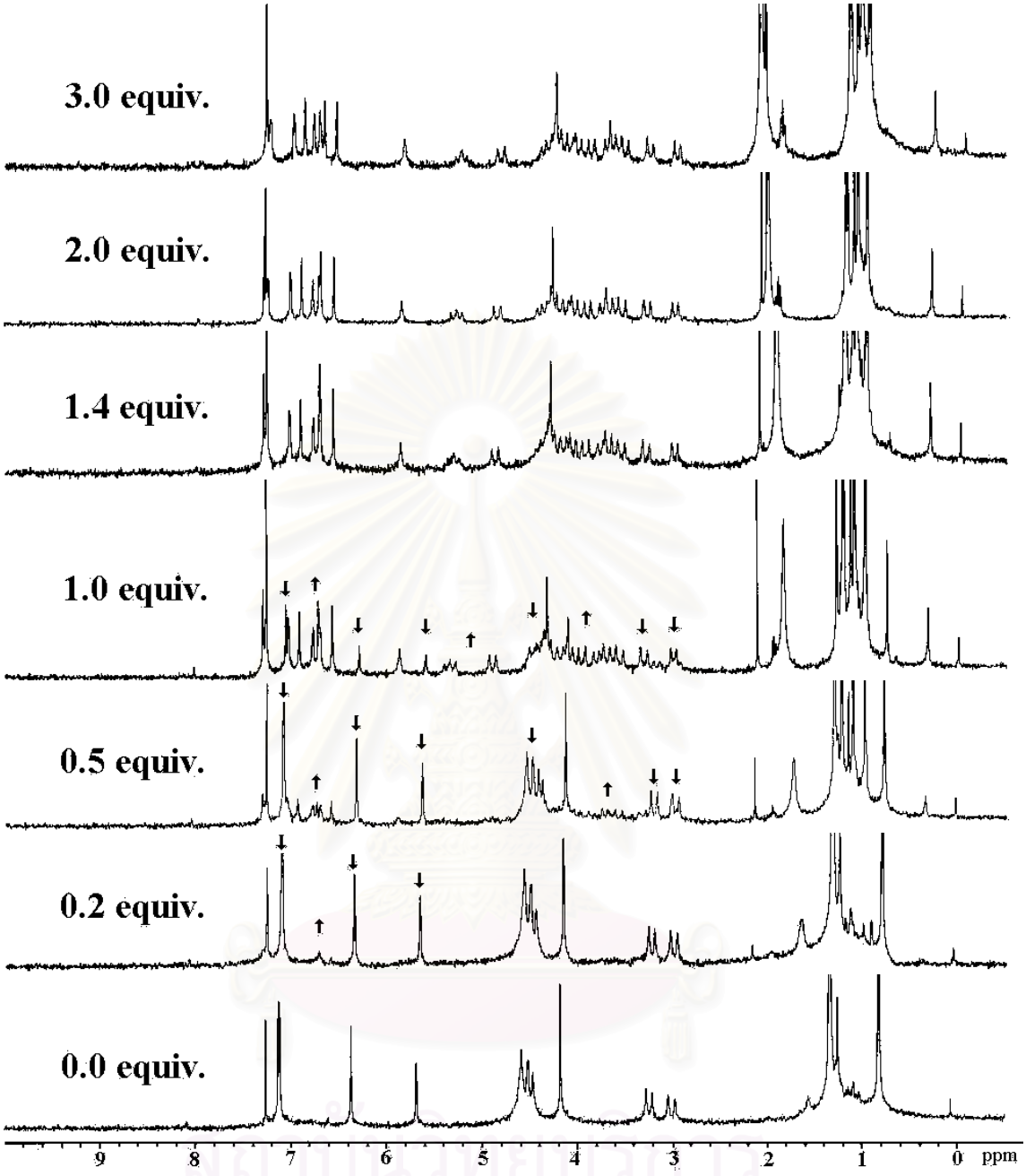

Figure 3.16 : ^{1}H-NMR ($CDCl_3$, 200 MHz) spectra of ligand **5c** with $LiClO_4$

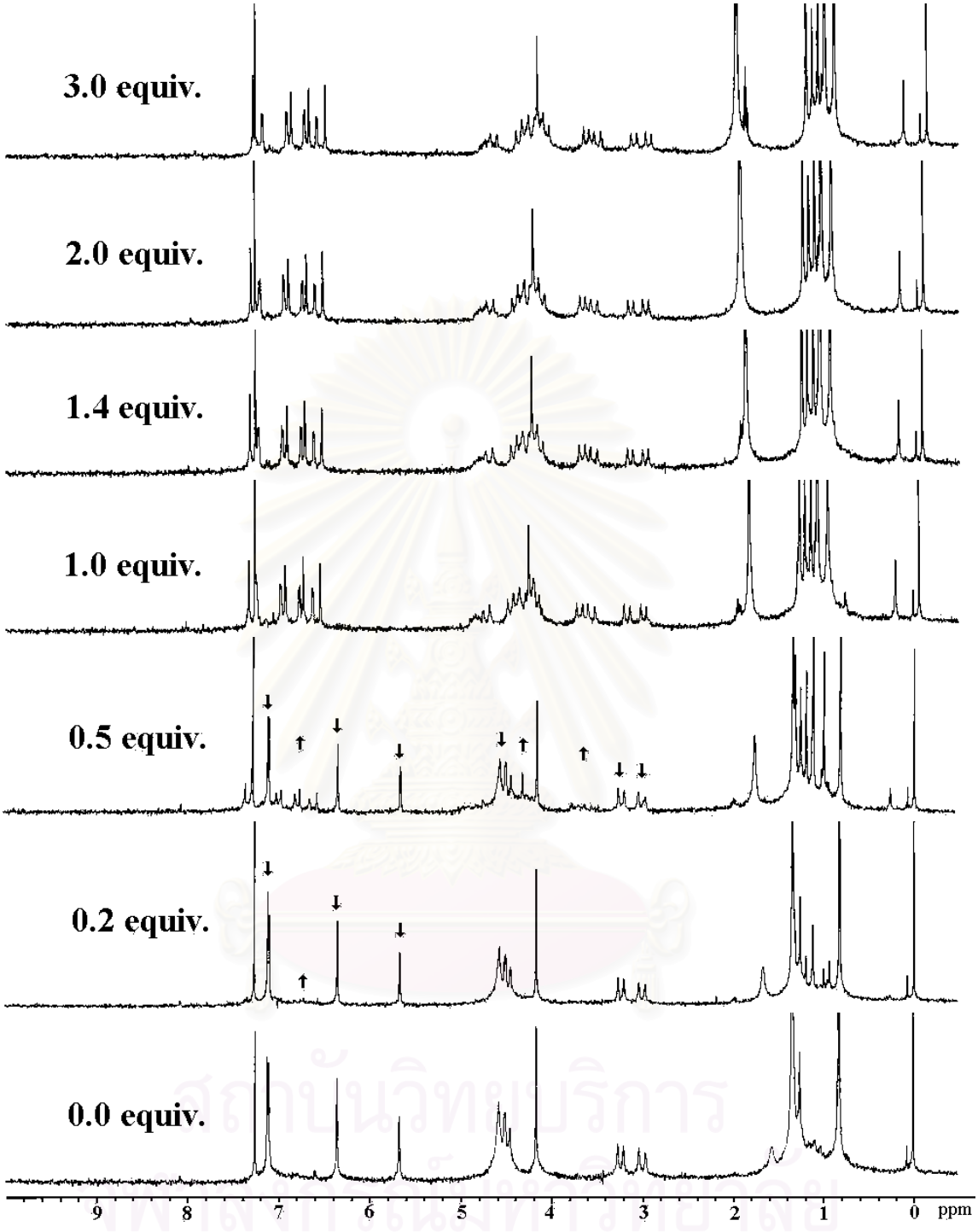

Figure 3.17 : ^{1}H-NMR ($CDCl_3$, 200 MHz) spectra of ligand **5c** with $NaClO_4$

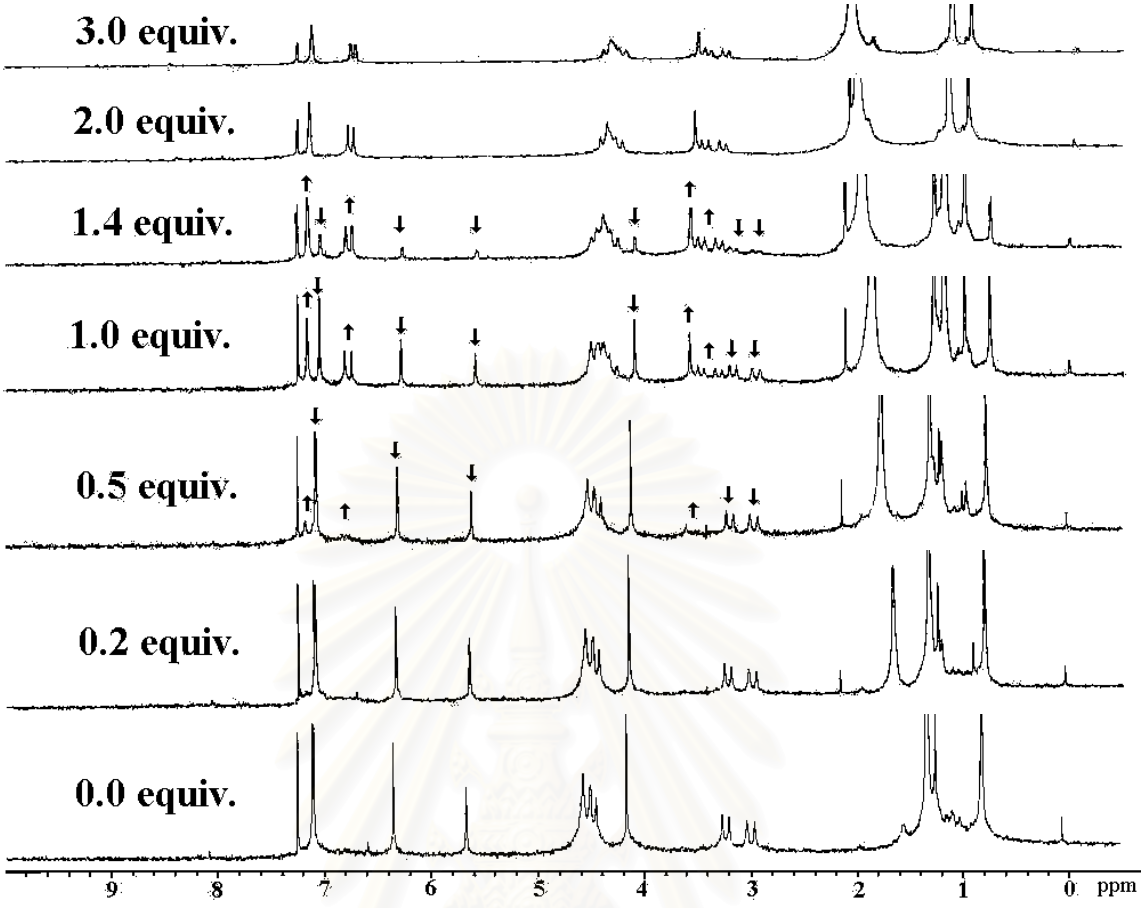

Figure 3.18 : ^{1}H-NMR ($CDCl_3$, 200 MHz) spectra of ligand **5c** with KPF_6

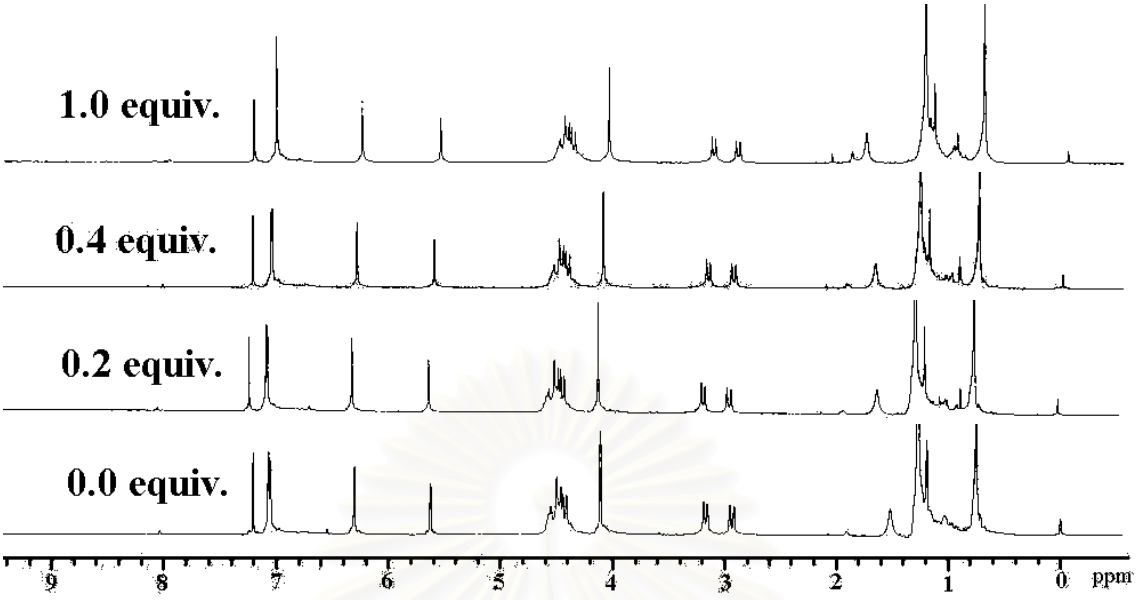

Figure 3.19 : ^{1}H-NMR ($CDCl_3$, 400 MHz) spectra of ligand **5c** with $CsPF_6$

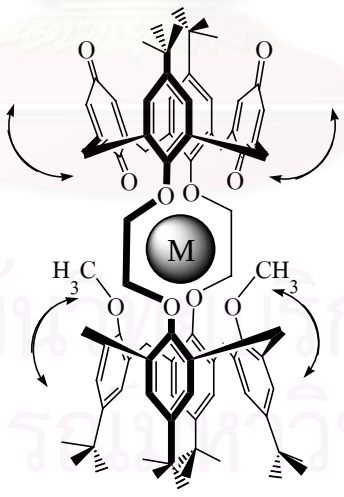

M = Li^+, Na^+ and K^+

Figure 3.20 : A proposed structure of complexation between ligand **5c** with various cations

3.2.4 Calculation of the Complexation Constant [45]

Nuclear magnetic resonance (NMR) spectroscopy is one of the most useful techniques available to chemists for the investigation of dynamic molecular process. Most basic treatments of NMR include at least a qualitative description of the effect of "exchange", reversible dynamic processes, on the appearance of NMR spectra.

One of the most active areas in modern chemical research involves "molecular recognition", the formation of so-called host-guest (or H-G) complexes (C).

$$H + G \underset{k_{-1}}{\overset{k_1}{\rightleftharpoons}} C \qquad (1)$$

$$K = \frac{k_1}{k_{-1}} = \frac{[C]}{[H]\,[G]} = \frac{n_c}{n_h\,[G]} = \frac{n_c}{(1-n_c)\,[G]} \qquad (2)$$

Where n_h is the mole fraction of uncomplexed host and n_c is the mole fraction of complexed host.

To use NMR methods to study such complexation phenomena, at least one site in the uncomplexed host (or guest) molecule must give rise to a signal at a chemical shift δ_h that is significantly different from the same site in the complexed host (or guest) molecule (δ_c). The magnitude of this difference ($\Delta\delta = \delta_h - \delta_c$) often gives information about the structure of the complex, and may be as large as several ppm.

With this information, we can determine the value of K under slow-exchange conditions by first rewriting equation **2** as

$$K = \frac{[C]}{([H]_o - [C])\,([G]_o - [C])} \qquad (3)$$

Where $[H]_o$ and $[G]_o$ are the formal (i.e., initial) concentration of host and guest ($[C]_o = 0$). The relative signal integrals at δ_h and δ_c give

$$\frac{I_c}{I_c + I_h} = n_c \qquad \text{(slow exchange)} \qquad (4)$$

and

$$[C] = n_c [H]_o \qquad (5)$$

Thus, equation **3** can be rewritten as

$$K = \frac{n_c / [H]_o}{(1 - n_c)(R - n_c)} \qquad (6)$$

Where R is the ratio $[G]_o/[H]_o$.

By using equation **6**, the complexation constant (K) can be calculated as shown in Table 3.1

Table 3.1 : Complexation Constant between double calix[4]arenequinones **5a**, **5b** and **5c** with alkali cations.

Alkaline cation	Ligand **5a**	Ligand **5b**	Ligand **5c**
Li^+	30415	897	860
Na^+	44335	9771	5112
K^+	1421	12993	458
Cs^+	NC^{**}	13748	NC^{**}

NC^{**} = No evidence of complexation was observed.

According to the results shown in Table 3.1, ligand **5a** and **5c** form a very stable complexes with Na^+ and exhibit the selectivity trend as $Na^+ > Li^+ >> K^+$ and $Na^+ >> Li^+ > K^+$ respectively. Both ligands **5a** and **5c** show high selectivity to Na^+ due to the optimal spacial fit of the sodium cation within the cavity of the ligands. In contrast, both ligands **5a** and **5c** exhibit low complexation constant with K^+ and no complexation with Cs^+ which could explain by the size of the cation which is larger than Na^+ and Li^+ and larger

than the cavity size. The smaller cavity size of ligand **5c** due to the steric from two methyl groups causes the complexation constants of ligand **5c** with various cations lower than those of ligand **5a**. In the case of ligand **5b**, it forms the most stable complex with Cs^+ and the least stable complex with Li^+. Its selectivity with larger cations such as K^+ and Cs^+ occurred due to the large cavity of the ligand and showed the binding trend as $Cs^+ > K^+ > Na^+ >> Li^+$. We expect that **5a**, **5b** and **5c** would be good sensors for Li^+, Na^+, K^+ and Cs^+. These sensoring properties will be studied by cyclic voltammetry and square wave voltammetry.

3.3 Electrochemical studies

Quinones are commonly used as a reflection of its importance in natural electron transfer systems. In nonaqueous aprotic solvents, quinones undergo two consecutive one-electron transfer processes. In addition, the reduced form of quinone can undergo a chemical reaction to produce hydroquinone according to the following equations.

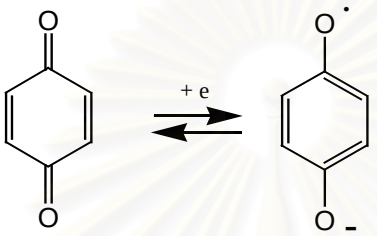

(3.1)

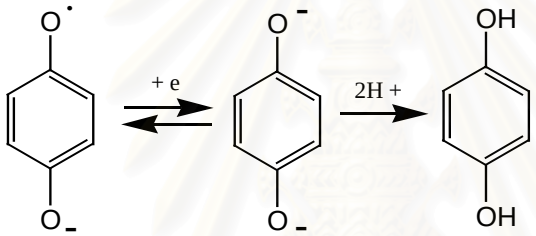

(3.2)

From cation complexation studies, double calix[4]arenequinones **5a**, **5b** and **5c** have been tested for the recognition of alkali cations. In this section, it is of interest to study their interactions with guest cations, in connection with the possibility of electrochemically recognizing alkali cations.

3.3.1 Electrochemical studies of ligand 5a with Li^+, Na^+ and K^+

In the light of the results from NMR titration experiments, ligand **5a** can form complexes with Li^+, Na^+ and K^+; therefore, we investigate the electrochemical properties of **5a** in the presence of Li^+, Na^+ and K^+.

The cyclic voltammogram of ligand **5a** in the mixture of CH_2Cl_2 and CH_3CN (4:1) are presented in Figure 3.21(A). Ligand **5a** exhibits essentially three broad redox waves at -1269, -1394 and -1510 mV, which implies multielectron transfers. Although ligand **5a** has four quinone molecules, one would expect to see 8 one-electron transfer signals in the voltammogram. By taking into account the known behavior of a calix[4]diquinone which can accept a total of four electrons by sequential two-electron reduction process,[26,30-31] the first large quasi-reversible redox wave designated as Ic (cathodic), with a related anodic peak Ia may be attributed to a four-electron reduction process in which a one-electron transfer takes place to each of the quinone moieties present in the ligand to form radical anions. The second and the third more cathodic waves, quasi-reversible reduction IIc and IIIc (related to anodic peak IIa and IIIa, respectively) are consistent with another two-electron reduction process which leads to the formation of dianions. Addition of $LiClO_4$ to electrochemical solution of ligand **5a**, Figure 3.21, led in all cases to the evolution of two new redox waves at -756 and -998 mV, IVc and Vc (related to anodic peak IVa and Va) that were substantially positively shifted relative to wave Ic, which diminished in current height concomitant with the growth of the new waves. Addition of 1.0 equiv. of $LiClO_4$ causes redox waves Ic, IIc and IIIc disappeared and found wave VIc at -1528 mV with a related anodic peak Va instead. The difference in peak potential between the complex and free ligand **5a** is shown in Table 3.3. Squarewave voltammograms also support the result that not only the new waves (IVc and Vc) gradually appears at less negative potential and increases but also the initial wave (Ic, IIc and IIc) decreases and disappears completely as shown in Figure 3.25.

In the case of Na^+, addition of 1.0 equiv. of $NaClO_4$ causes redox waves Ic, IIc and IIIc disappeared as shown in Figure 3.22. Three new redox waves at -1187, -1037 and -933 mV, VIc, Vc and IVc (related to anodic peak VIa, Va and IVa, respectively) appeared and suggested for the complex between ligand **5a** and sodium ion. The difference in peak potential between the complex and the free ligand **5a** is shown in Table

3.3. Square wave voltammograms also support the result that not only the new waves (IVc, Vc and VIc) gradually appear at less negative potential and increase but also the initial wave (Ic, IIc and IIIc) decreases and disappears completely as shown in Figure 3.26.

Upon addition of 1.0 equiv. of KPF_6 to the solution causes redox waves IIc and IIIc disappear as shown in Figure 3.23. A new irreversible redox wave at -1187 mV, Vc and one quasi-reversible wave at -994 mV, IVc (related to anodic peak IVa) appear and suggest the complex between ligand **5a** and potassium cation takes place. Quasi-reversible initial wave Ic became irreversible. The difference in peak potential between the complex and free ligand **5a** is shown in Table 3.3. The squarewave voltammograms (Figure 3.27) support the result that not only the new waves (IVc and Vc) gradually appear at less negative potential and increase but also the initial waves (IIc and IIIc) decrease and disappear completely.

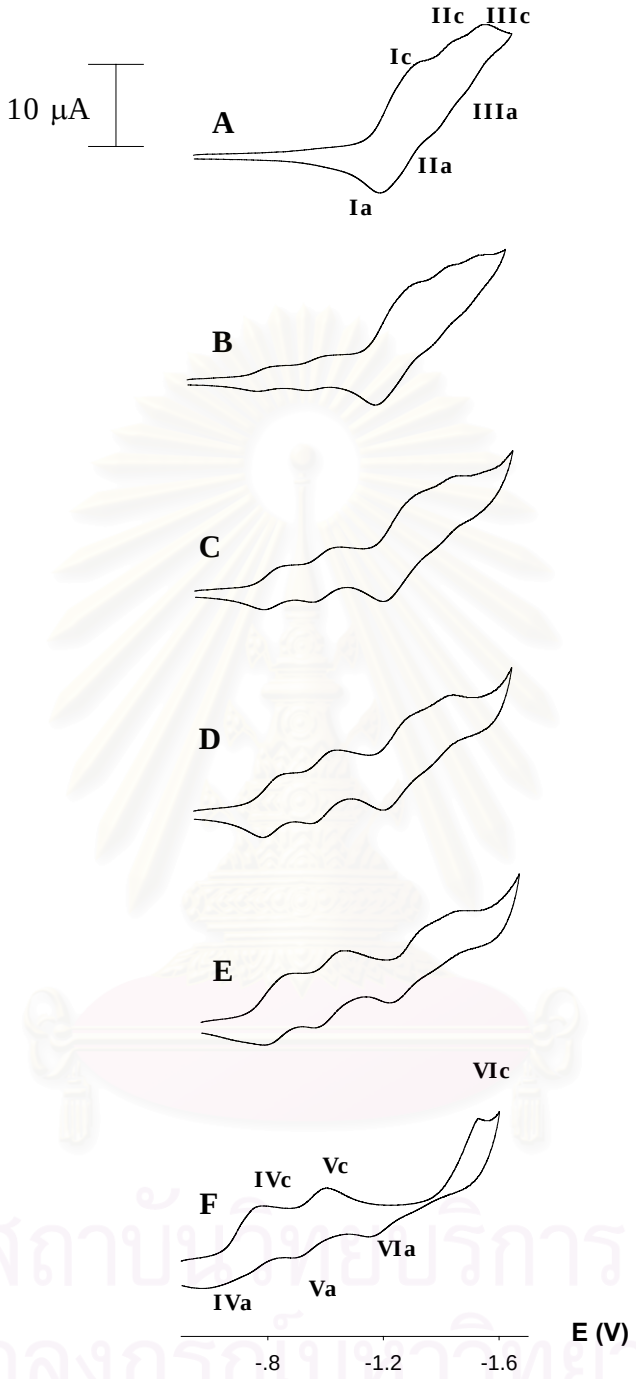

Figure 3.21 : CV of ligand **5a** + Li^+ (A) 0.0 equiv. (B) 0.2 equiv. (C) 0.4 equiv. (D) 0.6 equiv. (E) 0.8 equiv. (F) 1.0 equiv.

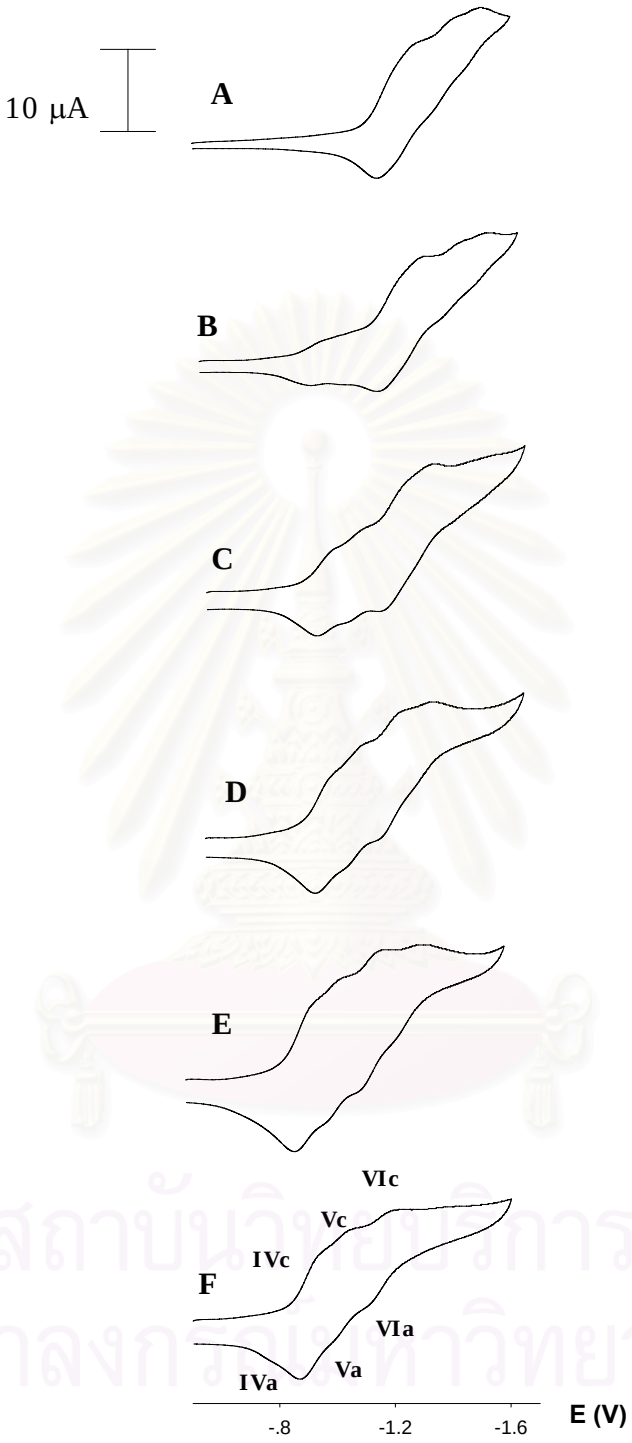

Figure 3.22 : CV of ligand **5a** + Na^+ (A) 0.0 equiv. (B) 0.2 equiv. (C) 0.4 equiv. (D) 0.6 equiv. (E) 0.8 equiv. (F) 1.0 equiv.

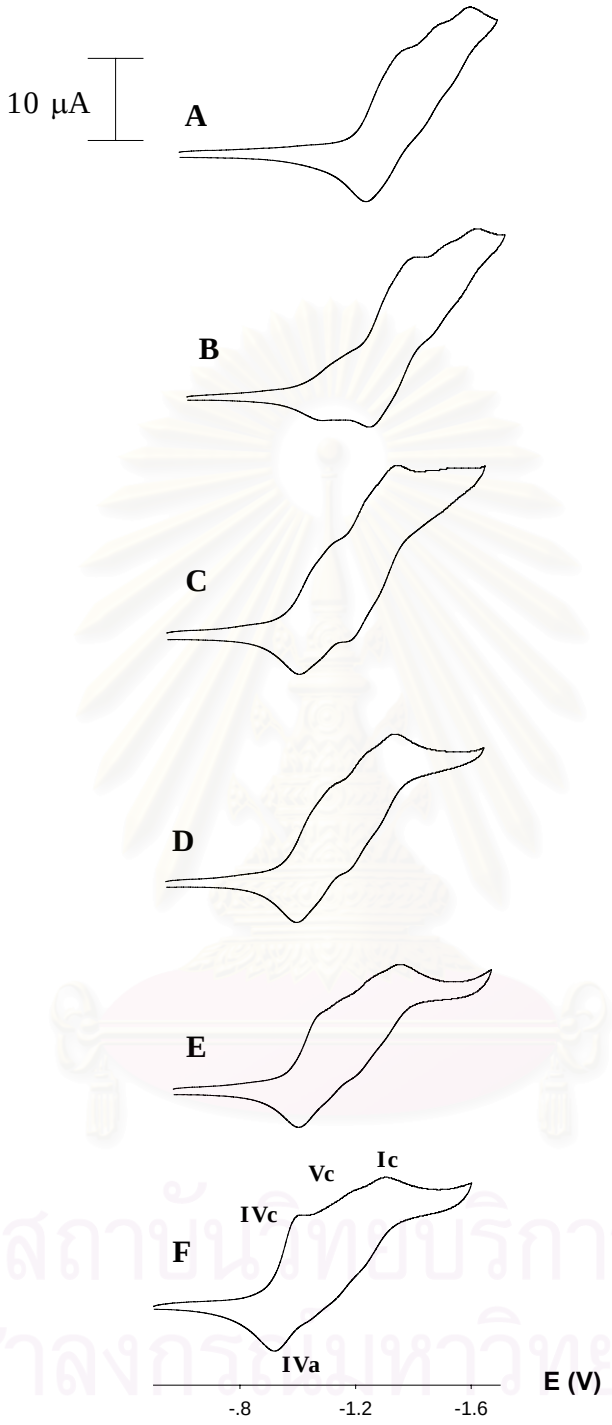

Figure 3.23 : CV of ligand **5a** + K^+ (A) 0.0 equiv. (B) 0.2 equiv. (C) 0.4 equiv. (D) 0.6 equiv. (E) 0.8 equiv. (F) 1.0 equiv.

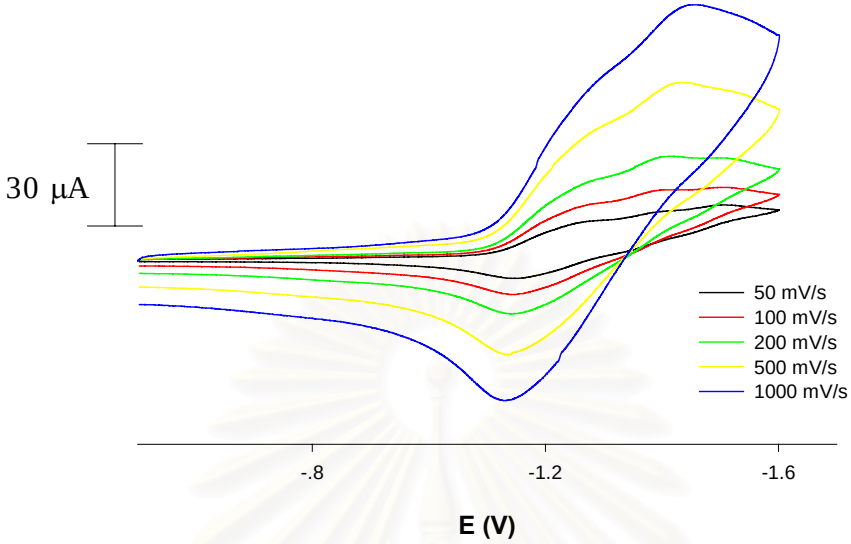

Figure 3.24 : CV of ligand **5a** at various scan rates

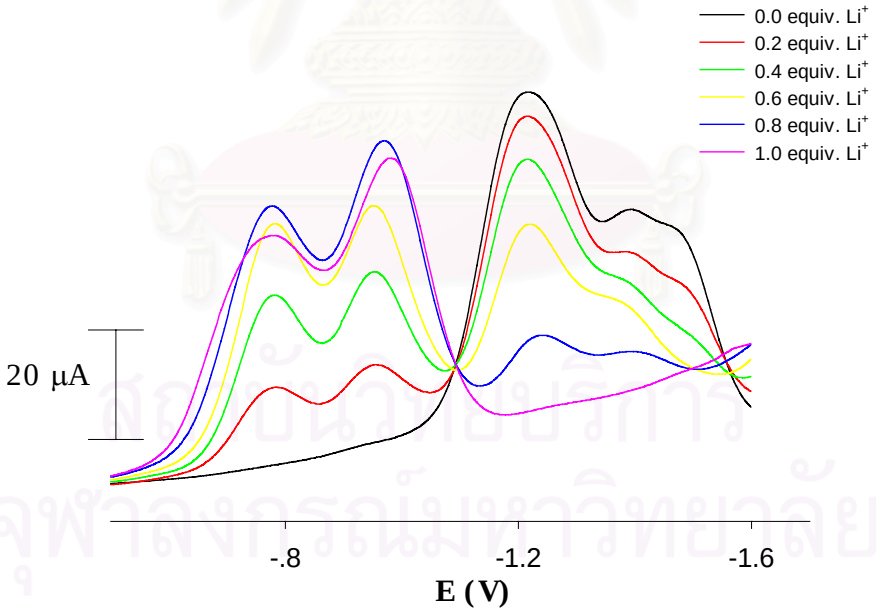

Figure 3.25 : SWV of ligand **5a** + Li^+

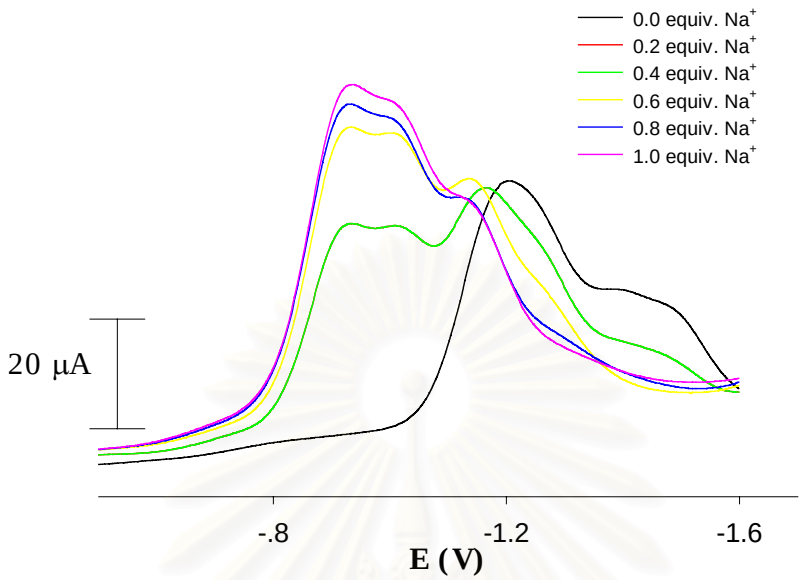

Figure 3.26 : SWV of ligand **5a** + Na^+

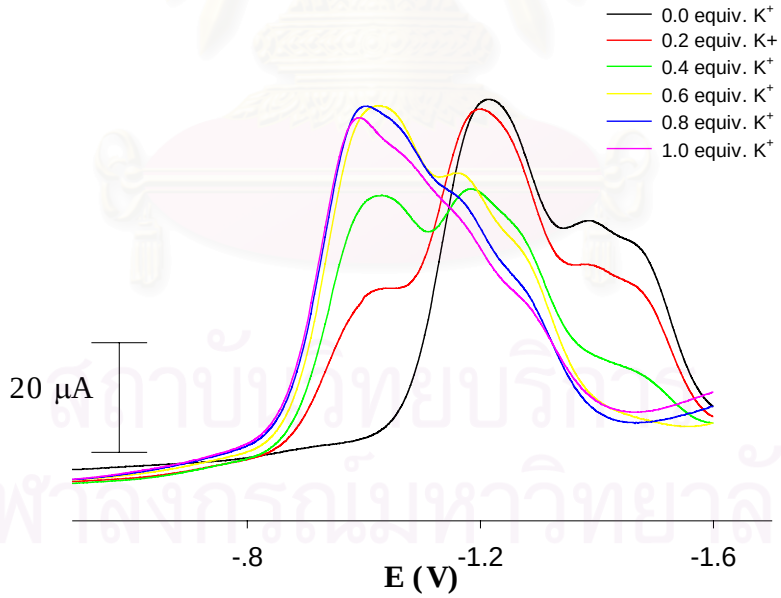

Figure 3.27 : SWV of ligand **5a** + K^+

3.3.2 Electrochemical studies of ligand 5b with Li^+, Na^+, K^+ and Cs^+

In the light of the results from NMR titration experiments, ligand **5b** can form complexes with Li^+, Na^+, K^+ and Cs^+; therefore, we investigate the electrochemical properties of **5b** in the presence of Li^+, Na^+, K^+ and Cs^+.

The cyclic voltammogram of ligand **5b** in the mixture of CH_2Cl_2 and CH_3CN (4:1) are presented in Figure 3.28(A). Compared to the ligand **5a**, ligand **5b** exhibits essentially two broad redox waves at -1269 and -1370 mV, which implies multielectron transfers. The first quasi-reversible redox wave designated as Ic (cathodic), with a related anodic peak Ia may be attributed to a four-electron reduction process in which a one-electron transfer takes place to each of the quinone moieties present in the ligand to form radical anions. The second more cathodic wave, quasi-reversible reduction IIc (related to anodic peak IIa) is consistent with another four-electron reduction process which leads to the formation of dianions. Addition of $LiClO_4$ to electrochemical solution of ligand **5b**, Figure 3.28, led in all cases to the evolution of two new redox waves at -765 and -936 mV, IIIc and IVc (related to anodic peak IIIa and IVa, respectively) that were substantially positively shifted relative to wave Ic, which diminished in current height concomitant with the growth of the new waves. Addition of 1.0 equiv. of $LiClO_4$ causes redox waves Ic and IIc reduced. The difference in peak potential between the complex and free ligand **5b** is shown in Table 3.3. Squarewave voltammograms also support the result that not only the new waves (IIIc and IVc) gradually appear at less negative potential and increase but also the initial waves (Ic and IIc) decrease as shown in Figure 3.33.

In the case of Na^+, addition of 1.0 equiv. of $NaClO_4$ causes redox waves Ic and IIc reduced as shown in Figure 3.29. Two new redox waves at -906 and -1040, IIIc and IVc (related to anodic peak IIIa and IVa, respectively) appeared and suggested for the complex between ligand **5b** and sodium cation. The difference in peak potential between the complex and the free ligand **5b** is shown in Table 3.3. Square wave voltammograms also support the result that not only the new waves (IIIc and IVc) gradually appear at less negative potential and increase but also the initial waves (Ic and IIc) decrease as shown in Figure 3.34.

Upon addition of 1.0 equiv. of KPF_6 to the solution causes redox waves Ic and IIc decreased as shown in Figure 3.30. Two new redox waves at -1016 and -1150 mV, IIIc and IVc (related to anodic peak IIIa and IVa, respectively) appear and suggest the complex between ligand **5b** and potassium cation takes place. The difference in peak potential between the complex and free ligand **5b** is shown in Table 3.3. The squarewave voltammograms (Figure 3.35) support the result that not only the new waves (IIIc and IVc) gradually appear at less negative potential and increase but also the initial waves (Ic and IIc) decrease.

With Cs^+, addition to 1.0 equiv. $CsPF_6$ causes redox waves Ic and IIc decreased as shown in Figure 3.31. Two new redox waves at -1022 and -1156 mV, IIIc and IVc (related to anodic peak IIIa and IVa, respectively) appear and suggest the complex between ligand **5b** and cesium cation takes place. The difference in peak potential between the complex and free ligand **5b** is shown in Table 3.3. The squarewave voltammograms (Figure 3.36) support the result that not only the new waves (IIIc and IVc) gradually appear at less negative potential and increase but also the initial waves (Ic and IIc) decrease.

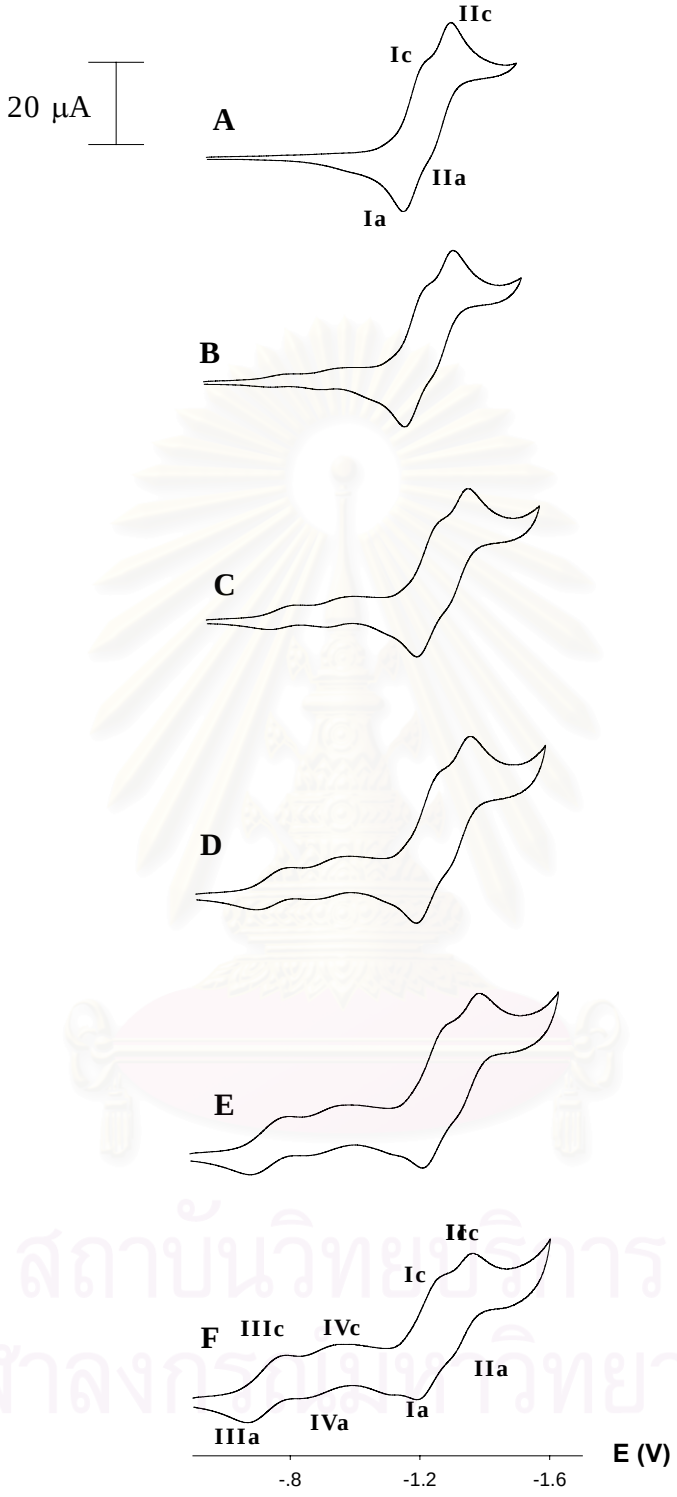

Figure 3.28 : CV of ligand **5b** + Li^+ (A) 0.0 equiv. (B) 0.2 equiv. (C) 0.4 equiv. (D) 0.6 equiv. (E) 0.8 equiv. (F) 1.0 equiv.

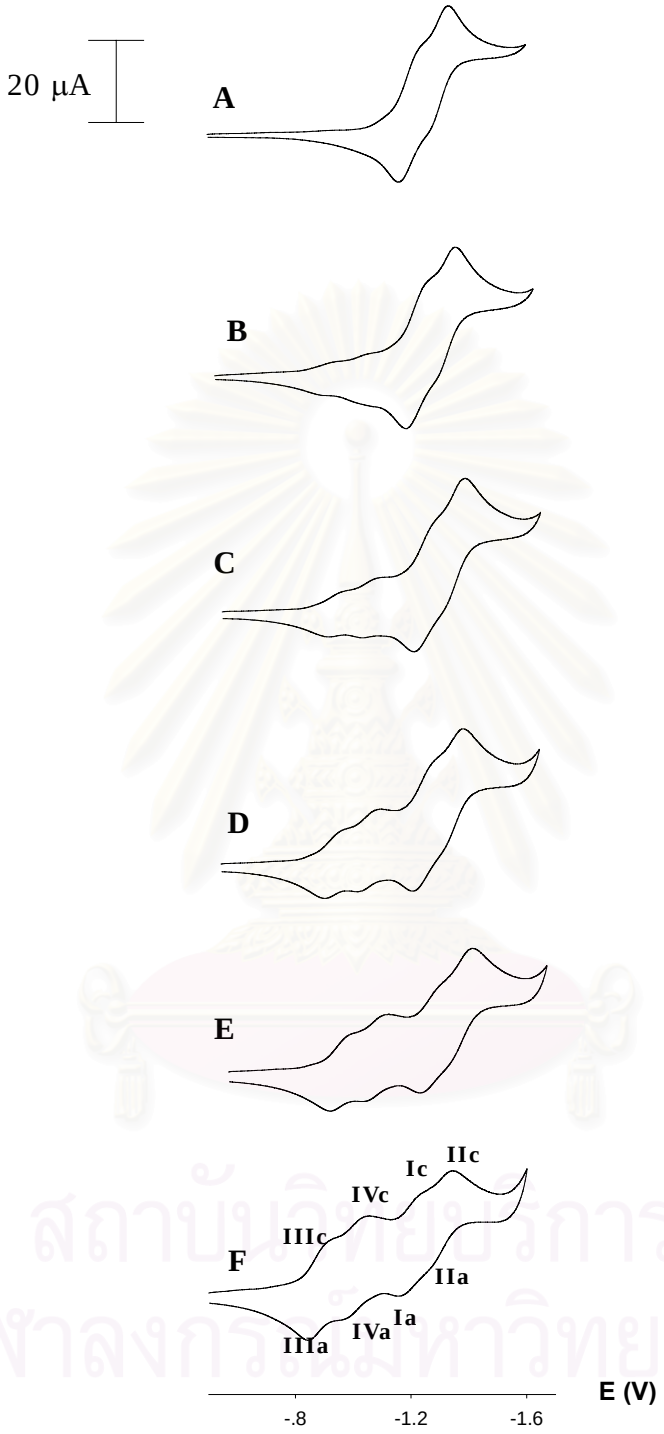

Figure 3.29 : CV of ligand **5b** + Na^+ (A) 0.0 equiv. (B) 0.2 equiv. (C) 0.4 equiv. (D) 0.6 equiv. (E) 0.8 equiv. (F) 1.0 equiv.

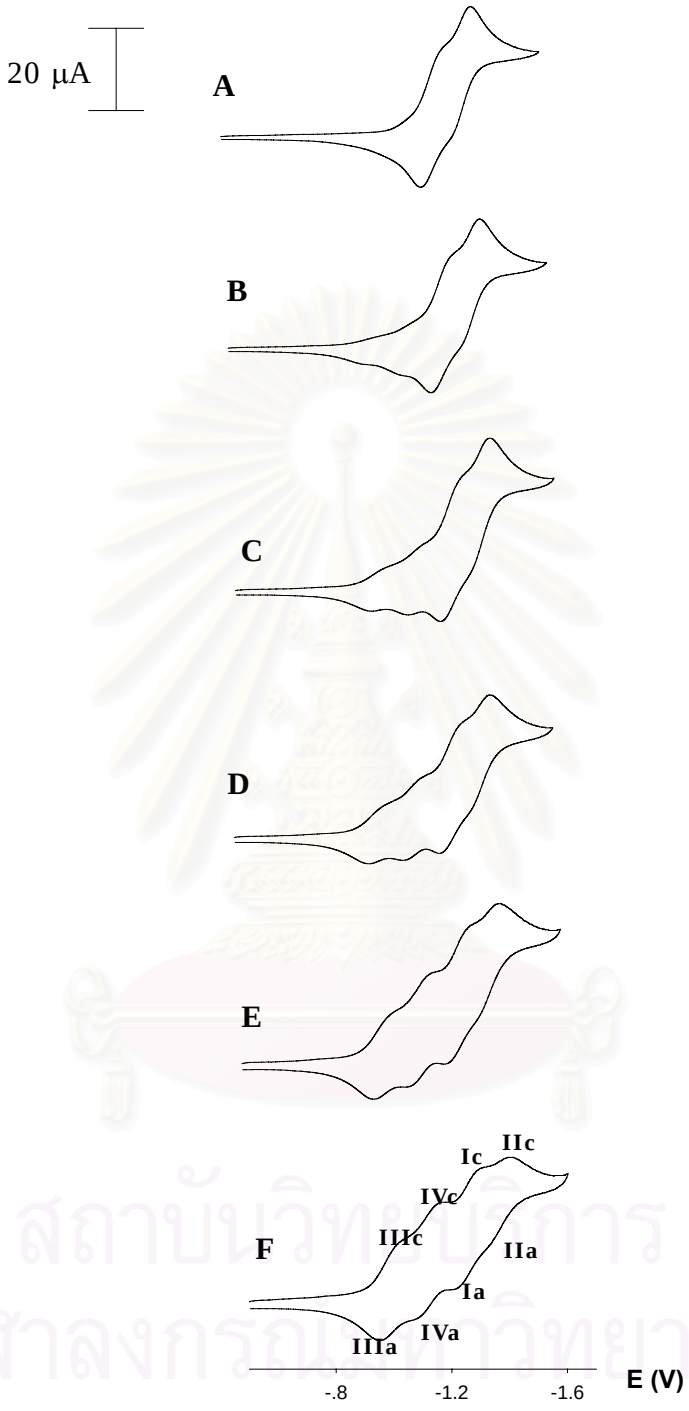

Figure 3.30 : CV of ligand **5b** + K^+ (A) 0.0 equiv. (B) 0.2 equiv. (C) 0.4 equiv. (D) 0.6 equiv. (E) 0.8 equiv. (F) 1.0 equiv.

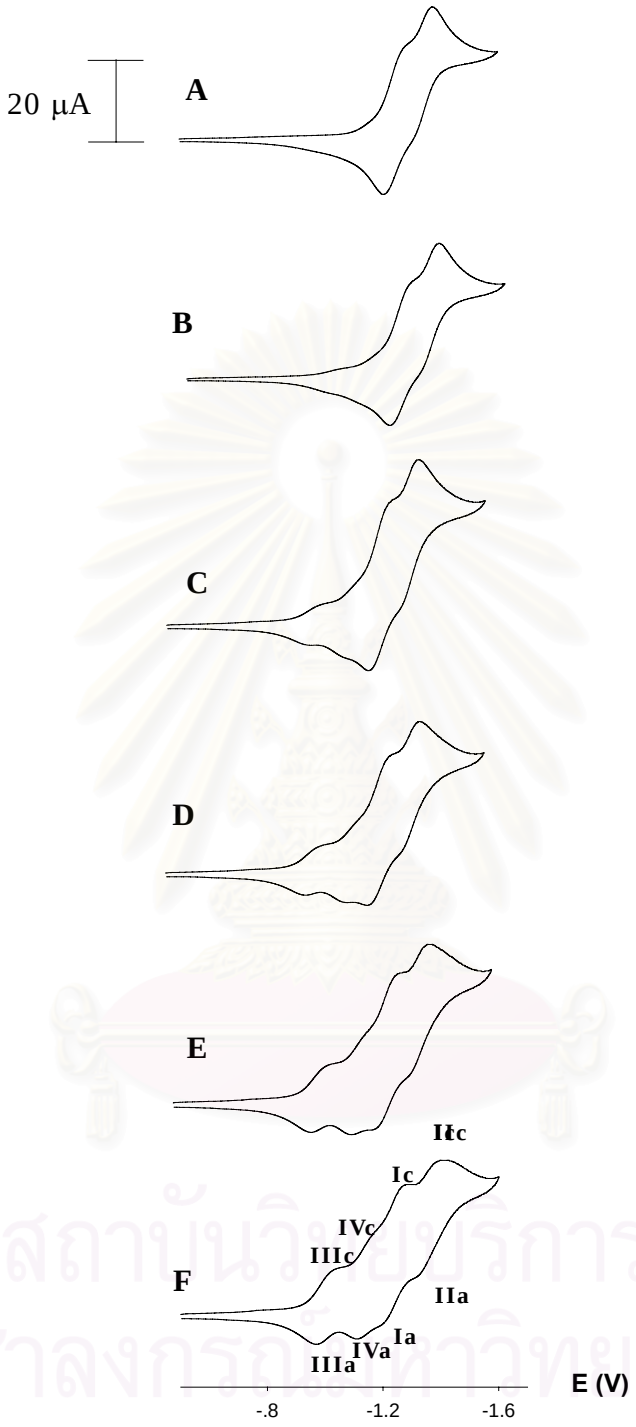

Figure 3.31 : CV of ligand **5b** + Cs^{+} (A) 0.0 equiv. (B) 0.2 equiv. (C) 0.4 equiv. (D) 0.6 equiv. (E) 0.8 equiv. (F) 1.0 equiv.

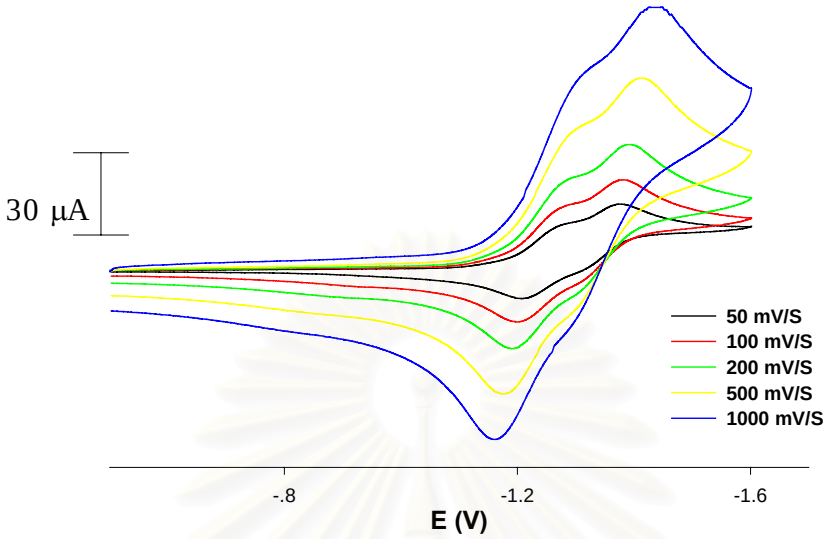

Figure 3.32 : CV of ligand **5b** at various scan rates

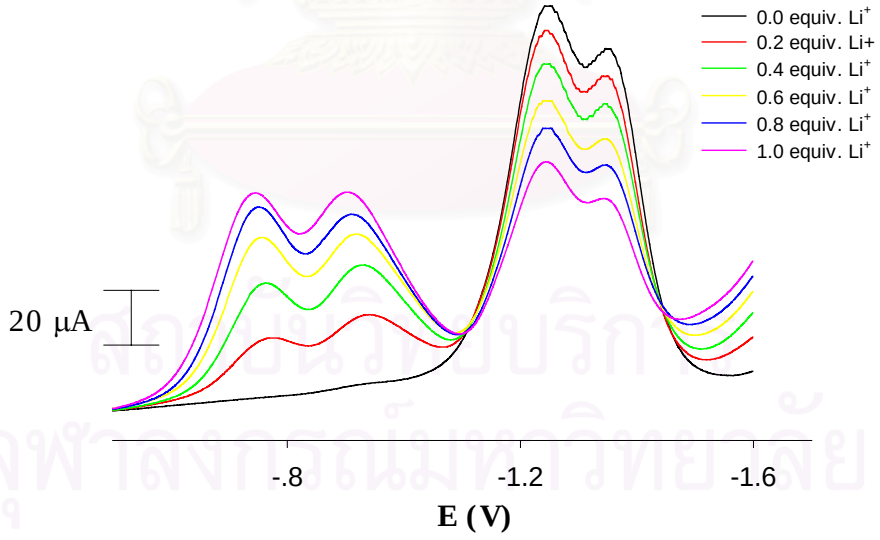

Figure 3.33 : SWV of ligand **5b** + Li^+

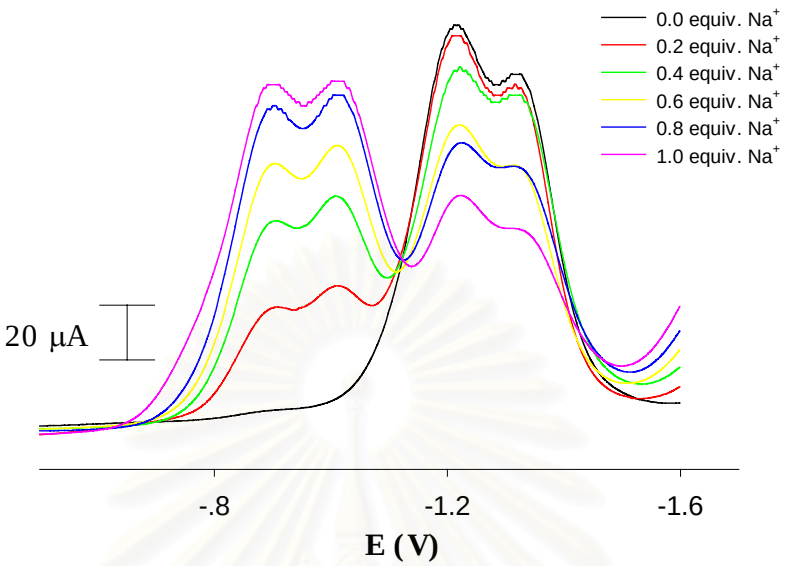

Figure 3.34 : SWV of ligand **5b** + Na^+

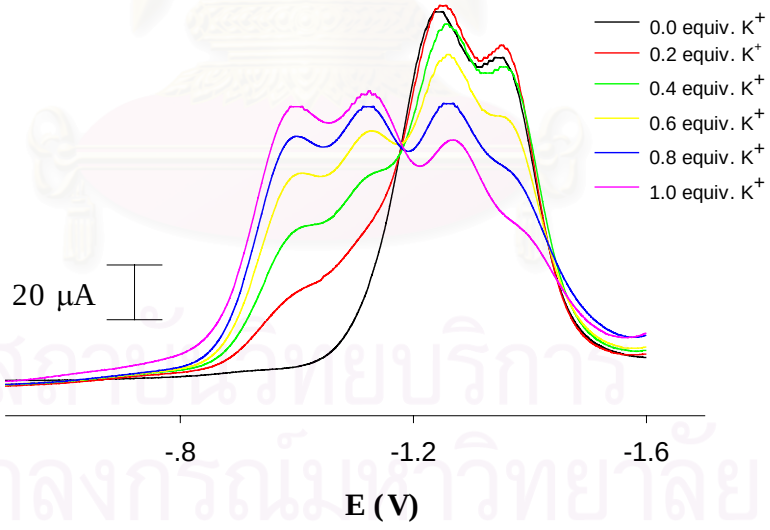

Figure 3.35 : SWV of ligand **5b** + K^+

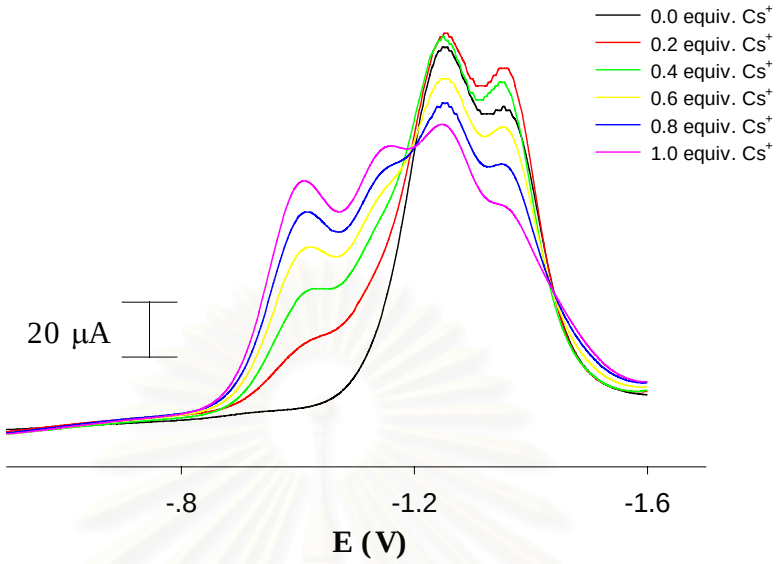

Figure 3.36 : SWV of ligand **5b** + Cs^{+}

3.3.3. Electrochemical studies of ligand 5c with Li^+, Na^+ and K^+

In the light of the results from NMR titration experiments, ligand **5c** can form complexes with Li^+, Na^+ and K^+; therefore, we investigate the electrochemical properties of **5c** in the presence of Li^+, Na^+ and K^+.

The cyclic voltammogram of ligand **5c** in the mixture of CH_2Cl_2 and CH_3CN (4:1) are presented in Figure 3.37(A). Ligand **5c** exhibits essentially two broad redox waves at -1300 and -1477 mV, which implies multielectron transfers. Althought ligand **5c** has two quinone molecules, one would expect to see 4 one-electron transfer signals in the voltammogram. By taking into account the known behavior of a calix[4]diquinone which can accept a total of four electrons by sequential two-electron reduction process. [26,30-31], the first quasi-reversible redox wave designated as Ic (cathodic), with a related anodic peak Ia may be attributed to a two-electron reduction process in which a one-electron transfer takes place to each of the quinone moieties present in the ligand to form radical anions. The second more cathodic wave, quasi-reversible reduction IIc (related to anodic peak IIa) is consistent with another two-electron reduction process which leads to the formation of dianions. Addition of $LiClO_4$ to electrochemical solution of ligand **5c**, Figure 3.37, led in all cases to the evolution of new quasi-reversible wave at -1049 mV, IIIc (related to anodic peak IIIa) that was substantially positively shifted relative to wave Ic, which diminished in current height concomitant with the growth of the new wave. Addition of 1.0 equiv. of $LiClO_4$ causes redox waves IIc disappeared and found Ic became an irreversible wave. The difference in peak potential between the complex and free ligand **5c** is shown in Table 3.3. Squarewave voltammograms also support the result that not only the new wave IIIc gradually appears at less negative potential and increases but also the initial wave IIc decreases and disappears completely as shown in Figure 3.41.

In the case of Na^+, addition of 1.0 equiv. of $NaClO_4$ causes redox waves Ic and IIc disappeare as shown in Figure 3.38. Two new redox waves at -906 and -1040, IIIc and IVc (related to anodic peak IIIa and IVa, respectively) appeared and suggested for the complex between ligand **5b** and sodium cation. The difference in peak potential between the complex and the free ligand **5b** is shown in Table 3.3. Square wave voltammograms also support the result that not only the new waves (IIIc and IVc) gradually appear at less

negative potential and increase but also the initial waves (Ic and IIc) decrease and disappear as shown in Figure 3.42.

Upon addition of 1.0 equiv. of KPF_6 to the solution causes redox waves Ic and IIc disappeared as shown in Figure 3.39. Two new redox waves at -946 and -1110 mV, IIIc and IVc (related to anodic peak IIIa and IVa, respectively) appear and suggest the complex between ligand **5c** and potassium cation takes place. The difference in peak potential between the complex and free ligand **5c** is shown in Table 3.3. The squarewave voltammograms (Figure 3.43) support the result that not only the new waves (IIIc and IVc) gradually appear at less negative potential and increase but also the initial waves (Ic and IIc) decrease and disappear completely.

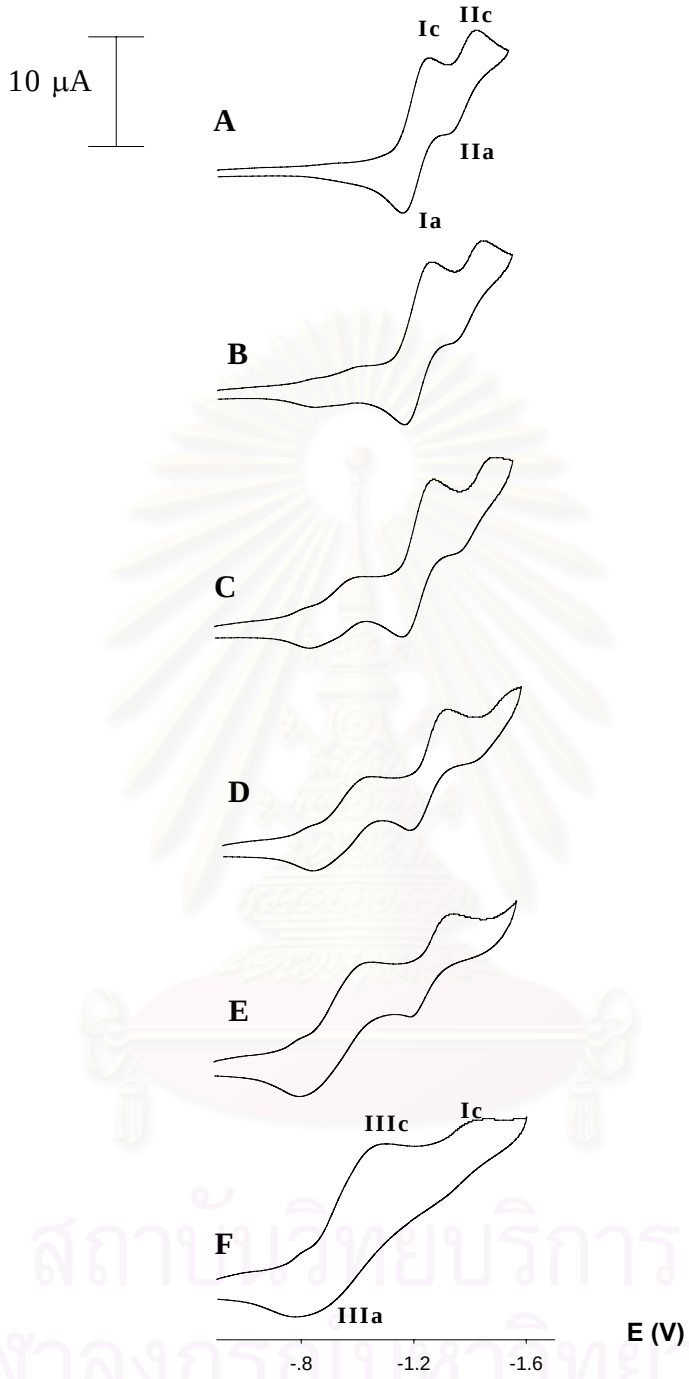

Figure 3.37 : CV of ligand **5c** + Li^+ (A) 0.0 equiv. (B) 0.2 equiv. (C) 0.4 equiv. (D) 0.6 equiv. (E) 0.8 equiv. (F) 1.0 equiv.

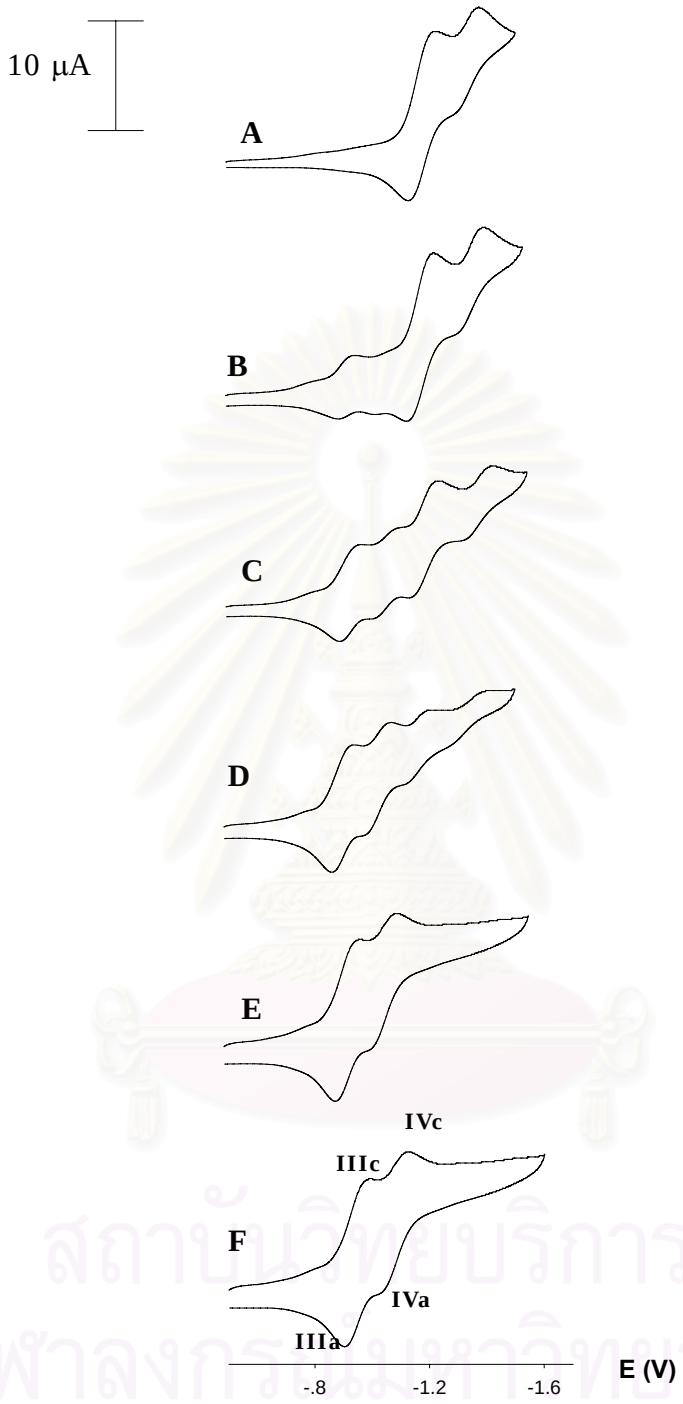

Figure 3.38 : CV of ligand **5c** + Na^+ (A) 0.0 equiv. (B) 0.2 equiv. (C) 0.4 equiv. (D) 0.6 equiv. (E) 0.8 equiv. (F) 1.0 equiv.

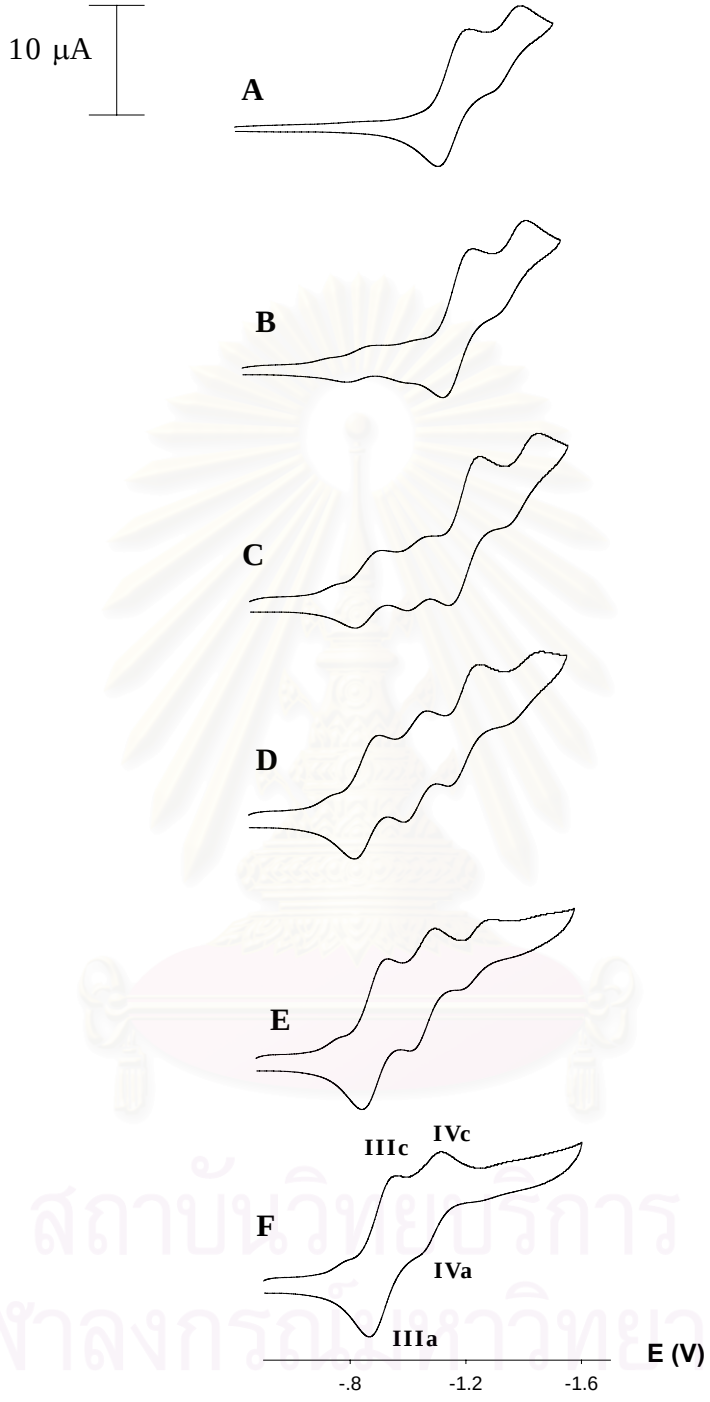

Figure 3.39 : CV of ligand **5c** + K^+ (A) 0.0 equiv. (B) 0.2 equiv. (C) 0.4 equiv. (D) 0.6 equiv. (E) 0.8 equiv. (F) 1.0 equiv.

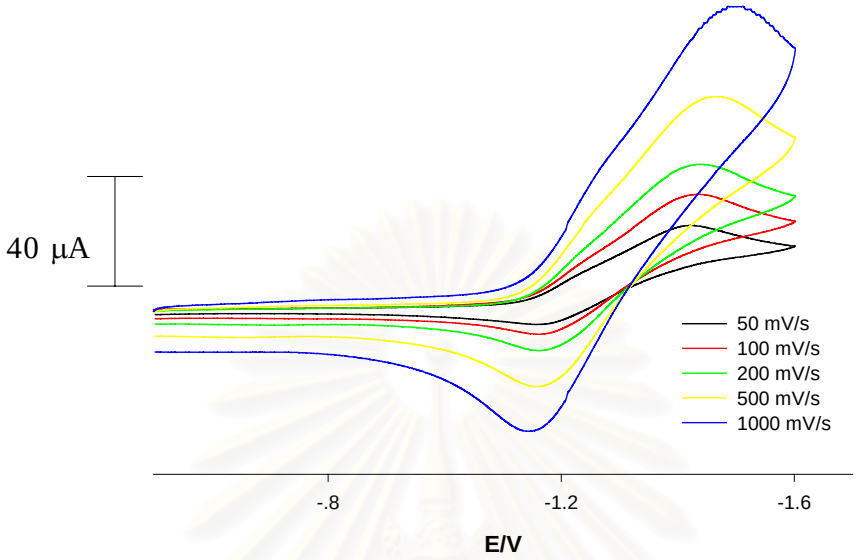

Figure 3.40 : CV of ligand **5c** at various scan rates

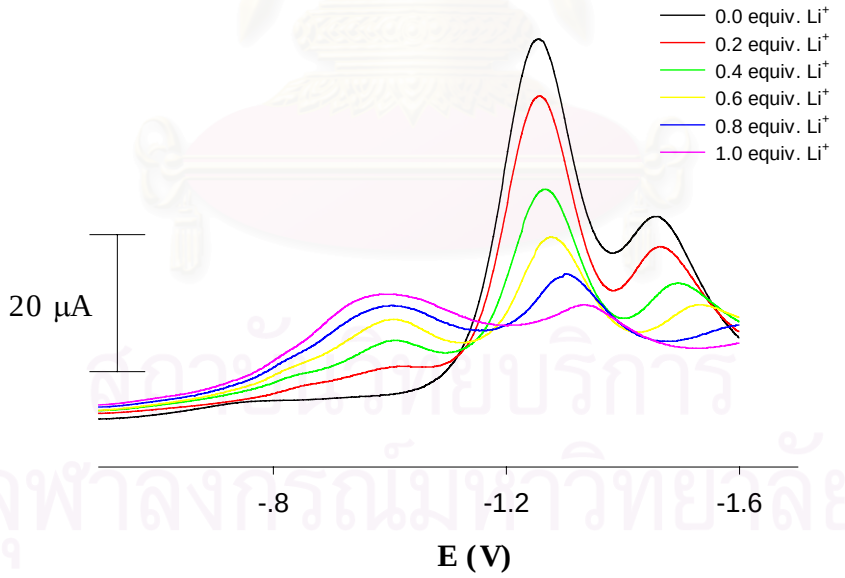

Figure 3.41 : SWV of ligand **5c** + Li^+

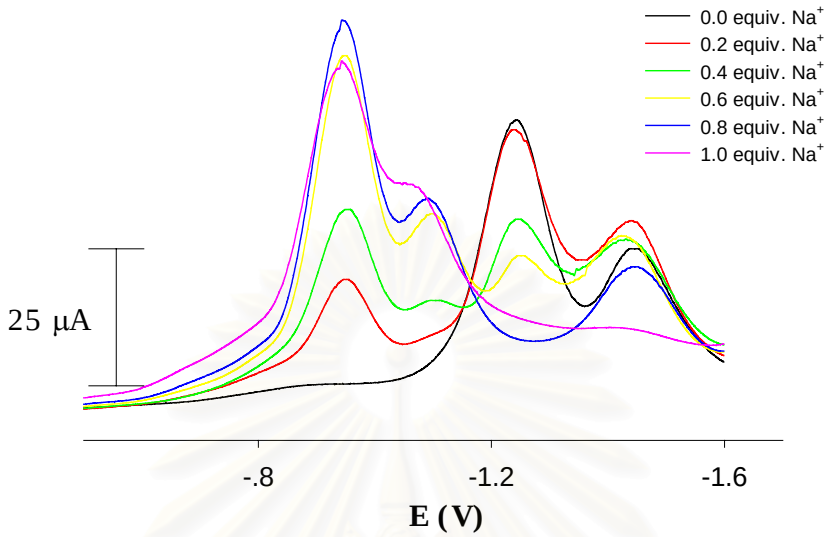

Figure 3.42 : SWV of ligand **5c** + Na^+

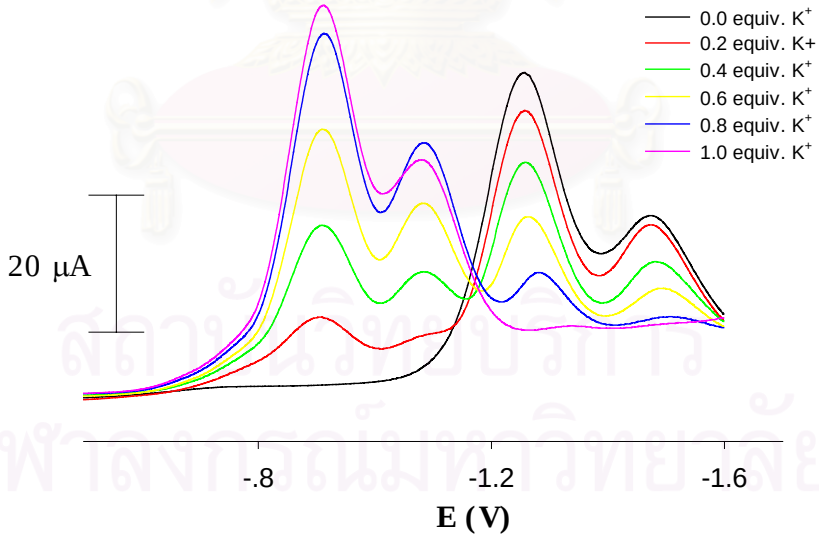

Figure 3.43 : SWV of ligand **5c** + K^+

Table 3.2 : Electrochemical data of ligands **5a**, **5b** and **5c** and their complexes with alkali cations from Figure 3.21-3.39.

	E(V) of each redox couple (mV)
Free ligand **5a**	Ic (q, -1269), IIc (q, -1394), IIIc (q, -1510)
	Ia (q, -1147), IIa (q, -1345), IIIa (q, -1443)
+ Li^+ 1.0 equiv.	IVc (q, -756), Vc (q, -998), VIc (q, -1528)
	IVa (q, -579), Va (q, -909), VIa (q, -1165)
+ Na^+ 1.0 equiv.	IVc (q, -933), Vc (q, -1037), VIc (q, -1187)
	IVa (q, -872), Va (q, -991), VIa (q, -1116)
+ K^+ 1.0 equiv.	IVc (q, -994), Vc (ir, -1187), Ic (ir, -1503)
	IVa (q, -921)
Free ligand **5b**	Ic (q, -1269), IIc (q, -1370)
	Ia (q, -1202), IIa (q, -1303)
+ Li^+ 1.0 equiv.	IIIc (q, -762), IVc (q, -936), Ic (q, -1254), IIc (q, -1361)
	IIIa (q, -674), IVa (q, -863), Ia (q, -1193), IIa (q, -1303)
+ Na^+ 1.0 equiv.	IIIc (q, -906), IVc (q, -1040), Ic (q, -1226), IIc (q, -1342)
	IIIa (q, -845), IVa (q, -979), Ia (q, -1165), IIa (q, -1284)
+ K^+ 1.0 equiv.	IIIc (q, -1016), IVc (q, -1150), Ic (q, -1290), IIc (q, -1400)
	IIIa (q, -952), IVa (q, -1086), Ia (q, -1220), IIa (q, -1336)
+ Cs^+ 1.0 equiv.	IIIc (q, -1022), IVc (q, -1156), Ic (q, -1269), IIc (q, -1400)
	IIIa (q, -970), IVa (q, -1110), Ia (q, -1205), IIa (q, -1327)
Free ligand **5c**	Ic (q, -1300), IIc (q, -1477)
	Ia (q, -1202), IIa (q, -1388)
+ Li^+ 1.0 equiv.	IIIc (q, -1049), Ic (ir, -1388)
	IIIa (q, -790)
+ Na^+ 1.0 equiv.	IIIc (q, -976), IVc (q, -1123)
	IIIa (q, -903), IVa (q, -1040)
+ K^+ 1.0 equiv.	IIIc (q, -946), IVc (q, -1110)
	IIIa (q, -866), IVa (q, -1052)

Definitions: c, cathodic peak potential; a, anodic peak potential; q, quasi-reversible; ir, irreversible.

Table 3.3: Peak potential shifts for cation complexes with ligand **5a**, **5b** and **5c**.

		Peak potential shifts (mV)
Ligand **5a**	+ Li^+ 1.0 equiv.	I-IV (513), II-V (396), III-VI (18)
	+ Na^+ 1.0 equiv.	I-IV (336), II-V (357), III-VI (323)
	+ K^+ 1.0 equiv.	I-IV (275), II-V (207)
Ligand **5b**	+ Li^+ 1.0 equiv.	I-III (507), II-IV (434)
	+ Na^+ 1.0 equiv.	I-III (363), II-IV (330)
	+ K^+ 1.0 equiv.	I-III (253), II-IV (220)
	+ Cs^+ 1.0 equiv.	I-III (247), II-IV (214)
Ligand **5c**	+ Li^+ 1.0 equiv.	I-III (251)
	+ Na^+ 1.0 equiv.	I-III (324), II-IV (354)
	+ K^+ 1.0 equiv.	I-III (354), II-IV (367)

Definition: X-Y, different cathodic peak potential between ligand at position X and complex at position Y from Figure 3.21-3.39.

In conclusion, ligand **5a**, which has four quinone units, exhibit three redox waves. Unlike ligand **5a**, ligands **5b** and **5c**, which have four and two quinone units exhibit two redox waves. Although ligand **5a** has the same structure as ligand **5b** except the glycolic linkages that are shorter, but cyclic voltammograms show the different redox wave signals. These phenomena can be described due to the poor solubility of ligand **5a** in the mixed solvent during experiments. On addition of alkali cations such as Li^+, Na^+, K^+ or Cs^+, a new set of peaks which indicated for the complex between ligand and cation are observed at a less negative potential than the original free ligand wave. This reflects the

stabilization of the reduced form of dianion and the stabilization of the complex as a result of the intramolecular interaction with ring-bound cation. From Table 3.3, the potential difference between the complex peak and the first peak of ligand is as large as 513 and 507 mV for ligand **5a** and **5b** with Li^+. Anodic shifts from ligand **5a**, **5b** and **5c** with another alkali cations also have high value in the range of 220-440 mV. The ΔE value of ligand **5a** and **5b** after complexation with a series of alkali cations exhibit the trend as $Li^+ > Na^+ > K^+ > Cs^+$ while **5c** exhibits the trend as $K^+ > Na^+ > Li^+$. Ligands **5a** and **5b** possess 4 quinone oxygens while **5c** contains only two quinone oxygens and two etheral oxygens. Therefore, **5a** and **5b** are harder acid than **5c** in the reduced forms and can form more stable complexes with smaller cations (Figure 3.44). This results in a larger shifts of cyclic voltammograms to less negative potential upon addition of metal ions. This suggests that hard-soft acid base shows important role in redox chemistry of the quinone moiety. All these phenomena imply double calix[4]arenequinones **5a**, **5b** and **5c** may be applicable to the fabrication of a molecular device that selectively recognizes a specific cation.

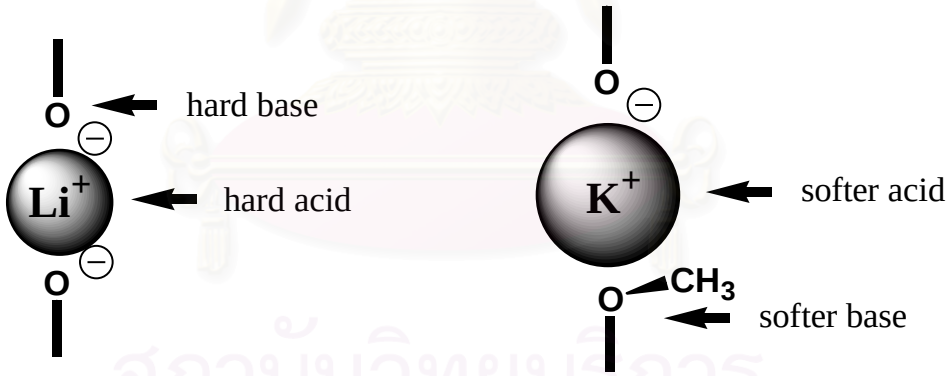

Figure 3.44: Effect of hard-soft acid base to peak potential shifts.

3.3.4 Calculation of binding enhancement factor

In a case when the formal potentials of both free (E_f) and complexed (E_c) forms of a redox active component can be obtained, the ratio of complex formation constants for reduced (K_{red}) and oxidized (K_{ox}) states of this component can be calculated from the difference between the formal potentials. From the cycle shown in Figure 3.44, where M represents the redox-active component and L is the ligand, it follows that [36,46-47]

$$RT\ln K_{ox} + nFE_c = nFE_f + RT\ln K_{red} \quad (\mathbf{7})$$

and

$$\Delta E = E_c - E_f = (RT/nF)\ln(K_{red}/K_{ox}) \quad (\mathbf{8})$$

or

$$K_{red}/K_{ox} = \exp\{\Delta EnF/RT\} \quad (\mathbf{9})$$

Figure 3.45 : Redox and complexation equilibria with a redox-active component M.

From cyclic voltammogram studies of complexes between ligands **5a**, **5b** and **5c** with cations suggested that only CV of ligand **5c** with Na^+ and K^+ can be used to calculated binding enhancement factors. This is due to cyclic voltammograms of ligands **5a** and **5b** with cations were too complicate to describe the mechanism. For ligand **5c** with Na^+ and K^+, the mechanism can described by the process shown in Figure 3.45.

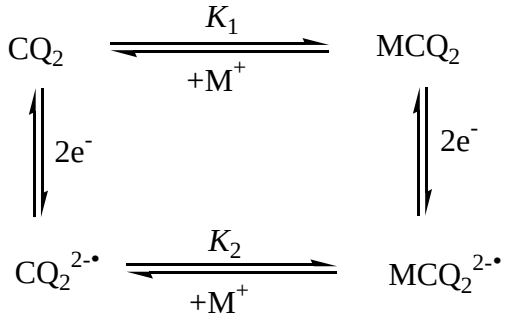

Figure 3.46 : A square sheme for cation binding redox mechanism of ligand **5c**

By using equation **9**, binding enhancement factor of ligand **5c** with Na^+ and K^+ can be calculated. K_2/K_1 values for Na^+ and K^+ complexes with ligand **5c** are 2.08 x 10^5 and 6.53 x 10^5, respectively. This reflects the binding enhancement through electrostatic attractions in the reduced forms. As mentioned above, we can conclude that the reduced forms of quinone prefer to bind cations more than the unreduced form.

CHAPTER 4

CONCLUSION

Three double calix[4]arenes, 25,27-di(ethyleneglycol)-bis-*p-tert*-butylcalix[4]arene, **1**, 25,27-di(diethyleneglycol)-bis-*p-tert*-butylcalix[4]arene, **2b**, and 25,27-di(methoxy)-26,28-di(ethyleneglycol)-bis-*p-tert*-butylcalix[4]arene, **4d**, have been synthesized by coupling reactions between *p-tert*-butylcalix[4]arene and 1,2-dibromoethane, diethylene glycol ditosylate (**2a**) and 25,27-di(methoxy)-26,28-di(methanesulfonyl)ethoxy-*p-tert*-butylcalix[4]arene (**4c**) in 12%, 14%, 52% yields, respectively. Coupling reactions to synthesize compounds **5b** and **5c** were carried out under high pressure. Three quinone derivatives, 25,27-di(ethyleneglycol)-bis-*p-tert*-butylcalix[4]tetraquinone, **5a**, 25,27-di (diethyleneglycol)-bis-*p-tert*-butylcalix[4]tetraquinone, **5b**, and 25,27-di(methoxy)-26,28-di(ethyleneglycol)-bis-*p-tert*-butylcalix[4]diquinone, **5c**, were synthesized by oxidizing compounds **1**, **2b** and **4d** with $Tl(CF_3COO)_3$ in CF_3COOH and were obtained in 52%, 68% and 38% yields, respectively.

^{1}H-NMR titrations show that **5a** and **5c** can form complexes with Li^+, Na^+ and K^+ ions. Compounds **5a** and **5c** selectively bind Na^+. However, the cavity in compound **5c** is possibly smaller than **5a**. Therefore, the stability constant of **5c**+Na^+ is much lower than that of **5a**+Na^+. The binding trends for **5a** and **5c** are as follows; $Na^+ > Li^+ >> K^+$ and $Na^+ >> Li^+ > K^+$. Compound **5b** which has a bigger cavity than **5a** and **5c** shows selectivity for Cs^+. The binding trend for **5b** is as $Cs^+ > K^+ > Na^+ >> Li^+$.

Electrochemical studies using cyclic voltammetry and square wave voltammetry showed significant changing of voltammogram of **5a**, **5b** and **5c** upon addition of alkali cations such as Li^+, Na^+, K^+ or Cs^+. A new set of peaks which indicate the complex between ligands and cations are observed at less negative potentials than the original free ligand waves. Anodic shift for ligands **5a** and **5b** upon addition of alkali cations exhibits the same trend as $Li^+ > Na^+ > K^+ > Cs^+$ while **5c** exhibits the trend as $K^+ > Na^+ > Li^+$.

Compounds **5a** and **5b** possess 4 quinone oxygens while **5c** contains only two quinone oxygens and two etheral oxygens. Therefore, **5a** and **5b** are harder acid than **5c** in the reduced forms and can form more stable complexes with smaller cations. This results in a larger shifts of cyclic voltammograms to less negative potential upon addition of metal ions. This suggests that hard-soft acid base shows important role in redox chemistry of the quinone moiety. All these phenomena imply that double calix[4]arenequinones **5a**, **5b** and **5c** may possibly be used as alkali metal ion sensors.

Suggestion for future works

From all obtained results and discussion, future works should be focused on;

1. X-ray crystal structures of ligands **5a**, **5b** and **5c** and their alkali metal complexes should be obtained in order to understand the structure of the synthetic receptors and their coordination chemistry with alkali metal ions.

2. UV-Visible and Fluorescence titrations of ligands **5a**, **5b** and **5c** with alkali metal ions should be investigated to obtain complexation constants and structural behaviors upon complexation.

3. Synthesize other derivatives of double calix[4]arenequinones such as a mono- or a triquinone to compare and study their complexation and electrochemistry.

REFERENCES

1. Kaifer, A.; Gómez-Kaifer, M. *Supramolecular Electrochemistry*. New York: Wiley-VCH Publishers, **1999**, p.103.
2. Asfari, Z.; Böhmer, V.; Harrowfield, J.; Vicens, J., Ed. *Calixarenes 2001*. London: Kluwer academic publishers, **2001**, p.627.
3. Beer, P. D. Transition-metal receptor systems for the selective recognition and sensing of anionic guest species. *Acc. Chem. Res*. **1998**, *31*, 71-80.
4. Arnaud-Neu, F.; Barrett, G.; Cremin, S.; Deasy, M.; Ferguson, G.; Harris, S. J.; Lough, A. J.; Guerra, L.; McKervey, M. A.; Schwing-Weill, M. J.; Schwinte, P. Cation complexation by chemically modified calixarenes. Part 10.Thioamide derivatives of *p-tert*-butylcalix[4]-, [5]- and [6]-arenes with selectivity for copper, silver, cadmium and lead. X-ray molecular structure of calix[4]arene thioamide-lead(II) and calix[4]arene amide-copper(II) complexed. *J. Chem. Soc., Perkin Trans.2* **1992**, 1119-1125.
5. Bocchi, V.; Foina, D.; Pochini, A.; Ungaro, R.; Andreetti, C. D. Synthesis, ^{1}H-NMR, ^{13}C-NMR spectra and conformational preference of open chain ligands on lipophilic macrocycles. *Tetrahedron* **1982**, *38*, 373-378.
6. Ferguson, G.; Kaiter, B.; McKervey, M. A.; Seward, E. M. Synthesis x-ray crystal structure and cation transfer properties of a calix[4]arene tetraketone. A new versatile molecular receptor. *J. Chem. Soc., Chem. Commum*. **1987**, 584-585.
7. Arnaud-Neu, F.; Barrett, G.; Harris, J.; McKervey, M. A.; Owens, M.; Schwing-Weill, M. J.; Schwinte, P. Cation complexation by chemically modified calixarene. 5. Protonation constants for calixarene carboxylates and stability constants of their alkali and alkaline-earth complexes. *Inorg. Chem*. **1993**, *32*, 2644-2650.
8. Muzet, N.; Wipff, G.; Casnati, A.; Domiano, L.; Ungaro, R.; Ugozzoli, F. Alkaline earth and uranyl cation complexes of a calix[4]arene-tetraamide MD and FEP simulations in aqueous and acetonitrile solutions and x-ray structure of its Sr (Picrate)$_2$ complex. *J. Chem. Soc., Perkin Trans.2* **1996**, 1065-1075.

9. Ghidini, E.; Ugozzoli F.; Ungaro, R.; Harkema, S.; Abu-El-Fadl, A.; Reinhoudt, D. N. Complexation of alkali metal cations by conformationally rigid, stereoisomeric calix[4]arene crown ethers : a quantitative evaluation of preorganization. *J. Am. Chem. Soc*. **1990**, *112*, 6979-6985.

10. Reinhoudt, D. N.; Dijkstra, P. J.; in't Veld, P. J. A.; Bugge, K. E.; Harkema, S.; Ungaro, R.; Ghidini, E. Kinetically stable complexes of alkali cations with rigidified calix[4]arenes. X-ray structure of a calixspherard sodium picrate complex. *J. Am. Chem. Soc*. **1987**, *109*, 4761-4762.

11. Gutsche, C. D. Calixarenes. *Acc. Chem. Res*. **1983**, *16*, 162-170.

12. Böhmer, V. Calixarenes, macrocycles with (almost) unlimited possibilities. *Angew. Chem. Int. Ed. Engl.* **1995**, *34*, 713-745.

13. Gutsche, C. D. *'Calixarene'-Monograph in Supramolecular Chemistry*, The Royal Society of Chemistry, Cambridge **1989**, p.36.

14. Ikeda, A. and Shinkai, S. Novel cavity design using calix[*n*]arene skeletons : Toward molecular recognition and metal binding. *Chem. Rev*. **1997**, *97*, 1713-1734.

15. Gutsche, C. D.; Muthukrishnan, R. Calixarenes. 1. Analysis of the product mixtures produced by the base-catalyzed condensation of formaldehyde with para-substituted phenols. *J. Org. Chem*. **1978**, *43*, 4905-4906.

16. Gutsche, C. D.; Dhawan, B.; No, K. H.; Muthukrishnan, R. Calixarenes. 4. The synthesis, characterization, and properties of the calixarenes from *p-tert*-butylphenol. *J. Am. Chem. Soc*. **1981**, *103*, 3782-3792.

17. Shinkai, S. Calixarenes-the third generation of supramolecules. *Tetrahedron* **1993**, *49*, 8933-8968.

18. Van Dienst, E.; Iwema-Bakker, W. I.; Engberson, J. F. J.; Verboom, W.; Reinhoudt, D. N. Calixarenes, chemical chameleons. *Pure & Appl. Chem*. **1993**, *65*, 387-392.

19. Pochini, A. and Ungaro, R. *Calixarenes and Related Hosts-Comprehensive Supramolecular Chemistry*. London: Elservier Science Ltd., **1996**, p.103.

20. Gutsche, C. D.; Dhawan, B.; Levine, J. A.; No, K. H.; Bauer, L. J. Calixarenes. 9. Conformational isomers of the ethers and esters of calix[4]arenes. *Tetrahedron* **1983**, *39*, 409-426.

21. Iwamoto, K.; Araki, K.; Shinkai, S. Syntheses of all possible conformational isomers of O-alkyl-*p-t*-butylcalix[4]arenes. *Tetrahedron* **1991**, *47*, 4325-4342.

22. Schmitt, P.; Beer, P. D.; Drew, M. G. B.; Sheen, P. D. Calix[4]tube : A tubular receptor with remarkable potassium ion selectivity. *Angew. Chem. Int. Ed. Engl*. **1997**, *36*, 1840-1842.

23. Ohseto, F.; Shinkai, S. Syntheses of and metal cation oscillation in ionophoric biscalix[4]arenes. *J. Chem. Soc. Perkin Trans.2* **1995**, 1103-1109.

24. Bethell, D.; Dougherty, G.; Coupertino, D. C. Selectivity in redox-switched calix [4]arene catiophores : Electrochemical detection of a conformational change on cation binding. *J. Chem. Soc. Chem. Commun*. **1995**, 675-676.

25. Akine, S.; Goto, K.; Kawashima, T. Synthesis, structure, and redox properties of a quinone-bridged calix[6]arene. *Tetrahedron Lett*. **2000**, *41*, 897-901.

26. Gómez-Kaifer, M.; Reddy, P. A.; Gutsche, C. D.; Echegoyen, L. Electroactive calixarenes. 1. redox and cation binding properties of calixquinones. *J. Am. Chem. Soc*. **1994**, *116*, 3580-3587.

27. Reddy, P. A.; Gutsche, C. D. Calixarenes : Reactions of calix[4]quinones. *J. Org. Chem.* **1993**, *58*, 3245-3251.

28. Suga, K.; Fugihara, M.; Monta, T.; Agawa, T. Electrochemical study on calix[4] quinone and calix[4]hydroquinone in N,N-dimethylformamide. *J. Chem. Soc. Faraday Trans*. **1991**, *87*, 1575-1578.

29. Beer, P. D.; Chen, Z.; Gale, P. A. Diester-calix[4]arenediquinone complexation and electrochemical recognition of group-1 and group-2, ammonium and alkyl ammonium guest cations. *Tetrahedron* **1994**, *50*, 931-940.

30. Beer, P. D.; Gale, P. A.; Chen, Z.; Drew, M. G. B., Heath, J. A.; Ogden, M. I.; Powell, H. R. New Ionophoric Calix[4]diquinones: coordination chemistry, electrochemistry, and x-ray crystal structure. *Inorg. Chem*. **1997**, *36*, 5880-5893.

31. Chung, T. D.; Choi, D.; Kang, S. K.; Lee, S. K.; Chang, S. K.; Kim, H. Electrochemical behavior of calix[4]arenediquinones and their cation binding properties. *J. Electroanal. Chem* **1995**, *396*, 431-439.

32. Bettega, H. C.; Moutet, J.; Ulrich, G.; Ziessel, R. Electrochemical cation recognition by novel 2,2'-bipyridine-grafted calix[4]arenequinones. *J. Electroanal. Chem*. **1996**, *406*, 247-250.

33. Webber, P. R. A.; Chen, G. Z.; Drew, M. G. B.; Beer, P. D. Cesium- and rubidium-selective redox-active bis(calix[4]diquinone) ionophores. *Angew. Chem. Int. Ed*. **2001**, *40*, 2265-2268.

34. Wang, J. *Analytical Electrochemistry*. New York: Wiley-VCH Publishers, **1994**, p.38-42, 161-164.

35. Plambeck, J. A. *Electroanalytical chemistry*. New York: Wiley-VCH Publisher, **1982**, p.310-312.

36. Schneider, H., Yatsimirsky, A. K. *Principles and methods in supramolecular chemistry*. New York: Wiley-VCH Publisher, **2000**, p.173-174.

37. Gutsche, C. D.; Iqbal, M. *p-tert*-Butylcalixarene *Org. Synth*. **1990**, *68*, 234-237.

38. Chen, C. F.; Zheng, Q. Y.; Zheng, Y. S.; Huang, Z. T. Functionalization of calix[4] arenes at the lower rim and synthesis of calix[4](aza)crowns. *Synthetic Communications* **2001**, *31*, 2829-2836.

39. Cobben, P. L. H. M.; Egberink, R. J. M.; Bomer, J. G.; Bergveld, P.; Verboom, W.; Reinhoudt, D. N. Transduction of selective recognition of heavy metal ion by chemically modified field effect transistors (CHEMFETs). *J. Am. Chem. Soc.* **1992**, *114*, 10573-10582.

40. Tomapatanaget, B.; Pulpoka, B.; Tuntulani, T. Preparation of diaza dioxa dithiacrown *p-tert*-butylcalix[4]arene by S-alkylation reactions: Use of metallocalix[4]arene complexes as reaction templates. *Chem. Lett*. **1998**, 1037-1038.

41. Tantrakarn, K.; Ratanatawanate, C.; Pinsuk, T.; Chailapakul, O.; Tuntulani, T. Synthesis of redox-active biscalix[4]quinones and their electrochemical properties. *Tetrahedron Lett*. **2003**, *44*, 33-36.

42. Asfari, Z.; Weiss, J.; Pappalardo, S.; Vicens, J. Synthesis and properties of double-calix[4]arenes, doubly-crowned calix[4]arenes, and double-calixcrowns. *Pure & Appl. Chem*. **1993**, *65*, 585-590.

43. Arduini, A.; Domiano, L.; Pochini, A.; Secchi, A.; Ungaro, R.; Ugozzoli, F.; Struck, O.; Verboom, W.; Reinhoudt, D. N. Synthesis of 1,2-bridged calix[4] arene-biscrowns in the 1,2-alternate conformation. *Tetrahedron* **1997**, *53*, 3767-3776.

44. Jaime, C.; Mendoza, J.; Prados, P.; Nieto, P. M.; Sanchez, C. ^{13}C NMR chemical shifts. A single rule to determine the conformation of calix[4]arenes. *J. Org. Chem*. **1991**, *56*, 3372-3376.

45. Macomber, R. S. An introduction to NMR titration for studying rapid reversible complexation. *J. Chem. Educ*. **1992**, *69*, 375-378.

46. Choi, D.; Chung, T. D.; Kang, S. K.; Lee, S. K.; Kim, T.; Chang, S. K.; Kim, H. Electrochemical recognition of ammonium and alkali metal cations with calix [4]arenediquinone. *J. Electroanal. Chem* **1995**, *387*, 133-134.

47. Miller, S. R.; Gustowski, D. A.; Chen, Z.; Gokel, G. W.; Echegoyen, L.; Kaifer, A. E. Rationalization of the unusual electrochemical behavior observed in lariat ethers and other reducible macrocyclic systems. *Anal. Chem*. **1988**, *60*, 2021-2024.

APPENDIX

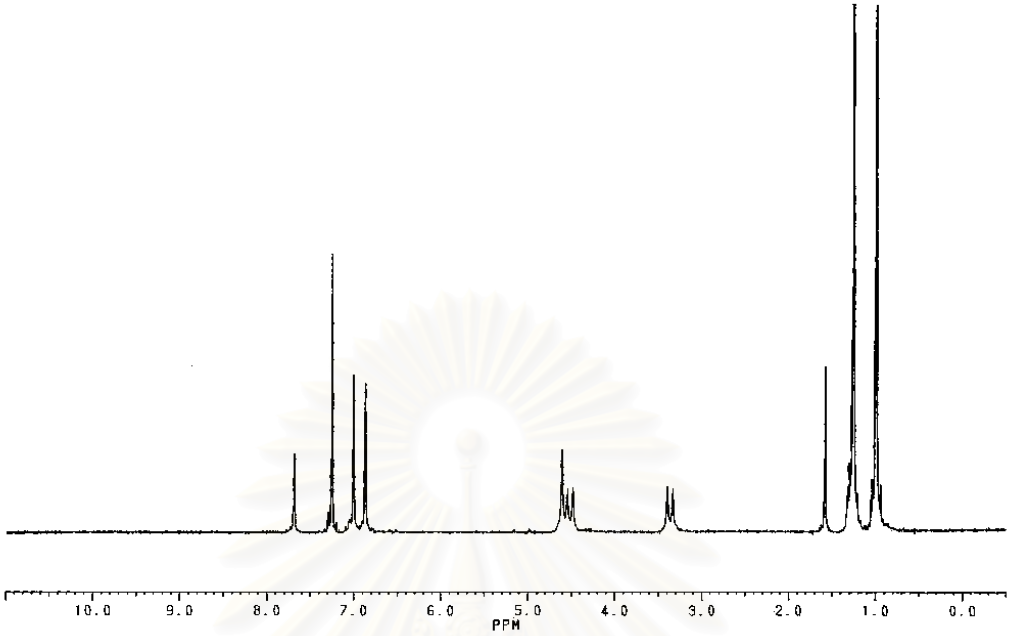

Figure A.1: ^{1}H-NMR (200 MHz, $CDCl_3$) spectrum of 25,27-di(ethyleneglycol)-bis-*p*-*tert*-butylcalix[4]arene (**1**)

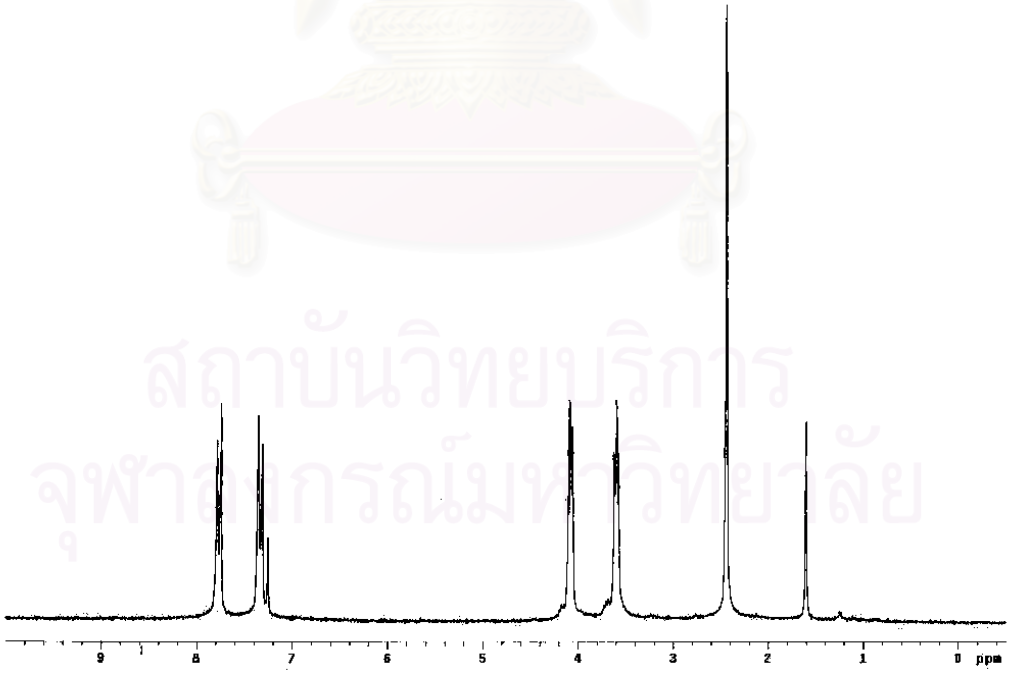

Figure A.2: ^{1}H-NMR (200 MHz, $CDCl_3$) spectrum of diethyleneglycol ditosylate (**2a**)

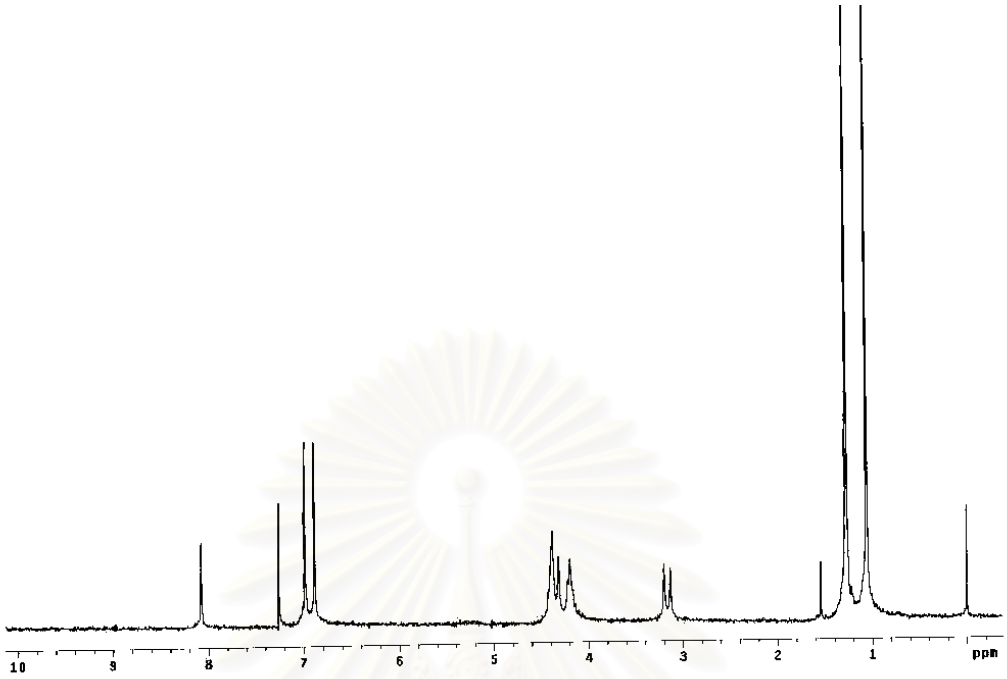

Figure A.3: ^{1}H-NMR (200 MHz, $CDCl_3$) spectrum of 25,27-di(diethyleneglycol)-bis-*p-tert*-butylcalix[4]arene (**2b**)

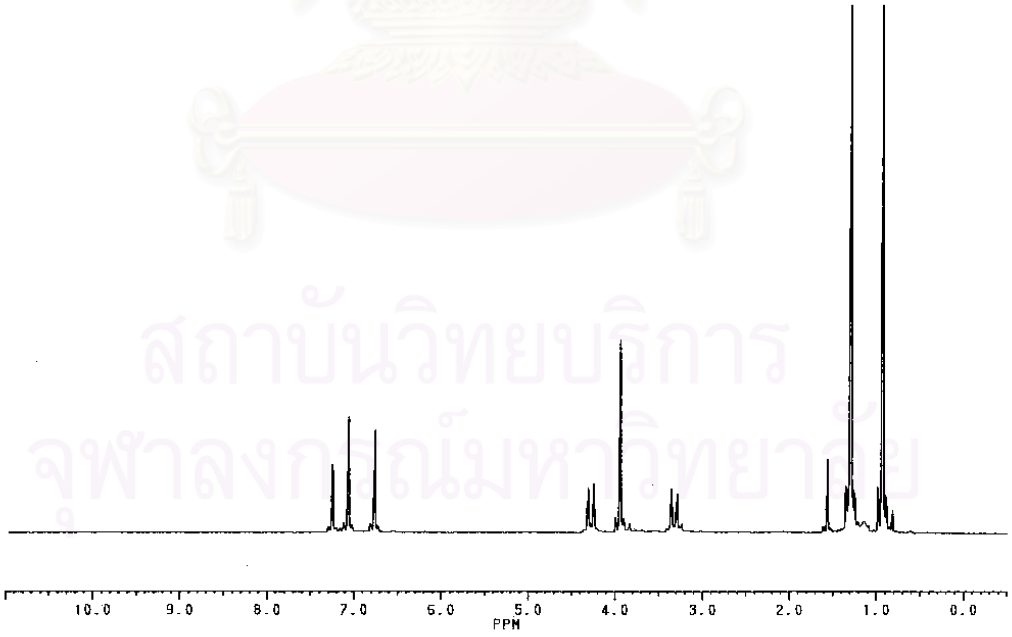

Figure A.4: ^{1}H-NMR (200 MHz, $CDCl_3$) spectrum of 25,27-di(methoxy)-*p-tert*-butylcalix[4]arene (**3a**)

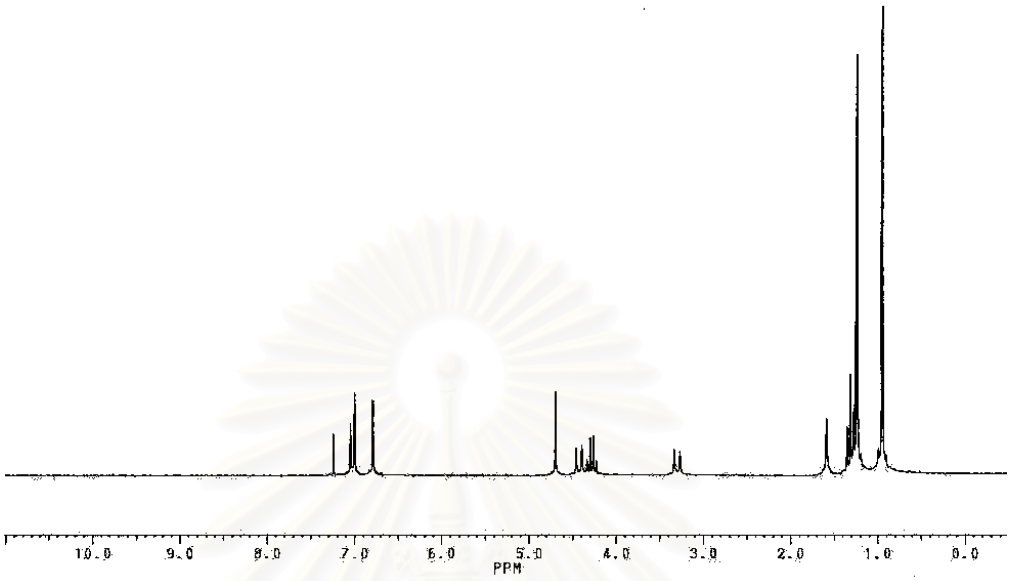

Figure A.5: ^{1}H-NMR (200 MHz, $CDCl_3$) spectrum of 25,27-di(carboethoxymethoxy)-*p-tert*-butylcalix[4]arene (**3b**)

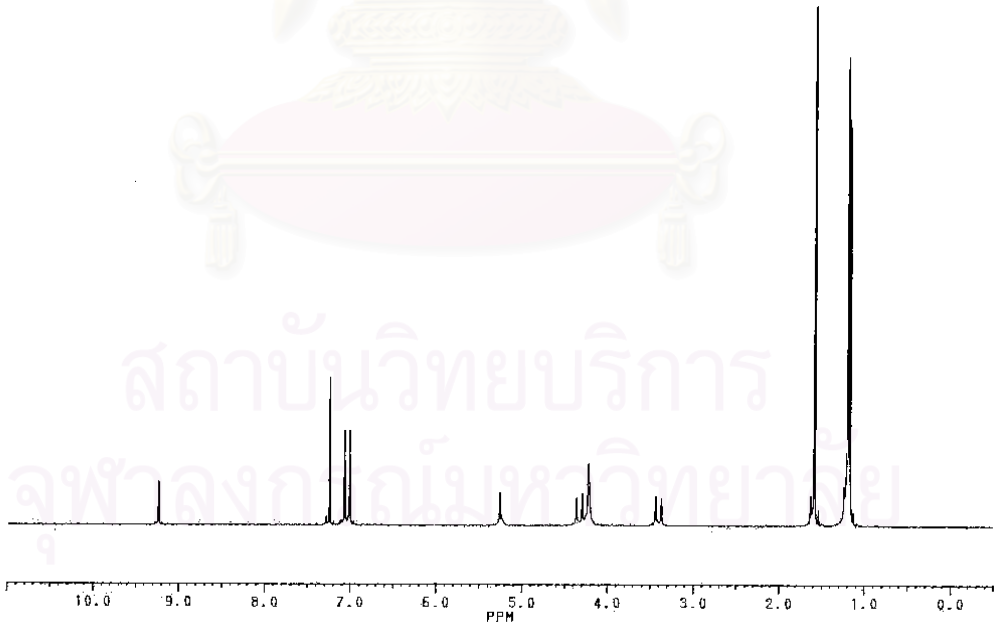

Figure A.6: ^{1}H-NMR (200 MHz, $CDCl_3$) spectrum of 25,27-di(2-hydroxyethoxy)-*p-tert*-butylcalix[4]arene (**3c**)

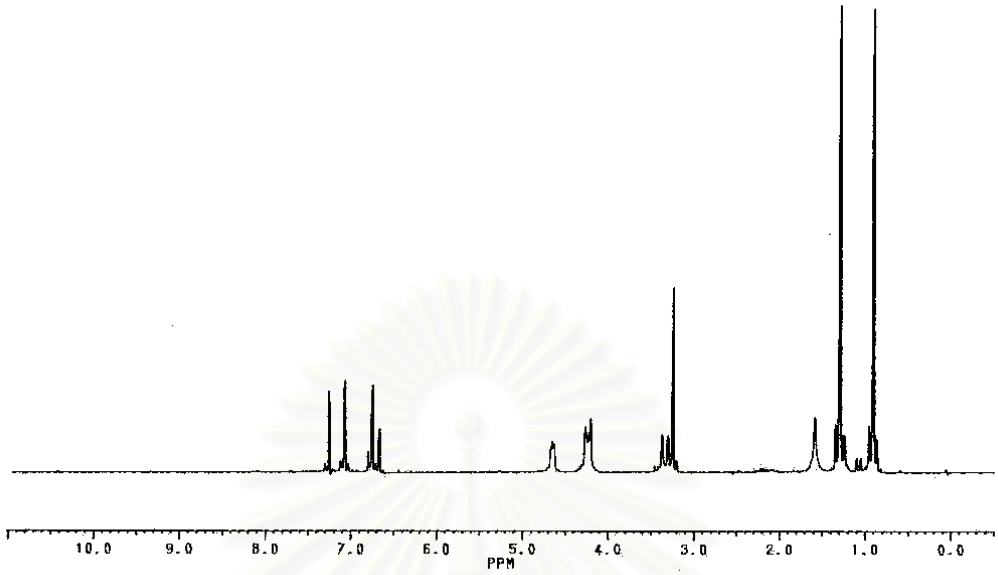

Figure A.7: ^{1}H-NMR (200 MHz, $CDCl_3$) spectrum of 25,27-di(methanesulfonyloxy-ethoxy)-*p-tert*-butylcalix[4]arene (**3d**)

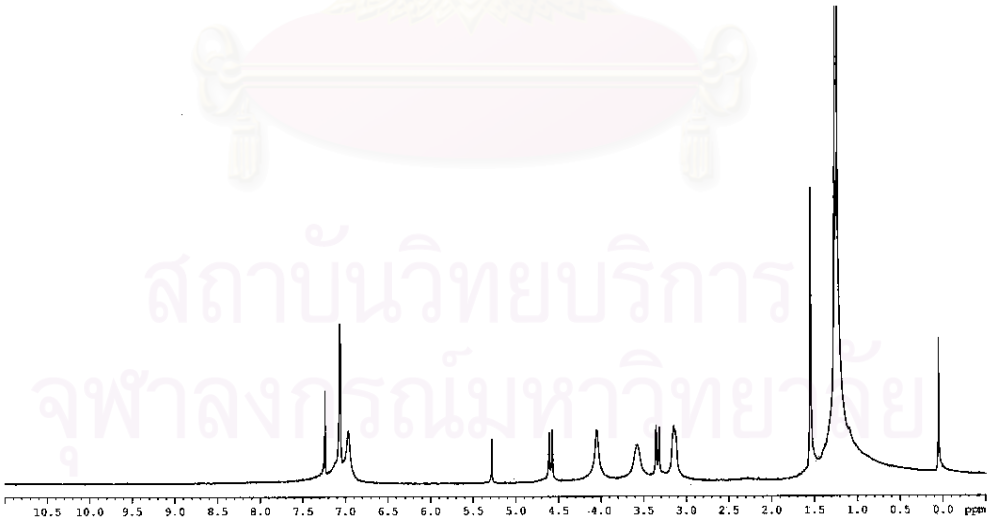

Figure A.8: ^{1}H-NMR (400 MHz, $CDCl_3$) spectrum of **3f**

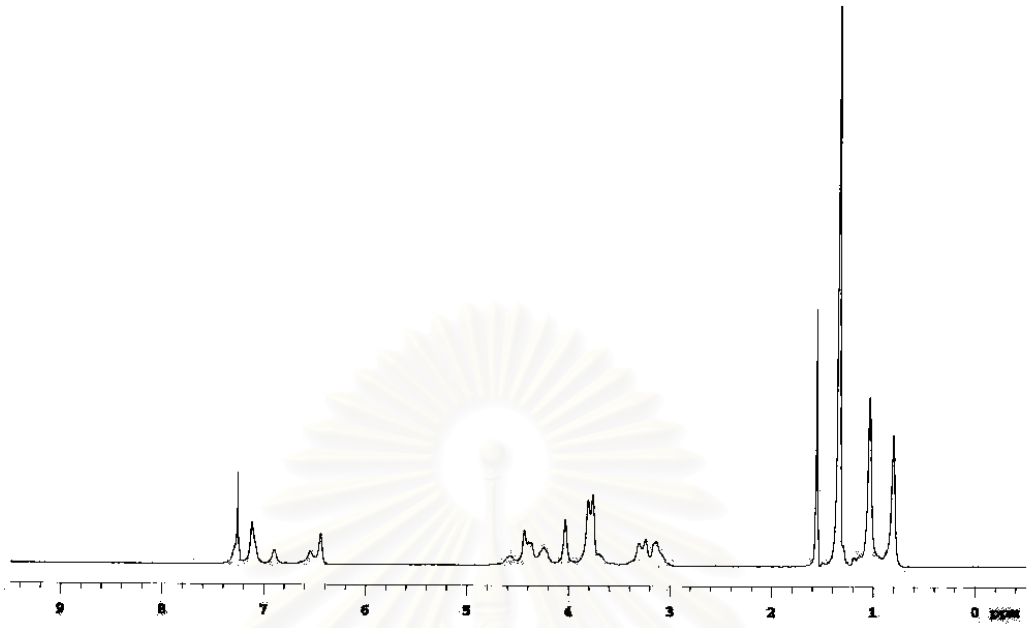

Figure A.9: ^{1}H-NMR (400 MHz, $CDCl_3$) spectrum of 25,27-di(methoxy)-26,28-di (carbomethoxymethoxy)-*p-tert*-butylcalix[4]arene (**4a**)

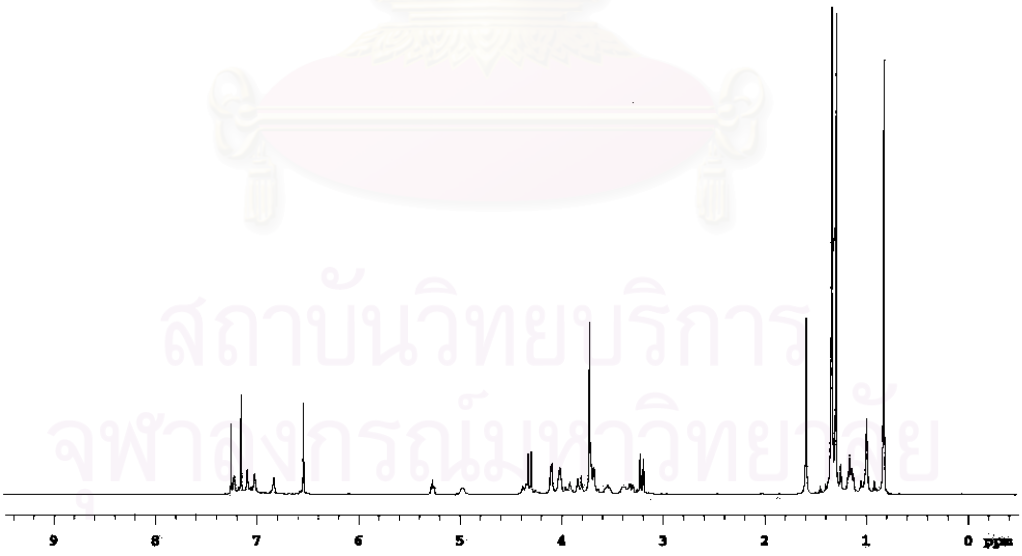

Figure A.10: ^{1}H-NMR (400 MHz, $CDCl_3$) spectrum of 25,27-di(methoxy)-26,28-di(2-hydroxyethoxy)-*p-tert*-butylcalix[4]arene (**4b**)

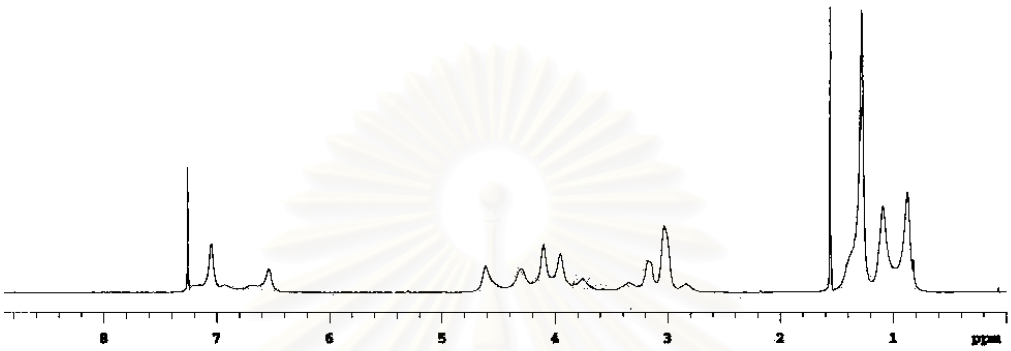

Figure A.11: ^{1}H-NMR (400 MHz, $CDCl_3$) spectrum of 25,27-di(methoxy)-26,28-di (methanesulfonyloxyethoxy)-*p*-*tert*-butylcalix[4]arene (**4c**)

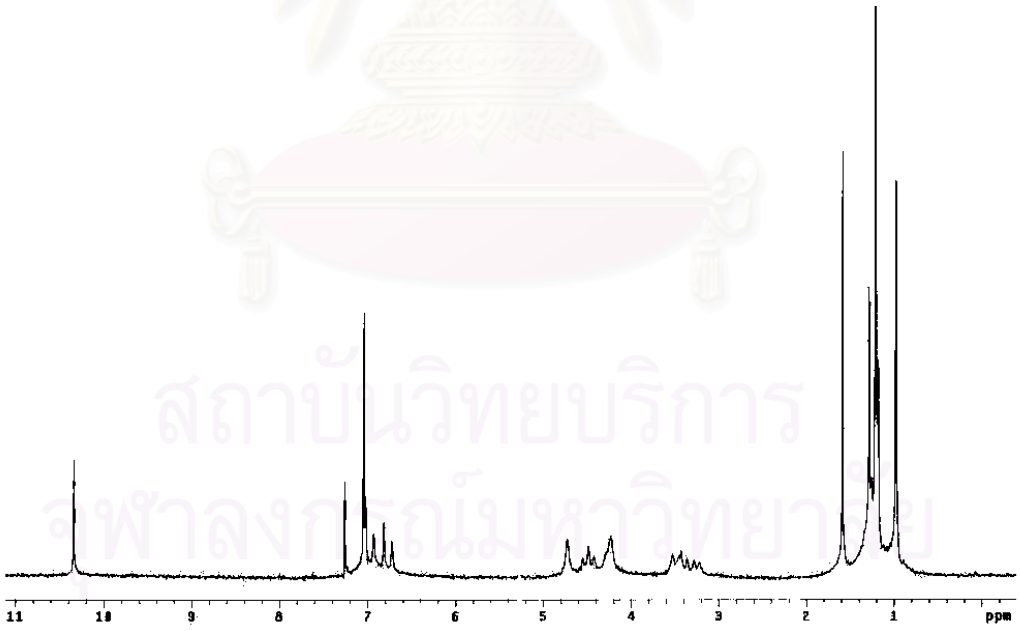

Figure A.12: ^{1}H-NMR (200 MHz, $CDCl_3$) spectrum of 25,27-di(methoxy)-26,28-di (ethyleneglycol)-bis-*p*-*tert*-butylcalix[4]arene (**4d**)

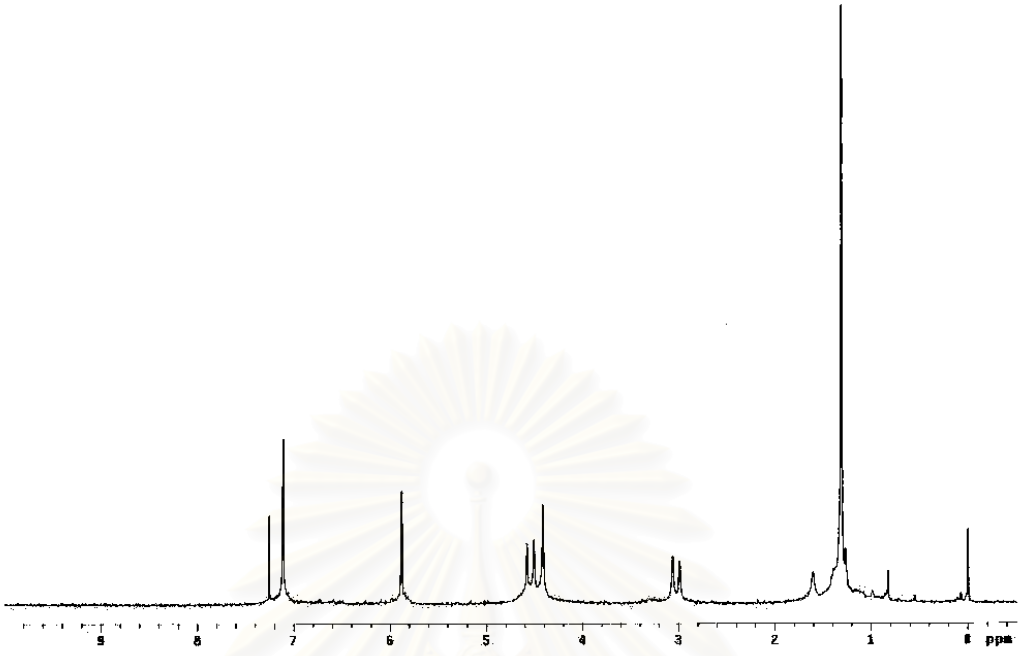

Figure A.13: ^{1}H-NMR (200 MHz, $CDCl_3$) spectrum of 25,27-di(ethyleneglycol)-bis-*p*-*tert*-butylcalix[4]tetraquinone (**5a**)

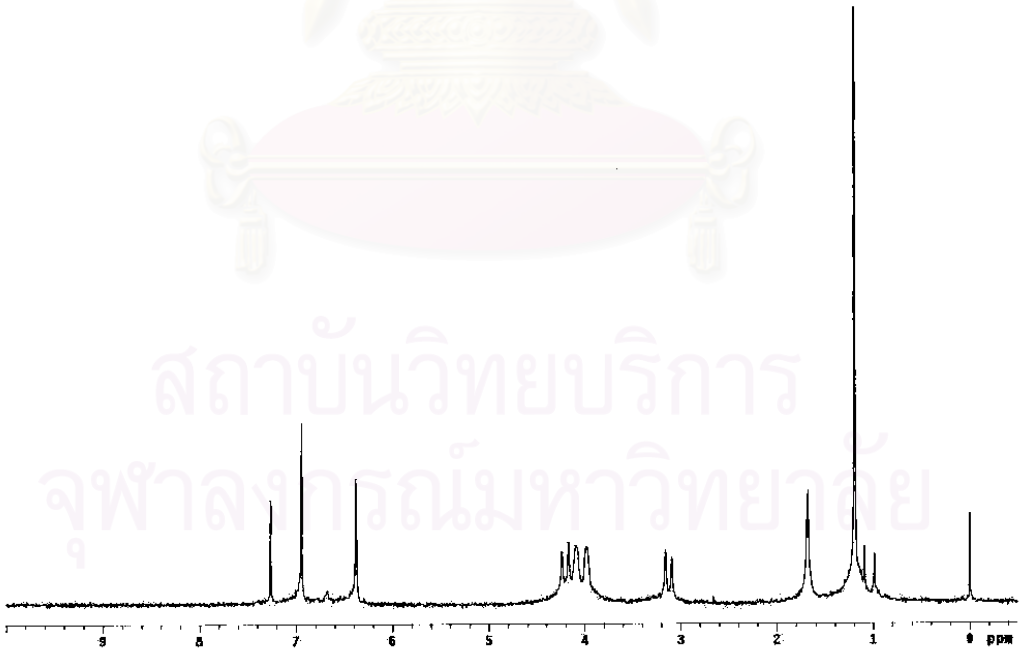

Figure A.14: ^{1}H-NMR (200 MHz, $CDCl_3$) spectrum of 25,27-di(diethyleneglycol)-bis-*p*-*tert*-butylcalix[4]tetraquinone (**5b**)

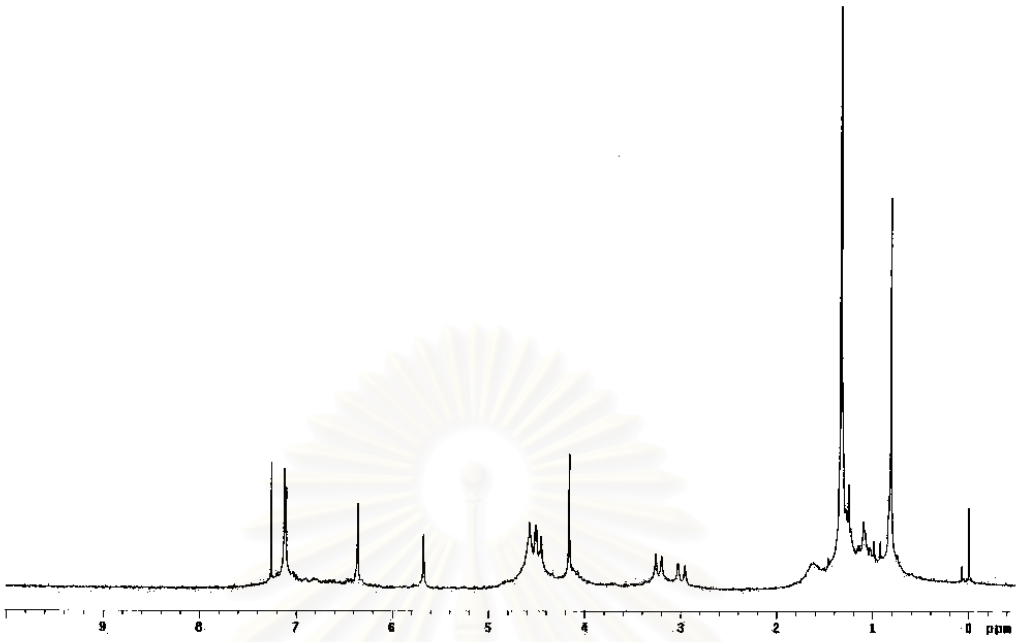

Figure A.15: ^{1}H-NMR (200 MHz, $CDCl_3$) spectrum of 25,27-di(methoxy)-26,28-di (ethyleneglycol)-bis-*p*-*tert*-butylcalix[4]diquinone (**5c**)

VITA

Mr. Nuttavut Kerdpaiboon was born on July 25, 1979 in Samutsakorn, Thailand. He graduated with a high school diploma from Suankularb School, Bangkok in 1995. He reveived his Bachelor's degree of Science in Chemistry from Chulalongkorn University in 1999. Since 2000, He has been a graduate student at the Department of Chemistry, Chulalongkorn University and become a member of the Supramolecular Chemistry Research Laboratory under supervision of Assistant Professor Dr. Thawatchai Tuntulani. He finished his Master's degree of Science in the academic year 2002.